Optimising the Plastic Optical Fibre Evanescent Field Biofilm Sensor

Yuen Mei Wong

A thesis submitted in part fulfilment
of the requirements of Liverpool John Moores University
for the degree of Doctor of Philosophy

School of Engineering

December 2008

BRITISH LIBRARY HSIIN

IMAGING SERVICES NORTH
Boston Spa, Wetherby
West Yorkshire, LS23 7BQ
www.bl.uk

APPENDICES 1 TO 11 AND FIG 3.7 EXCLUDED UNDER INSTRUCTION FROM THE UNIVERSITY

List of Contents

Appendices

Abbreviation	Meaning	Page first used
POF	Plastic Optical Fibre	xii
PMMA	Polymethylmethacrylate	xii
CLOOPT	Closed Loop Optimisation	xii
AQUA-STEW	Water Quality Surveillance Techniques for Early Warning by Interface Sensors	xii
GOF	Glass Optical Fibre	xvi
LAN	Local Area Network	xvi
Gbps	Gigabits per Second = Billions of Bits per Second	xvi
NA	Numerical Aperture	xvi
FBG	Fibre Bragg Grating	xvi
μm	Micrometer = 10^{-6}m	xvii
PCS	Polymer Clad Silica	xvii
mm	Millimetre=10^{-3}m	xvii
cm	Centimetre =10^{-2}m	xvii
Km	Kilometres=10^{3}m	xix
dB	Decibel	xix
nm	Nanometer=10^{-9}m	xix
mPOF	Microstructured POF	xx
EMI	Electromagnetic Interference	1
LPFG	Long Period Fibre Grating	5
sol-gel	Polymerization of molecular precursors which allows inorganic and organic components to be mixed at the nanometric scale	5
CVD	Chemical Vapour Deposition	5
PVD	Physical Vapour Deposition	5
FOI	Fibre Optic Interferometry	6
FFPI	Optical Fibre Fabry-Pérot Interferometer	7
FM	Frequency Modulated	7
AM	Amplitude Modulated	7
OTDR	Optical Time-Domain Reflectometry	8
TDM	Time Division Multiplexing	8
WDM	Wavelength Division Multiplexing	8
LED	Light Emitting Diodes	8
EW	Evanescent Wave	22
GRIN	Graded Index	24

Abbreviation	Meaning	Page first used
MBps	Megabytes per second	27
BER	Bit Error Ratio	26
PIN	Positive Intrinsic Negative	26
TIR	Totally Internally Reflected	29
μW	Microwatt= 10^{-6}w	47
LD	Laser Diode	53
mW	Milliwatt=10^{-3}w	53
V	Volt	53
AC	Alternating Current	53
CD	Compact Disc	54
DVD	Digital Versatile Disc	54
FWHM	Full-Width Half-Maximum	58
ST	Straight Tip Connector	61
SMA	Subminiature Version A	61
FET	Field Effect Transistor	64
pF	Pico Farad=10^{-12}F	64
BIFET	Bipolar Field Effect Transistor	66
DC	Direct Current	66
PC	Personal Computer	66
MSc	Master of Science	71
MIBK	Methylisobutylketone	93
EPS	Exopolysaccharide	115
LJMU	Liverpool John Moores University	115
XPS	X-Ray Photoelectron Spectroscopy	116
UV	Ultraviolet	124

List of figures

List of Tables

Abstract

This thesis describes the development, characterisation and application of large diameter multimode plastic optical fibre (POF) sensors using evanescent field modulation.

The exposed polymethylmethacrylate (PMMA) core of the POF fibre forms the sensor interface that detects refractive index changes of a measurand acting as the cladding. When a liquid measurand is used, the sensor can detect changes in refractive index, absorption and suspended particulates. It is this simple mechanism by which the evanescent field POF sensor operates. The evanescent field POF sensor has been characterised for refractive index of surrounding liquid from 1.33 to 1.49. The sensor demonstrated accuracy of $\pm 7 \times 10^{-3}$ refractive index units below 1.4 and $\pm 2 \times 10^{-3}$ refractive index units above 1.4.

Components have been selected and designed for this project to ruggedise the sensor, to make the sensor more self-contained and cheaper. The original design of the test conditions did not allow for optimum deployment of the sensor as it stripped out the very modes of light that were required for sensing purposes. The system was also operating under pressure, not reflecting the real conditions under which the sensor would be operating. The re-design of test conditions holds the sensor without straining the POF and operates under normal atmospheric pressure.

The POF sensor was demonstrated reacting to a real measurand eg biofilm in which initial growth affects the optical properties at the core cladding interface by refractive index modulation. This sensor was capable of measuring biofouling and scaling at water interfaces. The sensor was trialled in a European Commission funded project (CLOOPT) to study biofouling and scaling in closed loop water systems such as heat exchangers in the cooling tower of an electric power plant, and as an interface sensor for water quality monitoring (AQUA-STEW) involving biofilm removal and surface cleansing with a new application for contact lens protein removal systems.

Tapering multimode POF was a desirable goal as this increases the proportion of light coupled into the core available for sensing purposes, to achieve a more sensitive evanescent field POF sensor. Optically clear and consistent smooth tapering of ends and mid-lengths of POF fibre were achieved through chemical removal of material.

The tapered POF sensor was characterised with a range of refractive indices, and it exhibited two distinct regions; the water/alcohol region below 1.4 refractive index units, and the oil region above 1.4 suggesting the sensor's use as an oil-in-water, or water-in-oil sensor. From 95% confidence limits, the accuracy of the POF was ± 0.006 refractive index units (to 2 standard deviations) for fluids of refractive indices above 1.4. Tapered POF is sensitive to refractive index providing a cheap, easy to handle and rugged throwaway sensor for water and beverage process and quality monitoring.

DECLARATION

I declare that no portion of the work referred to in the thesis has been submitted in support of an application for another degree or qualification of this or any other university or other institute of learning.

COPYRIGHT STATEMENT

(i) Copyright in text of this thesis rests with the Author. Copies (by any process) either in full, or of extracts, may be made only in accordance with instructions given by the Author and lodged in the Liverpool John Moores University's Resource Centre. Details may be obtained from the Librarian. This page must form part of any such copies made. Further copies (by any process) of copies made in accordance with such instructions may not be made without the permission (in writing) of the Author.

(ii) The ownership of any intellectual property rights which may be described in this thesis is vested in Liverpool John Moores University, subject to any prior agreement to the contrary, and may not be made available for use by third parties without the written permission of the University, which will prescribe the terms and conditions of any such agreement.

(iii) Further information on the conditions under which disclosures and exploitation may take place is available from the Head of School of Engineering.

ACKNOWLEDGEMENTS

I wish to thank my supervisor, Dr P J Scully, for her patient and invaluable support and direction throughout this work, to Mr J C Yates for awarding me the sabbatical that has made the completion of this thesis possible and my colleagues at St Hilda's C.E. High School for their support.

My thanks to Liverpool John Moores University for giving me the opportunity to pursue my PhD degree and thanks to all the academics and staff at the university for their help and support along the way. Special thanks are due to Mr. Ron McGovern and Mr Brian Gray from the school's workshop for their technical and practical advice and for realising my designs with such great skill.

I thank the EU for their financial support via CLOOPT/AQUASTEW grants.

A final thank you to The University of Manchester for the use of their facilities and support of their staff in the completion of this thesis.

To Chau, my wonderful husband
you have been so patient and understanding

For my beautiful daughters, Jennifer and Emma
you are my inspiration and motivation

Introduction, Scope and Objectives

Introduction:

There is a constant and increasing demand for improvements in the quality of food and water[1]. Recycling is at the forefront of more people's minds than ever, fuel economy and efficiency leading to 'smarter' buildings, the maintenance of public common land, the health of our waterways and the quality of the water for our consumption.

There is a demand for structural health monitoring[2] which involves remote sensors which monitor buildings, pipelines and waterways. Strain sensors give early warning of fatigue in tall buildings, aeroplanes, ships, bridges, reservoir dams and various pipelines, allowing preventative action to be carried out at a more prudent time. Real time constant monitoring of our waterways is essential to maintain the health of the wildlife, ensure that leisure and recreational activities are without danger to participants, that water for human consumption is fit, all of which is dependent upon the close monitoring of industrial effluence.

As such there is a real demand for sensors for an increasingly diverse set of parameters. For simple light power monitoring, optical fibres offer real advantages in that they offer flexibility, miniaturisation, chemical, electrical, and magnetic immunity, are intelligence secure and can operate remotely over very long distances, kilometres, with the sensitised fibre in within specified targets.

Technology is constantly improving: faster, cheaper, more powerful computers; ever improving light emitters and detectors: higher optical powers, improved response, lower noise and wider wavelengths; introduction of new types of fibre and ongoing research and development in optical fibre sensors.

There are two basic types of optical fibres, categorised by the material of their core: silica based optical fibre or glass optical fibre (GOF) and polymer based optical fibre or plastic optical fibre (POF). Primarily manufactured for the telecoms business GOF is the first choice due to its low attenuation of signal over long distances, however over the shorter distances of local area networks (LANs) POF offers distinct advantages over GOF. 90% of all LANs cover less than 100m, a distance that POF supports data rates approaching 1Gbps.

The many advantages POF has over GOF are: high fracture toughness, GOF shatters easily when bent, relative flexibility in bending - tighter bend radius without damaging the operation of the fibre, durability in harsh chemical and environmental conditions, high elastic strain limit,[3,4,5] large core size, thus large numerical aperture (NA), which lead to the ease of non-skilled handling - easier to cleave and couple. It is more rugged, has safe disposability and at much lower cost.

Optical fibre is often modified to allow external perturbations to affect the fibre for sensor purposes. This includes removing the cladding, tapering, coating with reagents, adding grooves along its length, changing the refractive index of the core, writing gratings along its length or adding reagents to the core during manufacture.

The lower fabrication temperatures of POF enables the incorporation of organic chromophores and rare earth organic metallics that would be destroyed by the high temperatures used in GOF production to be added to POF facilitating doping with fluorophores and chemical reagents.

The fabrication of relatively low-attenuation single-mode POF at near-infrared wavelengths has permitted the writing of high deformation POF fibre Bragg grating (FBG) sensors and filters, Liu et al[6] demonstrated a 29% increase in strain sensitivity of POF FBG compared to similar GOF FBG.

POF in Everyday Life

Increasingly POF has applications in everyday life.[7] POF does have higher attenuation compared with GOF but are acceptable for short distance applications[11] for example in office blocks,[8] the home,[9,10] the car, and the person. A research group in Japan have installed a POF LAN system in a block of university halls[11,12] and a POF demonstration apartment was built in 2004 in Nuernberg.[13] Initially introduced to control entertainment systems, POF LANs can deliver as the demand for faster, bigger and better broadband internet connections in homes is driving optical telecommunications to producing high quality low cost optical fibre entertainment systems that could be extended to monitor environmental conditions for occupant comfort and safety. The car manufacture industry now includes POF networks within vehicles[14] initially used to interface in-car entertainment, navigation, mobile telephone systems with each other, over 22 models of cars including Mercedes E-Class, BMW 7 series, Porsche Cayenne, Saab 9-3, Audi A8 and Volvo XC90 being amongst the first to put this technology in commercially available models. BMW use a POF system to link 12 sensors (velocity, acceleration or pressure) called ByteFlight to evaluate the sensor data as to when to deploy airbags.

POF is being integrated into fabrics where it has the advantage over GOF. It can be woven into cloth during the manufacture of textiles.[15,16] It is rugged, flexible and is 10 times more sensitive to evanescent field than 200μm polymer-clad silica (PCS) fibre.[17] POF has a very small bend radius compared to GOF. 1mm diameter POF has a bend radius of 1cm, single mode POF of diameter 125μm has a bend radius of 0.125cm[18] and so is flexible and is easy to manipulate. GOF is brittle and may shatter when flexed by the wearer. The POF has applications as a communications and entertainment hub wired into a garment to integrate various gadgets but also as sensors

monitoring patients that require continuous medical assistance and treatment as a wearable heath system and also as protective clothing, detecting vital signals of the wearer's body or changes in the wearer's environment.[19,20]

Scope and Objectives:

The primary objective was to develop an Early Warning System for the Initial Onset of Biofilm Growth[21] an optimised, and rugged plastic optical fibre evanescent field sensors and interrogating instrumentation for applications that include, but not limited to the monitoring of biofilm growth in cooling towers, algal growth in natural waterways and water quality for contaminants at water processing plants. This was part of a European Commission project AQUASTEW* Fifth Framework Programme (FP5) Project Contract No. EVK1-CT-2000-00066 "Sustainable Management and Quality of Water". The sensor is to be deployed remotely in waterways by unskilled end-users and so must be rugged and easy to operate. The refractive index and spectral fingerprint of the biofilm needs to be known to be able to optimise the biofilm sensor. The technology should have the scope to be adapted for chemical sensing at manufacturing sites,[22] and monitoring of strain around concrete constructions, pipelines, aircraft or ship.[3,4,5]

This project consecutive to another European Commission project CLOOPT, Closed Loop Optimisation[23†] Fourth Framework Programme (FP4) Contract No. ENV 4-CT97-0634, "Environment and Climate". The sensor was successfully trialled at a power station cooling system and monitored scaling and fouling.

The processes involved in sensitising the optical fibre for sensor purposes must be refined and standardised. This involves the simple removal of the POF cladding to achieve sensing regions ranging from tens of millimetre lengths up to tens of

---

* Appendix 4
† Appendix 5

centimetres. These are to be deployed at targeted sites and connected to signal carrier optical fibres of tens of metres up to 10km, or to mobile telephone networks, allowing remote monitoring. The required response time of the sensors depends on their area of application. The build-up of biofilm, algae and chemicals would require daily sampling. Strains in concrete structures, aircraft and ships would also require daily sampling. Strains in pipelines may require a response time of 30 minutes to allow effective preventative actions to be initiated.

Intensity modulation is the simplest and cheapest type of sensor to develop. The greater the intensity of light available that is coupled into the sensor the greater its sensitivity. To this end, best practice methods for achieving the optimal termination of POF must be established, once achieved the fibre ends must be coupled in the most efficient manner.

The amount of light coupled out of a fibre, axially, is dependent upon the refractive index, colour and number of scattering particulates contained in the medium surrounding the fibre core. Light rays incident at the core/cladding face at angles larger than the critical angle result in a portion of that light refracting into the medium surrounding the core, both meridional and leaky skew rays contribute to absorption of the evanescent wave.

The quality of POF was improved 15 years ago. Attenuation dropped to 160 dB/km at 650nm, guiding 10^7 modes which made it suitable for use in multimode data communications up to 100m. POF is widely available in large diameters, typically 1mm, which ensures a large NA, allowing leaky modes to propagate into the fibre that will support tunnelling rays in addition to bound rays. Tunnelling rays have been demonstrated to contribute an extra 50% of the energy for modulation in the evanescent field of POF evanescent wave (EW) sensors. The distal end of the fibre has shown that

66% of power is contained in the bound modes and 33% in tunnelling modes – enabling maximum signal modulation of up to 13%, i.e. 13% of the total guided power exists in the evanescent field[24,25]. Due to the high attenuation of POF reveals itself to have 10 times greater sensitivity to evanescent field modulation than 200μm silica fibre.[26,27] Special emphasis has been put on intrinsic evanescent field sensors as these are the type developed by this project for detecting biofilm growth.

Optical fibres of smaller diameters have a greater proportion of coupled light in the evanescent field. The use of fibres with progressively smaller diameter cores should, therefore, lead to a more sensitive sensor. A 1mm diameter POF with a tapered region would be easier to handle and to couple light into than an optical fibre of smaller constant diameter. This would also enable the existing sensor to be optimised very easily with a straight swap-over of tapered fibre in place of the declad fibre presently used. To achieve this enhancement, a reliable method of producing mid-length POF tapers needs to be developed. The characterisation of both the declad and tapered fibre for their response to the refractive index of their cladding is desirable to assist in affecting the optimisation of sensor performance.

References

[1] Royal Commission on Environmental Pollution. Report No. FR/CL0005, "Assessing the Benefits of Surface Water Quality Improvements Manual", 1996

[2] KSC Kuang, ST Quek and M Maalej, "Assessment of an Extrinsic Polymer-based Optical Fibre Sensor for Structural Health Monitoring", Measurement Science and Technology vol.15, pp2133-2141, 2004

[3] KSC Kuang, WJ Cantwell, PJ Scully, "An Evaluation of a Novel Plastic Optical Fibre Sensor for Axial Strain and Bend Measurements", Measurement Science and Technology, vol.13, pp1523-1534, 2002

[4] KSC Kuang, WJ Cantwell, "Plastic Optical Fibre and Shape Memory Alloy for Damage Assessment and Damping Enhancement of Composite Materials", Measurement Science and Technology, vol.14, pp1305–1313, 2003

[5] KSC Kuang, Akmaluddin, WJ Cantwell, C Thomas, "Crack Detection and Vertical Deflection Monitoring in Concrete Beams Using Plastic Optical Fibre Sensors", Measurement Science and Technology, vol.14, pp205–206, 2003

[6] HB Liu, HY Liu, GD Peng, PL Chu, "Strain and Temperature Sensor Using a Combination of Polymer and Silica Fiber Bragg Gratings", Opt. Commun., vol.219, pp139-142, 2003

[7] K Poisel, D, Kalymnios, MM Werneck, K Krebber, JS Zubia, PJ Scully, "POF Sensors – Applications in Every Day's Life", ECOC07 Conference, POF Symposium, 2007

[8] GJ Grimes, "POF Applications in Broadband Networks", Proceedings ECOC2001,

[9] A Ng'oma,T Koonen, IT Monroy, H van den Boom, P Smulders, G Khoe, "Low Cost Polymer Optical Fibre Based Transmission System for Feeding Integrated Broadband Wireless In-house LANs", Proceedings Symposium IEEE/LEOS Benelux Chapter, pp214-217, 2002

[10] AMJ Koonen, A Ng'oma, MG Larrode, H Yang, K Wang, HPA van den Boom, "In-house Broadband Wireless Service Delivery Using Radio over Multimode Fibre", Proceedings POF2007, pp88-91, 2007

[11] T Ishigure, Y Koike, "Graded-index plastic optical fibres exceeding 10 Gigabit transmission rate", IEEE, Fibers and Waveguide components P1.11

[12] O Ziemann, W R White, "100Mbit/s – Gbit/s and beyond the Use of POF in Home Networking and Interconnection", ECOC07 Conference, POF Symposium, 2007

[13] POFAC Nuernberg "Paving the Optical Future with Affordable Lightning-fast Links" IST-FP6 STREP Project No.027549

[14] T. Freeman, "Plastic Optical Fibre Tackles Automotive Requirements", FibreSystems Europe, June 17 2004

[15] A Dhawan, T Ghosh, J Muth, "Incorporating Optical Fiber Based Sensors into Fabrics", Materials Research Society, proceedings of Sypmosium H, 2005

[16] A Harlin, M Mäkinen, A Vuorivirta, "Development of Polymeric Optical Fibre Fabrics as Illumination Elements and Textile Displays", AUTEX Research Journal, vol.3, No.1, 2003

[17] R Philip-Chandy, PJ Scully, P Eldridge, HJ Kadim, MG Grapin, MG Jonca, MG D'Ambrosio, F Colin, "An Optical Fiber Sensor for Biofilm Measurement Using Intensity Modulation and Image Analysis", IEEE Journal on Selected Topics in Quantum Electronics, vol.6, No. , pp764-772, 2000

[18] Paradigm Optics Inc.

[19] Enterprise Europe Network, Agencia de Inovacao, ref:08 DE 1698 OIET, "Smart Textiles with Integrated Optical Sensors for Medical and Health Care Applications"

[20] A Grillet, D Kinet, J Witt, M Schukar, K Krebber, F Pirotte A Depre, "Optical Fiber Sensors Embedded into Medical Textiles for Healthcare Monitoring", IEEE Sensors Journal, vol.8, No.7, pp1215-1222, 2008

[21] "Water Quality Surveillance Techniques for Early Warning by Interface Sensors" AQUA-STEW FP5 Project EVK1-CT-2000-00066

[22] OS Wolfbeis, "Fiber-Optic Chemical Sensors and Biosensors", Anal. Chem., vol.80, pp4269-4283, 2008

[23] CLOOPT - On line measurement for preventing fouling when closing Indutrial process water circuit. European Commission project CONTRACT N° ENV 4-CT97-0634

[24] AW Snyder, "Leaky-ray Theory of Optical Waveguides of Circular Cross-section", App. Phys. vol.4, pp273-298, 1974

[25] AW Snyder, DJ Mitchell, C Pask, "Number of modes on optical waveguides", J. Opt. Soc. Am., vol.64, p608, 1974

[26] J Vaughan, C Woodyatt, PJ Scully, "Polymer optical coatings for moisture monitoring", Lasers and Electro-Optics, 2007 and the International Quantum Electronics Conference. CLEOE-IQEC 2007. European Conference on Volume , Issue , 17-22 June 2007 Page(s):1 - 1

[27] MCJ Large, F Cox, A Arygros, R Lwin, G Barton, MA van Eijkelenborg, S Manos, L Poladian, A Bachmann, H Poisel, "Microstructured POF and Applications" Proceedings of the 12th International Plastic Optical Fibers Conference 2005

CHAPTER ONE

Sensors Based on Conventional Plastic Optical Fibres

1.1 Introduction

Optical fibre sensors bridge both optical fibre communications and optoelectronics industries. Adapting components developed for these sectors, optical fibre sensors bring numerous advantages over conventional electrical and mechanical devices. Optical fibres are made of a dielectric material (glass, plastic) that propagate photons rather than electrons. The systems tend to be small, light-weight and immune to electromagnetic interference (EMI) where the POF sensor is an intensity sensor. Optical fibre sensors therefore may be placed very close to large EMI sources (e.g., power generators, electrical motors) or on structures prone to lightning strikes (bridges, towers, and aircraft). In addition, the flexible nature of the fibre allows unobtrusive sensing combined with environmental ruggedness.

The most readily available optical fibres are manufactured to the specifications of the telecommunications industry. Transmission of light signal with minimal loss and

immunity to exterior conditions is the ultimate goal here. For sensor applications, however, the opposite is true; it is desirable for the optical fibre to be strongly affected by a certain physical parameter in its environment.[1,2] Since light is characterised by intensity, phase, wavelength, frequency and polarisation, changes in any one or more of these parameters are detected. This response to external influence is deliberately enhanced so that the resulting change in optical radiation can be used as a measure of the external perturbation. The optical fibre acts as a transducer converting changes due to measurand such as temperature, chemical reactions, stress, strain, rotation or electric and magnetic currents into a corresponding change in the optical radiation. The usefulness of an optical fibre therefore depends on the ability to measure and quantify the magnitude of change reliably and accurately.

Optical fibre sensors can measure more than 60 parameters.[3,45,6,7,8] A great number of the main types of sensors are described in this chapter to bring an appreciation of what is possible and has already been realised. The number of sensors described is extensive; however, as is the nature of list-making, there are omissions. There are endless opportunities for optical fibre sensing and the continual introduction of new materials and technologies make this an exciting and forward looking area of research and development.

1.2 Classification of Optical Fibre Sensors

Glass optical fibre (GOF) sensor technology is well established, the development of plastic optical fibre (POF) sensors is now emerging at a pace. Sensors using classical, commercial undoped or unmodified step-index polymethylmethacrylate (PMMA) optical fibres are based on ideas already used in silica glass sensors, but with the advantages of large core size, large numerical aperture, flexibility, ruggedness, ease of termination, coupling and lower cost. POF is now widely used in multimode intensity-based sensor applications. The high attenuation involved limit sensor length to tens of metres and the lower melt temperature of 80°C dictate areas of application. Within these parameters, however, POF sensors challenge corresponding GOF with their significantly lower costing systems.[9,1011,12,13,14,15] The optical fibre sensor developed by this project was an evanescent field modulated 1mm diameter intrinsic evanescent field POF sensor, and as such there will be a greater emphasis in their description.

1.2.1 Classification of Sensor by Application

Optical Fibre sensors may be classified by their application:

- Physical sensors: used to measure physical properties such as temperature, stress, pressure, displacement.
- Chemical sensors: used for pH measurement, gas analysis, spectroscopic studies, chemical coatings which react with analyte to produce optical changes.
- Bio-medical sensors: used in bio-medical applications such as measurement of blood flow, glucose content, in vivo applications.

Physical Sensors

Any changes in the orientation of an optical fibre will change the geometry or alignment of the fibre results in a change in the incident angle of the light rays travelling within. This modulates the signal from that point. Optical fibre is extremely sensitive to changes and will detect anything from very small perturbations, micro bending to catastrophic episodes.

Ioannides et al[16,17,18] developed a plastic optical fibre linear displacement sensor; a central fibre emits light that is reflected from a mirror surface that is captured by two outer fibres, has accuracy, resolution and stability better than 1%. Measurement of the frequency of large amplitude vibrating surfaces has also been demonstrated with this sensor.[19] This has been realised mainly due to the high numerical aperture (NA), section 2.3, of plastic optical fibre and its large core size. Various arrangements of the sensor measure wind speed and direction,[20] temperature,[21,22,23] changes in liquid level[24,25] and pressure.[26] The sensor was also used to monitor the reflectivity of a mirror surface as a function of condensation.[27] Other physical sensors monitor vibration[28] strain[29] and structural health.[30,31,32] POF may be further sensitised with the addition of

grooves[33] or the by regular changes of refractive index along its length producing Fibre Bragg Grating (FBG) in single mode optical fibre (single mode POF is not commercially available) which reflects some wavelengths and transmits others and Long Period Fibre Gratings (LPFG) which do not produce reflected light but serve as spectrally selective absorber.

Chemical and Bio-sensors[34]

Due to the low fabrication temperatures of POF, chromophores (organic dyes) may be included in the core or cladding of the fibres. Various types of radiation excite chromophores in the fibre, which then re-emit the radiation at altered wavelengths. Detection and measurement of the altered wavelength, decay time and intensity of the re-emitted wavelengths can then be related to various measurand. Such sensors may be used to measure humidity,[35,26] fluorescence,[36] toxicity and turbidity.[37] More recent work has a version of this sensor which measures the presence of oxygen and its effects.[38]

The cladding and ends of POF can be coated with a chemically sensitive optical coating by various methods: dip-coating using sol-gel technology, chemical vapour deposition (CVD), spray pyrolysis, physical vapour deposition (PVD), magnetron sputtering, nanobelts and tubes,[39] quantum dots.[40]

Requirements for medical sensors[41] centre on their physical size. They must be non-toxic and small enough to fit into arteries to measure pH, PCO_2, PO_2, electrolytes, enzymes, drugs, temperature, pressure and flow.[42,34] PMMA is clinically inert and so is ideal for clinical applications, it is used in the manufacture of rigid contact lenses and lens implants. PMMA is flexible compared with silica: large diameter POF can be used to carry light, bent through tighter diameters than GOF without breaking into dangerous shards, and the low cost of POF are all very important features. A huge market

potential for POF medical and bio sensors was estimated. Progress has not matched expectations; however sensors capable of the measurement of gastric fluid in a stomach, measurement of oxygen concentration in blood in vivo, measurement of respiratory chest movements or limbs in connection with a magnetic resonance scanner are a few current of such sensors.[43,44,45]

1.2.2 Classification of Sensor by Modulation Method

Optical fibre sensors are also classed by the modulation and demodulation method of a signal. As the detection of phase or frequency involves interferometric techniques, these are also called interferometric sensors. Fibre optic interferometric (FOI) sensor require single mode optical fibre, which is not commercially available in POF, however the various methods are described for completeness.

Polarisation Modulating Optical Fibre Sensing

The polarisation of light in an optical fibre can be affected by magnetic fields, pressure, temperature fluctuations which produce birefringence in the fibre causing rotation of the plane of polarised light proportional to the changes, the amount of rotational displacement that the field has undergone may be analysed to give magnitude of these changes. Optical arrangements lead to an extraction of the parameter of interest from the amount of field rotation, which is mapped into an intensity variation.[46]

Phase Modulating Interferometric Optical Fibre Sensing

These are usually based on single mode fibres which until recently was not available in POF.[47] The change in the phase of light launched into an optical fibre may be measured and interrogated. These are very minute changes and require sensitive and complex

optical arrangements. This method usually involves the splitting of a signal and measuring the delay between a reference signal that is isolated and the sensing signal that interacts with a measurand.[46] The arrival of the two signals in phase and same polarisation would result in a maximum output signal due to positive interference, as would a signal that was multiples of 360° phases, a limiting factor of this method. The output signal strength would diminish as the phase and polarisation become more out of step.

Changes in the phase of light may be affected by changes in pressure which alter the refractive index of the fibre which in turn changes the polarisation of the light.

FOI sensors are themselves categorised by the number of beams interrogated. Two beam interferometer configurations are the Michelson, Sagnac fibre-optic gyroscope[48,49,50] and the Mach-Zehnder. Optical fibre Fabry-Pérot interferometric (FFPI) sensors are multiple beam interferometer, they are of a much simpler configuration and offer high measurement sensitivity.

Frequency and Wavelength Varying Sensors

These sensors work by mapping a variation frequency[51,52] or wavelength[53] modulation of the optical field; analogous to FM vs. AM radio. In telecommunication, FM provides a larger signal dynamic range and better signal fidelity, with less sensitivity to amplitude variations, than does AM, however there is increased receiver complexity and tighter operating tolerances on the transmitter components. The change in spectral power distribution of the light source by modulation and the wavelength is referenced with use of either a spectrometer, a two wavelength detector or two detectors with filters.

Distributed and Multiplexed Sensors

Distributed sensors are able to sense changes at many points along a single fibre, using multiplexing techniques to interrogate output signals.[54]

Intrinsic Distributed Fibre Optic Sensors monitor a single measurand over a large number of points along a fibre or continuously over a long length of fibre. There are two types, one dependant upon frequency, Optical Frequency-Domain Reflectometry, and the other upon time, Optical Time-Domain Reflectometry (OTDR) which are further classified by the attenuation method: Rayleigh Scattering, Raman Scattering and Brillouin Scattering.[46]

Multiplexed sensing: the individual outputs from a network of sensors is multiplexed: *time division multiplexing (TDM)* measures the time delay between input and output pulse from individual sensors for measurement parameters such as strain, temperature and others that alter the length of the optical fibre sensor, hence the distance that the pulse travels, hence the time taken to travel that distance.

Wavelength division multiplexing (WDM) enables a series of sensors serviced by a single optical fibre. A broadband light source, such as light emitting diodes, LEDs, is coupled into a single optical fibre that illuminates a series of sensors that operate at different wavelength bands, their attenuated signals are returned along a single optical fibre and are separated out using gratings or prisms onto separate detectors.

Quasi-distributed Fibre Optic Sensors is where the measurand is measured at specific irregular points along a fibre. The sensing mechanism may be intrinsic or extrinsic. FBGs[55,56] along a length of a fibre is desirable to achieve a compact and cost effective quasi-distributed fibre optic sensor, over 100 wavelength bands may be utilised using WDM combined with TDM, in effect each acting as an individual sensor.

Amplitude and Intensity Based Sensors

By far the easiest and cheapest mechanisms to affect and detect is amplitude or intensity modulating sensor as it does not require the sophistication and expense required for tracking the frequency or phase of an optical field[46] which require single mode fibres.

There are numerous ways in which the intensity of the output signal is attenuated

The intensity of the output signal may be attenuated by physical or chemical means:

- The intensity of the output signal can be modified due to bending of the fibre, thus altering the incident ray angle and therefore the amount of light coupled into the cladding. This can be long length deflections or microbending to measure strain, pressure, force and position.
- The interrogating light is attenuated by the presence of a measurand, this can be either extrinsic or intrinsic

Parameters that may be measured include: deflection, bending, strain, microbending, chemical population due to reaction with reagents coating the sensor, refractive index changes due to biofilm growth, curing of epoxies, they are innumerable and are only limited by the imagination.

1.2.3 Classification of Sensors by Extrinsic or Intrinsic Modulation

Extrinsic optical sensors allow light from an optical fibre to leave the fibre core, interact with a measurand and then the resulting light is coupled into another optical fibre for detection. Intrinsic sensors are fibres which have a sensitised region along its length. Light is coupled into the sensor, a portion of which interacts with a measurand, the remaining continues along the fibre for detection.

The optical fibres of extrinsic sensors act as transmit/receive light conduit with signal modulation occurring outside of the fibre as shown in figure 1.1. A property of the measurand, such as its refractive index, its colour, particle density or a change in the alignment of the fibres, changes the characteristics of the interrogating light. The attenuated light is detected by the second fibre and is interrogated to reveal these changes.[46] Extrinsic sensors are easier to use, they are more easily multiplexed and are subject to interference into and out of the light modulator and contamination of optical surfaces. They are also sensitive to vibrations and are highly attenuated due to light losses at the coupling of light in and out of the fibre nature of its operation. Polarisation preserving optical fibre and low birefringence fibres enable polarisation to be present and single mode enable phase interference.

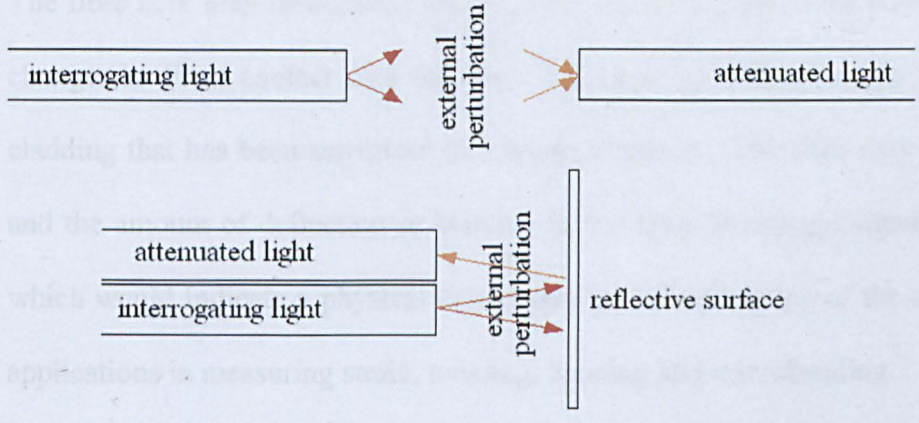

Figure 1.1 Extrinsic optical fibre pressure sensors: light leaves optical fibre, modified light is detected by fibre.

The optical fibres of intrinsic sensors have a sensitised region along its length. Light does not leave the fibre, but is coupled into the sensor, a portion of which interacts with a measurand, the remaining continues along the fibre for detection. Intrinsic sensors, figure 1.2 are more difficult to shield from unwanted external perturbations, they are "all fibre" thereby reducing or eliminating the sensing region connector problems of extrinsic sensors, less attenuating due to light not leaving fibre for modulation.

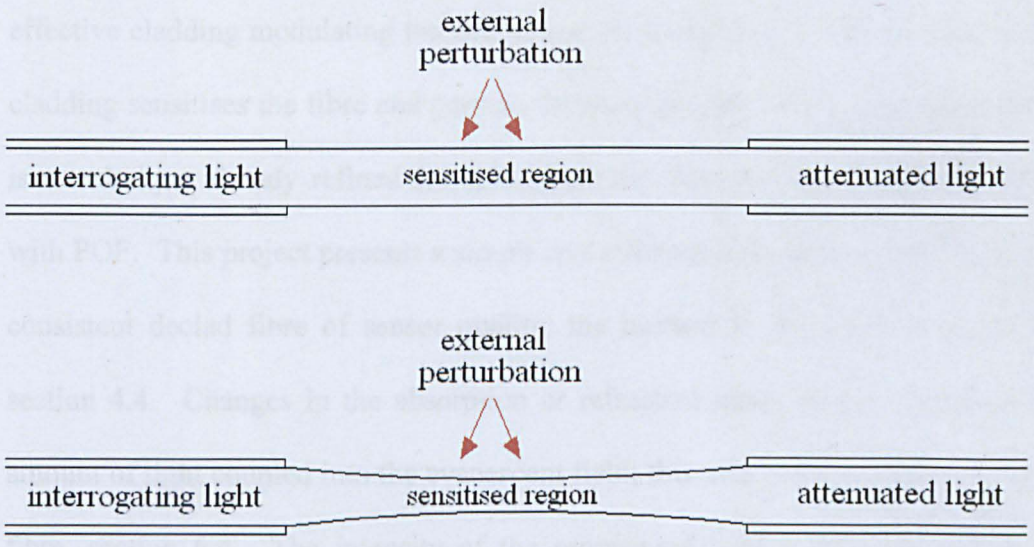

Figure 1.2 Intrinsic optical fibre sensor: light within the fibre itself undergoes modulation *above*: declad fibre core *below*: tapered fibre core.

The fibre core may be exposed and the light signal is affected by chemical or physical changes in direct contact with the core. The exposed fibre core may be coated with a cladding that has been sensitised to a target chemical. The fibre may be left unaltered and the amount of deflection or bending in the fibre affects the signal within the core which would indicate a physical disturbance to the orientation of the optical fibre with applications in measuring strain, twisting, bending and microbending.

Evanescent Wave Sensors

At every reflection of light along an optical fibre length a very small fraction of that light is refracted into the cladding. The light beyond the core is called the evanescent field more details of which may be found in section 2.5 of this thesis.

The sensor developed by this project is an intensity modulated, intrinsic evanescent field biosensor and a thorough description of the sensor may be found in chapter five. The intensity of the light in the fibre core is modulated by changes in its effective cladding modulating the evanescent field, figure 1.3. The removal of the fibre cladding sensitises the fibre and permits the manipulation of the evanescent field. This is a technique already refined for silica fibre and has now been successfully adopted with POF. This project presents a simple and efficient chemical method[57] that produces consistent declad fibre of sensor quality, the method is discussed in more detail in section 4.4. Changes in the absorption or refractive index of the cladding affect the amount of light coupled into the evanescent field; this affects the intensity of light in the fibre, section 6.4. The intensity of the propagated light is modulated due to these changes at the core/cladding interface. The measurand is in intimate contact with an exposed fibre core acting as the cladding. The larger core diameter and NA of POF leads to an evanescent field that is greater than the usual 200μm silica fibre sensors.[58] A fibre with a tapered region has a greater evanescent field at the taper region for sensing purposes[59] as shown in figure 1.3.

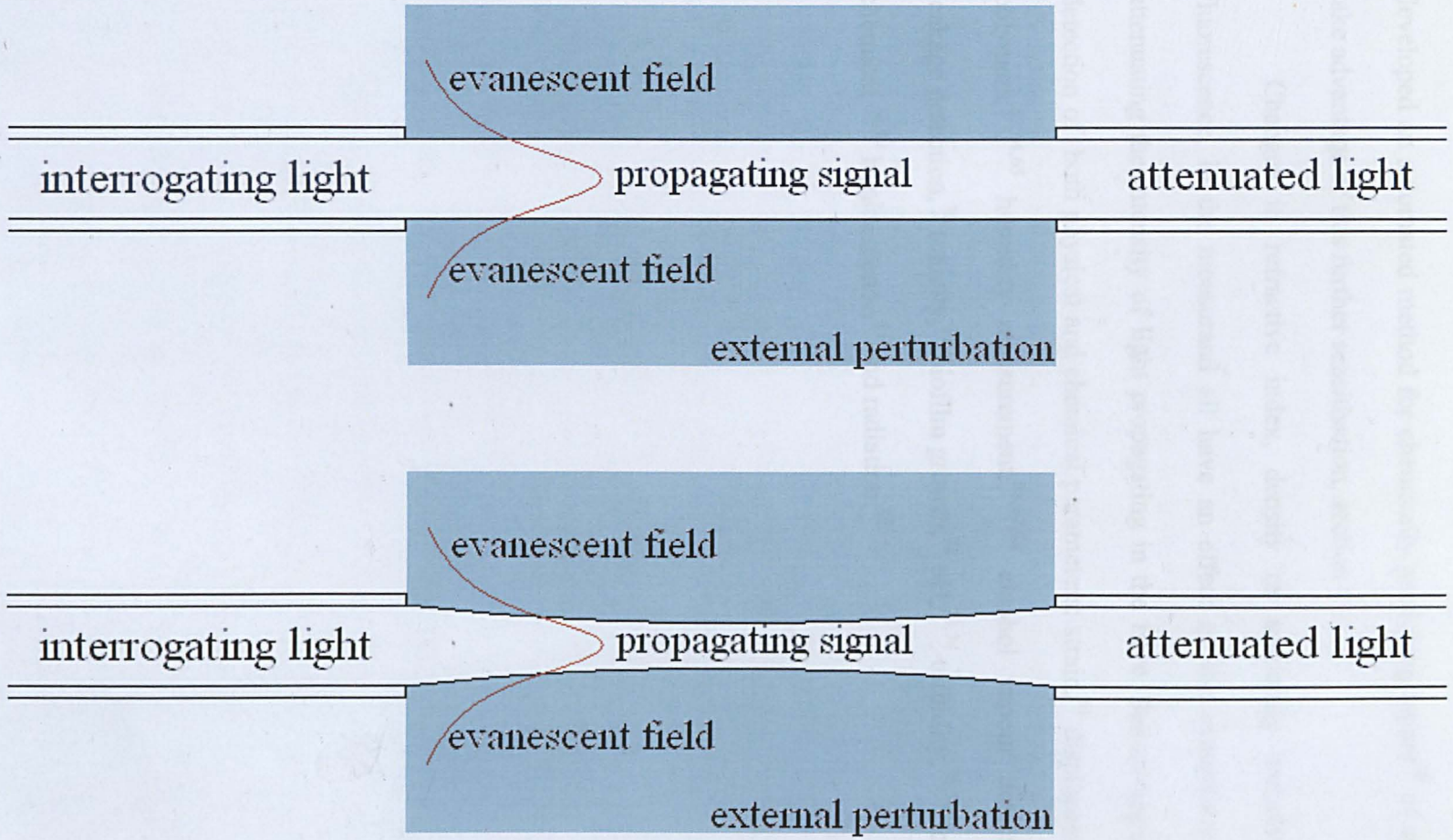

Figure 1.3 A single mode evanescent field sensor above: declad fibre core below: tapered fibre core note the increased proportion of light in the evanescent field. 1mm diameter POF sensor has 10^5 modes

This project produced chemically tapered fibres[57] and the author of this thesis has developed an automated method for chemically producing tapers[60] of sensor quality to take advantage of this further sensitisation, section 4.5.

Changes in refractive index, density of scattering particles, colour, and fluorescence, in the measurand all have an effect on the evanescent field strength, attenuating the intensity of light propagating in the fibre. Sensor applications include detection of both physical and chemical parameters: strain,[61] displacement,[62] curing of polymers,[63,64,65] humidity measurement,[66,67,68] alcohol vapour detection,[69] gasoline leakage detection,[70] toxicity,[71] biofilm growth,[72] pH,[73,74] turbidity,[75,76] scaling,[77] gas,[78,79] chemical,[76,80] luminescence,[81] and radiation.[82]

1.3 Summary

Optical fibre sensors have been categorised according to their application, modulation method and whether that modulation is extrinsic or intrinsic. This is by no means a comprehensive list, but gives an overview of the technologies available and show that the parameters that may be detected are only restricted by our own imagination. This is a fairly new science and there is a huge scope for great advances to be made. Special emphasis has been put on intrinsic evanescent field sensors in this thesis as these are the type developed by this project for detecting biofilm growth.

POF sensors have the advantage over GOF sensors due to their high fracture toughness, relative flexibility in bending - tighter bend radius without damaging the operation of the fibre, durability in harsh chemical and environmental conditions, high elastic strain limit,[83,84,85] large core size, large NA, ease of non-skilled handling - easier to cleave and couple, ruggedness, safe disposability and lower cost.

Evanescent field sensing presents itself as the most suitable method for the sensing the early onset of biofilm growth as:

- scattering due to particulates and spectral identity and refractive index changes, and at the core/cladding interface dictate the extent of the evanescent field.
- the resulting intensity due to these changes is simple to detect and monitor.
- the refractive index of biofilm changes as it attaches and increases in thickness, and often includes particulates in its matrix.[86]
- the biofilm measured has spectral markers.

The use of large diameter multimode POF has in its favour:

- a large NA, resulting in more of the lossy modes propagating along the fibre, increasing the proportion of light coupled into the evanescent field for sensing purposes, section 2.4

- 10 times more sensitive to evanescent field than 200μm PCS silica fibre.[86]
- large angle of curvature, facilitates microbial attachment
- the process of decladding gives a keyed surface which also facilitates microbial attachment
- sensitisation of POF is easy to perform
- easy to handle
- rugged.

New structures of optical fibres are constantly being introduced with new sensing opportunities presented. FBG consists of short segments of optical fibre that have grating written[87] into them which reflect only particular wavelengths of light and transmits all others. LPFG[88] do not produce reflected light but selectively absorbs spectra. Cladding technology is making advances, most recent and exciting are the advances made in nano-structures. Microstructured POF, mPOF aka 'holey fibres' are the most recent and exciting introduction and bring with them endless possibilities for sensing[89] all of which make this an exciting and forward looking area of research and development.

References

[1] DA Kronh, "Optical Fibre Sensors" Instrument Society of America, 2nd edition., 1991

[2] U Steiger, "Sensor Properties and Applications of POF", Proceedings of the Seventh International Conference on Plastic Optical Fibres and Applications – POF'98, Berlin (Germany), pp171-177, 1998

[3] D.Hogg, R Turner, R Measures, "Polarimetric fibre optic structural strain sensor characterization," Proc SPIE, vol.1170, pp542-550, 1990

[4] RM Measures, AT Alavie, R Maaskant, M Ohn, R Lee, S Karr, T Coroy, S Huang, "Smart structure interface issues and their resolution: Bragg grating laser sensor and the optical synapse," Proc SPIE, vol.1918, 1993

[5] J Dunphy, G Meltz, W Morey, "Optical fibre Bragg grating sensors: A candidate for smart structure applications," Ch. 10 in Fibre Optic Smart Structures, Ed. E Udd, John Wiley; 1995

[6] E. Udd, "Fibre Optic Sensors for Scientists and Engineers", Wiley, 1993

[7] T Vais, D Hogg, R Measures. "Composite material embedded fibre optic Fabry-Perot strain gauge." Proc SPIE, vol.1370, pp154-161, 1991 J Blake, S Huang, B Kim, "Elliptical core two-mode fibre strain gauge," Proc SPIE, vol.838, p332, 1987

[8] J Blake, S Huang, B Kim, "Elliptical core two-mode fibre strain gauge," Proc SPIE, vol.838, p332, 1987

[9] E Udd, Fibre Optic Sensors, Wiley, 1991; D. Kalymnios, "Plastic Optical Fibres (POF) – Characteristics, Metrology and Applications", NATO ASI Series, E285, Ch.45, pp747-770, 1994

[10] D Kalymnios, PJ Scully, J Zubia, H Poisel, "POF Sensor Overview", Proceedings of the Thirteenth Plastic Optical Fibres Conference, pp237-244, 2004

[11] B Gholamzadeh, H Nabovati, "Fiber Optic Sensors", Proceedings of World Academy of Science, Engineering and Technology vol.32, 2008

[12] D Kalymnios, "Plastic Optical Fibres (POF) in Sensing – Current Status and Prospects", invited paper at the 17th International conference on optical fibre sensors. Proceedings of SPIE vol.5855

[13] RJ Bartlett, R Philip-Chandy, P Eldridge, DF Merchant, R Morgan, PJ Scully, "Plastic Optical Fibre Sensors and Devices", Transactions of the institute of Measurement and Control, vol.22, No.5, pp431-457, 2000

[14] B Lee "Review of the present status of optical fiber sensors", Optical Fiber Technology 9 pp57–79; 2003

[15] J Kruszewski, M Borecki, M Beblowska, "Plastic optical fibers in sensors - a review", Proceedings of SPIE vol.5576, pp234–238, 2004

[16] N Ioannides, D Kalymnios, I Rogers, " An Optimised Plastic Optical Fibre (POF) Displacement Sensor", Proceedings of the Fifth International Conference on Plastic Optical Fibres and Applications-POF'96, pp251-255, 1996

[17] N Ioannides, D Kalymnios, IW Rogers, "A POF-based Displacement Sensor for use over Long Ranges", Proceedings of the Fourth International Conference on Plastic Optical Fibres and Applications – POF'95, pp157-161, 1995

[18] D Kalymnios, "Linear and Scalable Optical Sensing Technique for Displacement Sensors VI, Technology Systems and Applications, IOP Publishing Ltd., pp291-293, 1993

[19] N Ioannides, D Kalymnios "A Plastic Fibre (POF) Vibration Sensor", Proceedings of the Applied Optics Divisional Conference of the IOP, Brighton, UK, pp163-168, 1998

[20] J Zubia, O Aresti, J Arrue, J Miskowicz, ML Amo, "Barrier Sensor Based on Plastic Optical Fibre to Determine the Wind Speed at a Wind Generator", IEEE Selected Topics in Quantum Electronics, vol.6, No.5, pp73-779, 2000

[21] MN Alahbabi, YT Cho, TP Newson, " 100km Distributed Temperature Sensor Based on Coherent Detection of Spontaneous Brillouin Backscatter", Measurement Science & Technology vol.15, No.8, pp1544-1547, 2004

[22] E Ito, J Muramatu, T Kanazawa, E Nihei, KY Kioke, U Yagi, T Sobukawa, K Takada, "Plastic Optical Fibre Thermosensor", Proceedings of the Third International Conference on Plastic Optical Fibres and Applications-POF'94, pp52-55, 1994

[23] M McSherry, C Fitzpatrick, E Lewis, S Wylie, C Wright, A Al-Shamma'a, J Lucas, " Development of an Extrinsic Optical Fibre Temperature Sensor for Monitoring Liquid Temperature in Harsh Industrial Environments", Journal of Optics A – Pure and Applied Optics, vol.7, No.6, pp331-339, 2005

[24] JD Weiss, "The Pressure Approach to Fibre Liquid Level Sensors". Proceedings of the Fourth International Conference on Plastic Optical Fibres and Applications-POF'95, pp167-170, 1995

[25] S Vargas, C Vászques, AB Gonzalo, JMA Pena, "A Plastic Fibre-Optic Liquid Level Sensor", Proceedings of the Second European Workshop on Optical Fibre Sensors, SPIE vol.5502, pp148-151, 2004

[26] KF Klein, H Poisel, D Kalymnios, "Fluorescent Polymer Optical Fibres for New Applications", Proceedings SPIE vol.5131 pp205-212, 2003
[27] S Hadjiloucas, S Karatzas, DA Keating, MJ Usher, "Optical Sensors for Monitoring Water Uptake in Plants", Journal of Lightwave Technology, vol.13, No.7, pp1421-1428, 1995
[28] TK Gangopadhyay, S Chakravorti, K Bhattacharya, S Chatterjee, " Wavelet Analysis of Optical Signal Extracted from a Non-contact Fibre-optic Vibration Sensor using and Extrinsic Fabry-Perot Interferometer", Measurement Science & Technology, vol.16, No.5, pp1075-1082, 2005
[29] A Minardo, R Bernini, L Zeni, L Thevenaz, F Briffod, " A Reconstruction Technique for Long-range Stimulated Brillouin Scattering Distributed Fibre-Optic Sensors: Experimental Results", Meas. Sci. & Tech., vol. 16, 4, pp900-908, 2005
[30] G Kister, D Winter, J Tetlow, R Barnes, G Mays, GF Fernando, " Structural Integrity of Reinforced Concrete Structures. Part 1: Evaluation of Protection Systems for Extrinsic Fibre Fabry-Perot Sensors", Engineering Structures, vol.27, No.3, pp411-419, 2005
[31] KSC Kuang, ST Quek, M Maalej, " Assessment of an Extrinsic Polymer-based Optical Fibre Sensor for Structural Health Monitoring", Measurement Science & Technology, vol.15, No.10, pp2133-2141, 2004
[32] W Baker, I Mckenzie, R Jones, " Development of Life Extension Strategies for Australian Military Aircraft, using Structural Health Monitoring of Composite Repairs and Joints", Composite Structures, vol. 66, No.1-4, pp133-143, 2004
[33] R Philip-Chandy, P J Scully, R Morgan, "The design, development and performance characteristics of a fibre optic drag-force flow sensor" , Meas. Sci. Technol. vol.11, pp31–35, 2000
[34] ME Bosch, AJR Sánchez, FS Rojas, CB Ojeda, "Recent Development in Optical Fiber Biosensors", Sensors, vol.7, pp797-859, 2007
[35] S Muto, H Sato, T Hossaka, "Fluorescent POF Humidity Sensor: Theoretical and Experimental Analyses", Proceedings of the Third International Conference on Plastic Optical Fibres and Applications-POF'94, pp46-48, 1994
[36] KF Klein, H Poisel, D Kalymnios, "Fluorescent Polymer Optical Fibres for New Applications", Proceedings SPIE vol.5131, pp205-212, 2003
[37] R Philip-Chandy, PJ Scully, C Whitworth, "Integrated, Multi-angle, Low Turbidity Measurement using Fluorescent Plastic Optical Fibre", OFS2000, 14th International Conference on Optical Fibre Sensors, 2000
[38] H Hecht, M Kolling, "A Low Cost Optode-array Measuring System Based on a 1mm Plastic Optical Fibres – New Technique for In-situ Detection and Quantification of Pyrite Weathering Processes", Sensors and Actuators B vol.81, pp 76-82, 2001
[39] A Bismuto, S Lettieri, PMaddalena, C Baratto, E Comini, G Faglia, G Sberveglieri and L Zanotti, "Room-Temperature Gas Sensing Based on Visible Photoluminescence Properties of Metal Oxide Nanobelts", J. Opt. A: Pure Appl. Opt. vol.8, pp585–588, 2006
[40] PAS Jorge, M Mayeh, R Benrashid, P Caldas, JL Santos, F Farahi, "Applications of quantum dots in optical fiber luminescent oxygen sensors", APPLIED OPTICS vol.45, No.6, pp3760 3767, 2006
[41] AG Mignani, F Baldini "Fibre-optic sensors in health care" Phys. Med. Biol. vol.42, pp967–979, 1997
[42] NB Kosa, "Key Issues in Selecting Plastic Optical Fibres used in Novel Medical Sensors", SPIE, vol.1592, pp114-121, 1991
[43] PJ Scully, R Holmes, GR Jones, "Optical Fibre-based Goniometer for Sensing Patient Position and Movement Within a Magnetic Resonance Scanner Using Chromatic Modulation", Journal of Medical Engineering and Technology, vol.17, No.1, pp1-8, 1993
[44] F Baldini, "In Vivo Monitoring of the Gastrooesophageal System using Optical Fibre Sensors", Analytical and Bioanalytical Chemistry, vol.375, No.6, pp723-743, 2003
[45] F Baldini, S Bracci, P Bechi, "Plastic Optical Fibres for the Detection of pH in the Foregut", Proceedings of the Fifth International Conference on Plastic Optical Fibres and Applications-POF'96, pp238-243, 1996
[46] F Yu, S Yin, "Fiber Optic Sensors" Marcel-Dekker, CRC Press2002
[47] Z Li, H Ma, Q Zhang, H Ming, "Birefringence Grating Within a Single Mode Polymer Optical Fibre with Photosensitive Core of Azobenzene Copolymer", Journal of Optoelectronics and Advanced Materials, vol.7, No.2, pp1039 -1046, 2005
[48] H Lefevre, "The Fiber Optic Gyroscope", Artech, Norwood, 1993
[49] RB Smith, Editor, "Selected Papers on Fiber Optic Byroscopes", SPIE Milestone Series, 1989
[50] WK Burns, Editor, "Optical Fiber Rotation Sensing, Academic Press, San Diego, 1994

[51] SR Kidd, PG Sinha, JS Barton, JDC Jones, "Interferometric Fiber Sensor for Measurement of Surface Heat-transfer Rates on Turbine-Blades", Optics and Lasers in Engineering, vol.16, No 2-3, pp207–221, 1992
[52] AJ Coleman, E Draguioti, R Tiptaf, N Shotri, JE Saunders, "Acoustic Performance and Clinical Use of a Fibreoptic Hydrophone", Ultrasound in Medicine and Biology, vol.24, No.1, pp 143 – 151, 1998
[53] A Michie, I Bassett, J Haywood, "A Low Coherence Interferometric Sensing Method with Analysis and Experimental Results for Voltage Sensing", Proc. SPIE, vol.5855, pp206-209, 2005
[54] C Saunders and P J Scully, "Sensing applications for POF and hybrid fibres using a photon counting OTDR", Meas. Sci. Technol. Vol.18, pp615–622, 2007
[55] CM Davis, EF Carome, MH Weik, S Ezekiel, RE Einzig, "Fibre Optic Sensors Technology Handbook", Optical Technologies – a Division of Dynamic System Inc, Virginia
[56] JR Casas, PJS Cruz, M Asce, "Fiber Optic Sensors for Bridge Monitoring", Journal of Bridge Engineering", pp262 - 373, 2003
[57] DF Merchant, PJ Scully, NF Schmitt, "Chemical Tapering of Polymer Optical Fibre", Sensors and Actuators, vol.76, pp365-371, 1999
[58] ZH Zhang, E Lewis, PJ Scully, "An Optical Fibre Sensor for Particle Concentration Measurement in Water Systems Based on Inter-fibre Light Coupling Between Polymer Optical Fibres", Transactions of the Institute of Measurement and Control vol.22, No.5, pp413-430, 2000
[59] AW Snyder, JD Love, "Optical Waveguide Theory" Ch.5, Chapman and Hall
[60] YM Wong, PJ Scully, R Bartlett, V Alexiou, HJ Kadim, "Automation and Characterisation of Chemical Tapering of Plastic Optical Fibres", Sensors and Their Applications XI, pp203-208, 2001
[61] KSC Kuang, WJ Cantwell, PJ Scully, "An Evaluation of a Novel Plastic Optical Fibre Sensor for Axial Strain and Bend Measurements", Measurement Science and Technology, vol.13, pp1523-1534, 2002
[62] VPN Nampoori, ST Lee, CPG Vallabhan, P Radharishnan, "Macro Bending in Fibre Optic Interferometer Sensor for Displacement and Weight Measurement", SPIE Conference in Transducing Materials and Devices, Brugge, Belgium, 2002
[63] E Chailleux, M Salvia, N Jaffrezic-Renault, V Matejec, I Kasik, "In-situ Study of the Epoxy Cure Process using a Fibre-optic Sensor", Smart Materials and Structures, vol.10, pp194-202, 2001
[64] GR Powell, PA Crosby, DN Waters, CM France, RC Spooncer, GF Fernando, "In-situ Cure Monitoring Using Optical Fibre Sensors – a Comparative Study", Smart Materials and Structures vol.7, pp577-568, 1998
[65] F Fouchal, JAG Knight, PM Dickens, "Monitoring the Polymerisation of a Diglycidyl Ether Bisphenol-A/2.2 '-dimethyly-4,4 '- Methylenebis (cyclohexylamine) Matrix with a Fourier Transform Infrared Optical Fibre Sensor", Proceedings of the Institution of Mechanical Engineers Part L – Journal of Materials – Design and Applications, vol.218, L4, pp331-342, 2004
[66] S Muto, O Susuki, T Amano, M Morisawa, "A Plastic Optical Fibres Sensor for Real-time Humidity Monitoring" Measurement Science and Technology, vol.14, pp746-750, 2003
[67] M Morisawa, Y Amemiya, H Kohzu, CX Liang, S Muto, "Plastic Optical Fibre Sensor for Detecting Vapour Phase Alcohol", Measurement Science and Technology, vol.12, pp877-881, 2001
[68] D King, WB Lyons, C Flanagan, E Lewis, "A Multipoint Optical Fibre Sensor System for use in Process Water Systems Based on Artificial Neural Network Pattern Recognition Techniques", Sensors and Actuators A – Physical vol.115, 2-3, pp293-302, 2004
[69] M Morisawa, Y Amemiya, H Kohzu, CX Liang and S Muto, "Plastic Optical Fibre Sensor for Detecting Vapour Phase Alcohol", Measurement Science and Technology vol.12 pp877- 881, 2001
[70] M Morisawa, K Uchiyama, G Vishnoi, S Muto, "Improvement of Sensitivity in Plastic Optical Fibre Gasoline Leakage Sensors", SPIE vol. 3540, pp175-182, 1998
[71] D Merchant, PJ Scully, R Edwards, J Grabowski, "Optical Fibre Fluorescence and Toxicity Sensor", Sensors and Actuators 76, pp365-371, 1998
[72] YM Wong, PJ Scully, RJ Bartlett, KSC Kuang, WJ Cantwell, "Plastic Optical Fibre Sensors for Environmental Monitoring: Biofouling and Strain Applications", Strain, vol.39, No.3, pp115-119, 2003
[73] BJ Deboux, E Lewis, PJ Scully, R Edwards, "A Novel Technique for Optical Fibre pH Sensing Based on Methylene Blue Adsorption", Journal of Lightwave Technology vol.3, pp1407-1212, 1995
[74] S Navneet, BD Gupta, "Fabrication and Characterisation of a Fibre-optic pH Sensor for the pH Range 2 to 13", Fibre and Integrated Optics, vol.23, No4, pp327-335, 2004
[75] FH Zhang, PJ Scully, E Lewis, "A Novel Optical Fibre Sensor for Turbidity Measurement", Applied Optics and Optoelectronics, pp 370-373, 1996
[76] WB Lyons, H Ewald, C Flanagan, E Lewis, " A Multi-point Optical Fibre Sensor for Condition Monitoring in Process Water Systems Based on Pattern Recognition", Measurement, vol.34, No.4 pp301-312, 2003

[77] R Philip-Chandy, PJ Scully, D Thomas, "A Novel technique for Novel On-line Measurement of Scaling using a Multimode Optical Fibre Sensor for Industrial Applications", Sensors and Actuators B, vol.71, pp19-23, 2000

[78] C Bariain, IR Matias, C Fdez-Valdivielso, CElosua, A Luquin, J Garrido, M Laguna, "Optical Fibre Sensors Based on Vapochromic Gold Complexes for Environmental Applications", Sensors & Actuators B – Chemical, vol.108, iss 1-2, pp535-541, 2005

[79] M Benounis, N Jaffrezic-Renault, JP Dutasta, K Cherif, A Abdelghani, "Study of a New Evanescent Wave Optical Fibre Sensor for Methane Detection Based on Cryptophane Molecules", Sensors & Actuators B – Chemical, vol.107, No.1, pp32-39, 2005

[80] WB Lyons, H Ewald, C Flanagan, E Lewis, " A Multi-point Optical Fibre Sensor for Condition Monitoring in Process Water Systems Based on Pattern Recognition", Measurement, vol.34, No.4 pp301-312, 2003

[81] WB Lyons, C Fitzpatrick, C Flanagan, E Lewis, "A Novel Multipoint Luminescent Coated Ultra Violet Fibre Sensor Utilising Artificial Neural Network Pattern Recognition Techniques", Sensors and Actuators A – Physical, vol.15, 2-3, pp267-272, 2004

[82] E Takada, D Yamada, H Kuroda, "A New Optical Fibre Sensor for Multipoint Radiation Measurement with Sensing Regions in its Cladding", Measurement Science & Technology, vol.15, No.8, pp1479-1483, 2004

[83] KSC Kuang, WJ Cantwell, PJ Scully, "An Evaluation of a Novel Plastic Optical Fibre Sensor for Axial Strain and Bend Measurements", Measurement Science and Technology, vol.13, pp1523-1534, 2002

[84] KSC Kuang, Akmaluddin, WJ Cantwell, C Thomas, "Crack Detection and Vertical Deflection Monitoring in Concrete Beams Using Plastic Optical Fibre Sensors", Measurement Science and Technology, vol.14 pp 205–206, 2003

[85] KSC Kuang, WJ Cantwell, "Plastic Optical Fibre and Shape Memory Alloy for Damage Assessment and Damping Enhancement of Composite Materials", Measurement Science and Technology, vol.14, pp1305–1313, 2003

[86] R Philip-Chandy, PJ Scully, P Eldridge, HJ Kadim, MG Grapin, MG Jonca, MG D'Ambrosio, F Colin, "An Optical Fiber Sensor for Biofilm Measurement Using Intensity Modulation and Image Analysis", IEEE Journal on Selected Topics in Quantum Electronics, vol.6, No.5, pp764-772, 2000

[87] KO Hill, "Photosensitivity in Optical Fiber Waveguides: Application to Reflection Fiber Fabrication", Appl. Phys. Lett. Vol.32, p647

[88] AM Vengsarkar, PJ Lemaire, JB Judkins, V Bhatia, JE Sipe, T Erdogan, "Long Period Fiber Gratings as Band-rejection Filters", OFC'95, PD4-2, 1995

[89] MCJ Large, F Cox, A Arygros, R Lwin, G Barton, MA van Eijkelenborg, S Manos, L Poladian, A Bachmann, H Poisel, "Microstructured POF and Applications" Proceedings of the 12th International Plastic Optical Fibers Conference 2005

CHAPTER TWO

Optical Fibres

2.1 Introduction

This chapter is vital to the understanding of the operation and mechanism of the sensor developed in this project. The different characteristics of readily available telecommunications optical fibre are discussed to inform the choice of optical fibre in order to design a device with optimum performance. The fibre must be least attenuating in the operational wavelengths of the signal light source launched into it to maximise the available light for the measurand to interact with. Losses due to termination and connections must be within acceptable functional limits. Guiding of light rays and the

modes in which they propagate along a length of fibre are described together with dependence upon fibre geometry and material of both core and cladding.

The explanations of evanescent fields and tunnelling rays are given in detail as these are fundamental to the operation of the sensor developed in this project. Evanescent field modulation is described; the evidence for increased penetration depth of tunnelling rays in POF is described, which justifies the use of large diameter POF[1].

Most GOF sensors operating within the operational limitations of POF may be realised with POF with the advantage of lower cost. Most importantly previous research has demonstrated that POF evanescent wave (EW), sensors based on multimode large diameter fibre are an order of magnitude more sensitive than multimode GOF EW sensors and can sense parameters such as refractive index, strain, turbidity, scaling, fouling and flow. For weakly guiding multimode fibre such as 200μm diameter PCS fibre the proportion of light available in the evanescent field is less than 1%, this can be maximised by exciting higher order modes to optimise penetration depth to increase the sensitivity of the sensor.

POF is widely available in large diameters, typically 1mm that will support tunnelling rays in addition to bound rays.[2,3,4] Tunnelling rays have been demonstrated to contribute an extra 50% to the energy for modulation in the evanescent field of POF EW sensors. The distal end of the fibre has shown that 66% of power is contained in the bound modes and 33% in tunnelling modes – enabling maximum signal modulation of up to 13%, i.e. 13% of the total guided power exists in the evanescent field.[2,4]

2.2 The Physical Properties of Optical Fibre

The basic design for an optical fibre consists of an optically transmissive signal-carrying core surrounded by a cladding designed to prevent loss of signal. These structures are shown below, Figure 2.1,[5] both three dimensionally and in cross section.

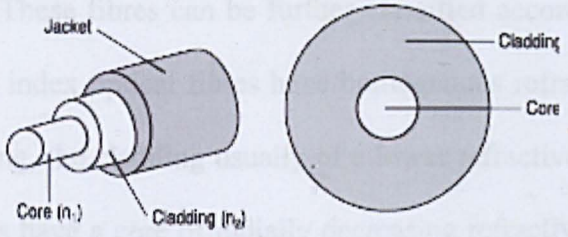

Figure 2.1 Jacketed step index optical fibre 3 D view and basic cross section

Step Index and Graded Index Optical Fibre

Both core and cladding in a step index optical fibre are homogenous but with different indices of refraction: core refractive index, n_1, and the cladding refractive index, n_2; The refractive index of the core must be greater than the refractive index of the cladding, $n_1 > n_2$, to ensure light rays are guided in the core. The difference in refractive index is very small; typically POF core of PMMA is 1.492 with a cladding of fluorinated

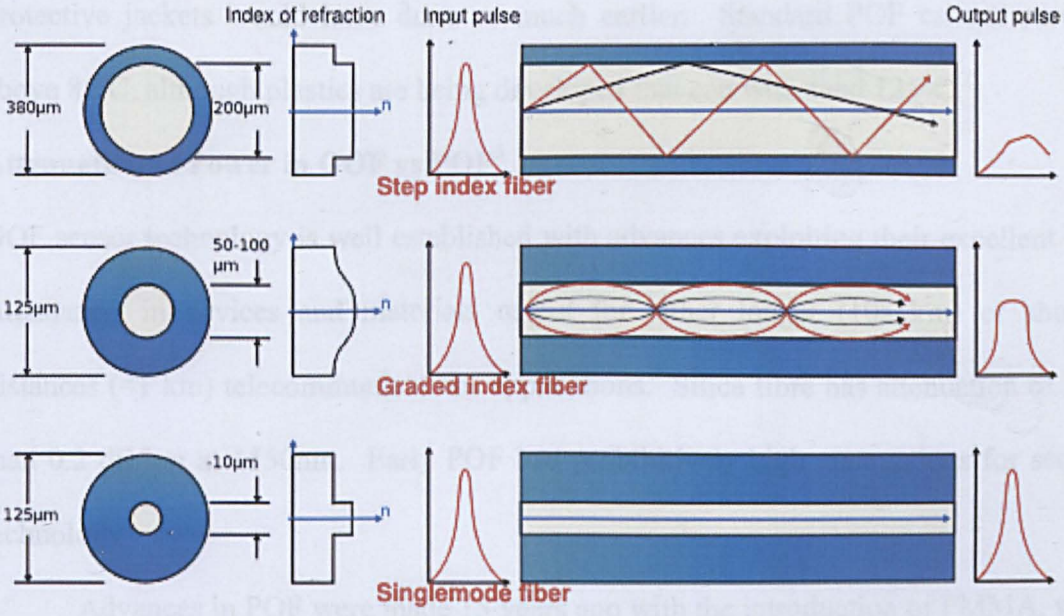

Figure 2.2 Optical fibre types

PMMA of refractive index 1.405; glass optical fibre typically has a core refractive index of 1.62 with a cladding of 1.52.

There are two general types of optical fibre core material, silica glass core and polymer core. GOF may have cladding of either glass or polymer, PCS, POF are always all polymer. These fibres can be further classified according to their refractive index profiles. Step index optical fibres have homogenous refractive index profiles in their core and cladding, the cladding usually of a lower refractive index. Graded index (GRIN) optical fibres have a core of radially decreasing refractive index profile until it reaches the refractive index of the cladding. Figure 2.2[6] depicts multimode step index, graded index and single mode optical fibre, how the refractive index varies axially and the modes supported by each. Optical fibre cable for communications purposes has an additional coating around the cladding called the jacket, this usually consists of one or more layers of polymer which acts as a shock absorber, but also provides protection from abrasions, solvents and other contaminants.

GOF can withstand high temperatures before melting, although their cladding and protective jackets would have done so much earlier. Standard POF cannot survive above 85°C, although plastics are being developed that can withstand 125°C.[7]

Attenuation of Power in GOF vs POF[5]

GOF sensor technology is well established with advances exploiting their excellent low attenuation in devices and materials useful for either longer (10s km) or shorter distances (<1 km) telecommunications applications. Silica fibre has attenuation of less than 0.2 dB/km at 1550nm. Early POF had prohibitively high attenuations for sensor technology.

Advances in POF were made 15 years ago with the introduction of PMMA, with improved attenuation, 160 dB/km at 650nm, guiding 5000 modes, suitable for

multimode data communications up to 100m. Figure 2.3[8] shows attenuation at various wavelengths. POF and GOF sensors share advantages but in addition POF also brings large core size, large NA, improved flexibility, ease of non-skilled handling, tighter bend radius, easier to cleave and couple, ruggedness, safe disposability and lower cost. POF has higher attenuation compared with GOF but are acceptable for short distance applications. The lower fabrication temperatures of POF enables the incorporation of organic chromophores and rare earth organic metallics that would be destroyed by the high temperatures used in GOF production to be added to POF facilitating doping with fluorophores and chemical reagents. Table 2.1[5] gives the attenuation and bandwidth characteristics of various fibre optic cables.

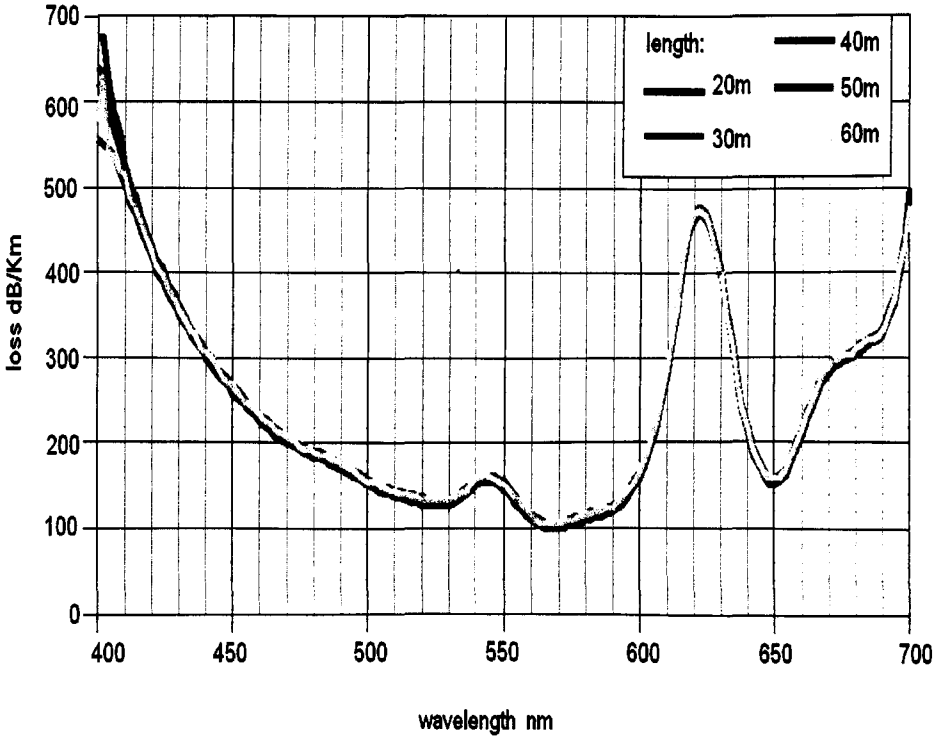

Figure 2.3 Attenuation vs wavelength of POF[8]

Mode	Material	Index of Refraction Profile	λ microns	Size (microns)	Atten. dB/km	Bandwidth MHz/km
Multi-	Glass	Step	800	62.5/125	5.0	6
Multi-	Glass	Step	850	62.5/125	4.0	6
Multi-	Glass	Graded	850	62.5/125	3.3	200
Multi-	Glass	Graded	850	50/125	2.7	600
Multi-	Glass	Graded	1300	62.5/125	0.9	800
Multi-	Glass	Graded	1300	50/125	0.7	1500
Multi-	Glass	Graded	850	85/125	2.8	200
Multi-	Glass	Graded	1300	85/125	0.7	400
Multi-	Glass	Graded	1550	85/125	0.4	500
Multi-	Glass	Graded	850	100/140	3.5	300
Multi-	Glass	Graded	1300	100/140	1.5	500
Multi-	Glass	Graded	1550	100/140	0.9	500
Multi-	Plastic	Step	650	485/500	240	5 @ 680
Multi-	Plastic	Step	650	735/750	230	5 @ 680
Multi-	Plastic	Step	650	980/1000	220	5 @ 680
Multi-	PCS	Step	790	200/350	10	20
Single-	Glass	Step	650	3.7/80 or 125	10	600
Single-	Glass	Step	850	5/80 or 125	2.3	1000
Single-	Glass	Step	1300	9.3/125	0.5	*
Single-	Glass	Step	1550	8.1/125	0.2	*

Table 2.1 Attenuation and Bandwidth characteristics of different fibre optic cable candidates *Too high to measure accurately, effectively infinite[5].

Splicing

Although this section applies to data transmission it gives some indication of the intensity of light available for sensing. Splices may be required at building entrances, wiring closets, couplers and literally any intermediary point between transmitter and receiver. To determine whether the fibre optic link design can meet the sensitivity required it must be analysed. How much power reaches the detector must be determined, and is done with a fibre optic data link power budget.

A power budget for a particular example is presented in Table 2.2.[5] This example corresponds to the design of a fibre optic data link with the following attributes:

1. Data Rate of 50 Megabytes per second (MBps).
2. Bit Error Ratio (BER) of 10-9.
3. Link length of 5 km (premises distances).
4. Multi-mode, step index, glass fibre optic cable having dimensions 62.5/125.Transmitter uses light emitting diode (LED) at 850 nm.
5. Receiver uses PIN semiconductor detector and has sensitivity of -40 dBm at 50 MBps.
6. Fibre optic cable has one splice.

Table 2.2[5] clearly shows that the optical power at the receiver is greater than that required by the sensitivity of the PIN semiconductor detector to give the required BER. The loss margin specifies the amount by which the received optical power exceeds the required sensitivity. In this example it is 15.75 dB. Good design practice requires it to be at least 10 dB to account for the unforeseen losses.

LINK ELEMENT	**VALUE**	**COMMENTS**
Transmitter LED output power	3 dBm	Specified value by vendor
Source coupling loss	-5 dB	Accounts for reflections, area mismatch etc.
Transmitter to fibre optic cable connector loss	-1 dB	Transmitter to fibre optic cable with ST connector. Loss accounts for misalignment
Splice loss	-0.25 dB	Mechanical splice
Fibre Optic Cable Attenuation	-20 dB	Line 2 of Table 2-1 applied to 5 km
Fibre optic cable to receiver connector loss	-1 dB	Fibre optic cable to Receiver with ST connector. Loss Accounts for misalignment
Optical Power Delivered at Receiver	-24.25 dB	
Receiver Sensitivity	-40 dBm	Specified in link design. Consistent with Figure 2-14
LOSS MARGIN	15.75 dB	

Table 2.2 Example Power Budget for a fibre optic data link

2.3 Propagation of Light in Optical Fibres

It is well known that light has a dual nature, in traditional geometrical and physical optics light is considered to travel in straight lines as 'rays', but some light behaviour can only be described in terms of particles, and as a transverse electromagnetic wave. Ray propagation theory describes light in the former guise. The refractive index of the

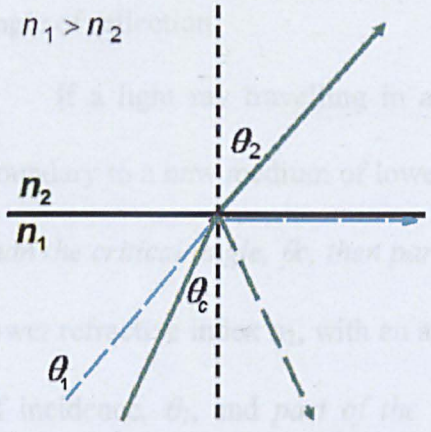

Figure 2.4 An incident light ray less than critical angle partly transmits through second lower refractive index material and partly reflected into the original material of higher refractive index

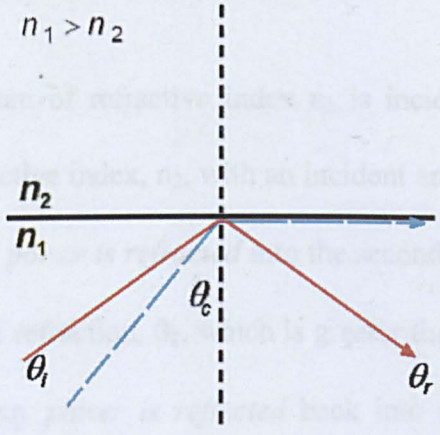

Figure 2.5 An incident light ray greater than the critical angle is fully internally reflected at the boundary to a medium of lower refractive index.

core and cladding material of a step index optical fibre are constant. The cladding material has a lower refractive index than the core. Refractive index is the measure of the ratio of the speed of light within a material to that in a vacuum. When a light ray crosses an interface into a medium of lower refractive index the light bends away from the normal as shown in figure 2.4.

Snell's law relates the indices of refraction of two media in the directions of propagation in terms of the angles to the normal:

$$n_1 \sin\theta_1 = n_2 \sin\theta_2 \qquad \text{---2.1}$$

The critical angle is the angle of incidence at which the resulting angle of refraction is 90°, i.e. the incident light ray does not leave the first material as illustrated in figure 2.5.

$$\sin\theta c = n_2/n_1 \qquad \text{---2.2}$$

A light ray, travelling in a medium of refractive index n_1 is incident upon a boundary into a new medium of lower refractive index, n_2 with an incident angle, θ_1, *greater than the critical angle,* θc, all of its power is reflected back into the original medium, the light energy is *totally internally reflected (TIR).* The angle of incidence is equal to the angle of reflection.

If a light ray travelling in a medium of refractive index n_1 is incident upon a boundary to a new medium of lower refractive index, n_2, with an incident angle, θ_1, *less than the critical angle,* θc, *then part of its power is refracted* into the second medium of lower refractive index n_2, with an angle of refraction, θ_2, which is greater than the angle of incidence, θ_1, and *part of the light ray power is reflected* back into the original medium, the angle of incidence being equal to the angle of reflection.

Acceptance Angle and Numerical Aperture

The significant angle for light rays travelling in air, n_o, to refract into a higher refractive index core, n_1, is called the acceptance angle, θ_a, of the optical fibre in question, figure 2.6. This is the angle at which the transmitted ray encounters the core/cladding

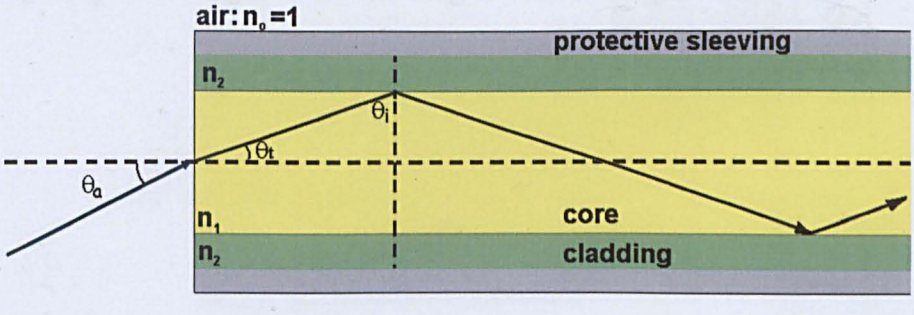

Figure 2.6 Propagation of a light ray along an optical fibre
θ_a=acceptance angle of fibre θ_t= angle of transmission θ_i= angle of incidence.

interface at the aforementioned critical angle for that core/cladding interface. Any angle of light ray coupled into the fibre that is less than θ_a will result in an angle of incidence

greater than the critical angle for the core/cladding interface it will undergo TIR and propagate along the fibre.

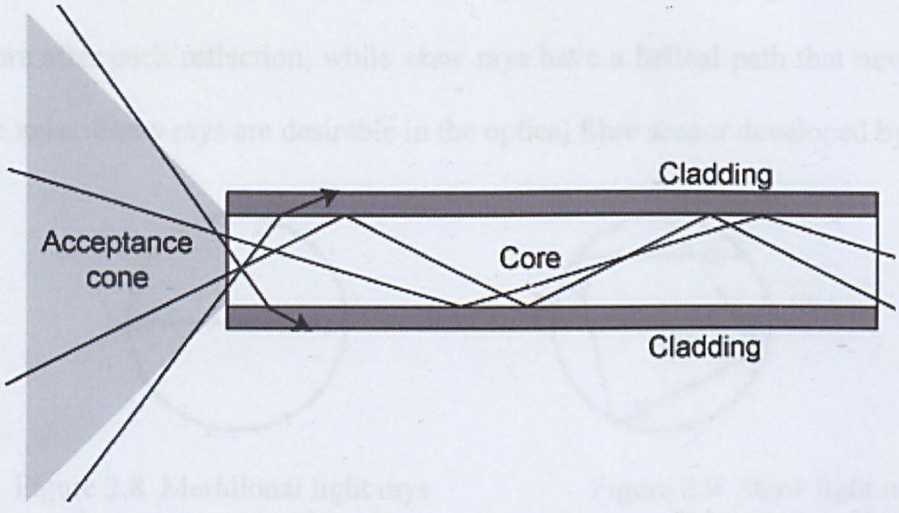

Figure 2.7. Acceptance cone of an optical fibre, incident light of an angle less than acceptance angle will undergo TIR

The sine of this acceptance angle, θ_a, is called the numerical aperture, *NA*

$$\sin\theta_a = \sqrt{n_1^2 - n_2^2} = NA \qquad \text{---2.3}$$

The larger the acceptance angle, and therefore, NA, the larger the proportion of light coupled into the fibre core. Any angle larger than the acceptance angle will result in the light ray refracting into the cladding as shown in figure 2.7.

2.4 Types of Light Rays in Optical Fibre Core

Light rays propagating in a fibre are referred to as bound rays and may be classified as *meridional* figure 2.8 or *skew* figure 2.9 rays. *Meridional* rays pass through the axis of a fibre after each reflection, while *skew* rays have a helical path that never crosses the fibre axis. Skew rays are desirable in the optical fibre sensor developed by this project

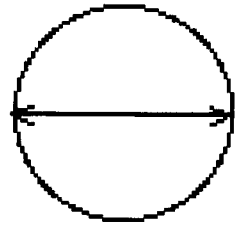

Figure 2.8 Meridional light rays pass through the axis of the fibre.

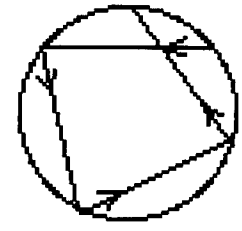

Figure 2.9 Skew light rays propagate through an optical fibre without passing through its axis.

as this ensures that the number of rays which have an incident angle with the core/cladding interface greater than the critical angle are maximised. These rays couple the most light into the cladding.

Classification of Rays

Snell's laws are derived for reflection from a planar interface, whereas the optical fibre interface is curved. As shown above, the condition for a ray to be *bound* is $0 \leq \theta_i \leq \theta_c$ independent of the angle between projection of path onto the fibre cross section and the azimuthal direction. This represents a cone of angles at each position in the core cross sections and includes meridional and skew rays. The remaining skew-ray directions which are not included in either *bound* or *refracting* rays belong to a third class of rays called *tunnelling rays.*[3] Rays which are not bound, i.e. tunnelling and refracting rays, are known as *leaky rays.*

Modes

A mode is a defined path in which light rays travel. Electromagnetic modes can be regarded as transverse resonances of the fields of the optical fibre, by analogy with the normal modes of vibration of a membrane fixed at its periphery. However, whereas the membrane has an infinite number of bound modes, an optical fibre can only support a *finite* number of bound modes. The guided portion of the fields store electromagnetic energy in the optical fibre and transports power along the fibre length. A fraction of this energy is stored in the fields of each bound mode, and these fields also transport a portion of the total power.

Single Mode Fibre

Guided rays occur when light rays propagate along or are constrained by the physical boundaries of an optical fibre. When a core diameter is small enough that the number of possible totally internally reflected rays is reduced to one, thus allowing only a single

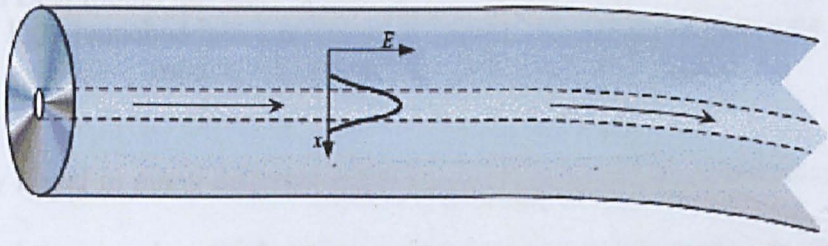

Figure 2.10 Fundamental mode guided by single mode fibre

mode of guided light, the concept of rays changes to modes, which bend with or are guided by the core. Single mode optical fibre, figure 2.10, has a diameter of 8 microns or less that supports only one mode of transmission, the *fundamental mode*, which travels parallel to the axis of the fibre with very little pulse dispersion. Not all light travels through the core of the fibre but is distributed through both the core and the cladding. The "mode field" is the distribution of light through the core and cladding of a particular fibre. The portion of this field in the cladding is called the evanescent field.

Multimode Fibre

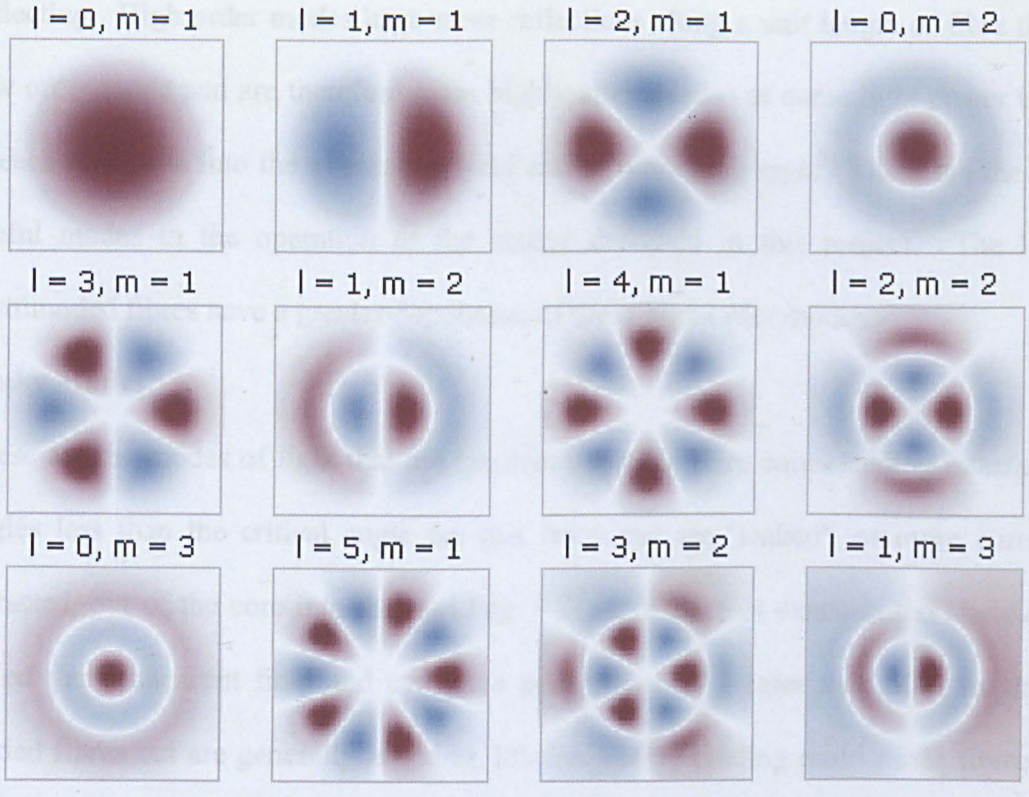

Figure 2.11 The guided modes of a multimode fibre. The lowest order mode (l=1,m=0 is called LP_{01} mode) has and intensity profile similar to that of a Gaussian beam. In general, light launched into a multimode fibre will excite a superposition of different modes, which can have a complicated shape[9]

Light may travel in many different paths along the optical fibre; groupings of light rays are referred to as modes which arrive separately at a receiving point as shown in figure 2.11. Multimode fibres typically have core diameters up to 100 microns that allow many modes of transmission, figure 2.12. The mode in which light rays travel depends on geometry, the index profile of the fibre and the wavelength of the light.

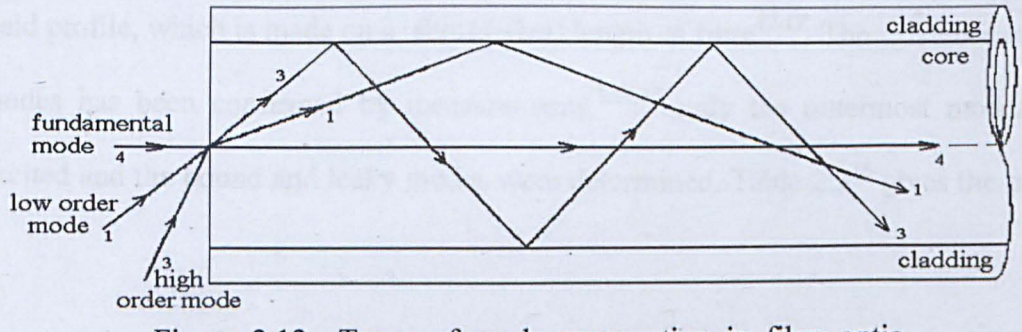

Figure 2.12 Types of mode propagation in fibre optic

The fundamental mode is the lowest order mode and propagates along the fibre without reflecting. High order modes have more reflections along a unit length of fibre than a low order mode and are therefore more highly attenuated – as some light power is lost at each reflection into the evanescent field and to tunnelling rays.[3] These are the most useful modes in the operation of the sensor designed in this project. The larger multimoded fibres have a greater population of these high order modes.

Leaky Modes

These are the modes of light that are incident upon the fibre core/cladding interface at angles less than the critical angle for that fibre and are 'leaked', or more correctly refracted, out of the core into the cladding.[3,4,10] The light that exists in the cladding is called the evanescent field and can have penetration of greater than 50% in single-moded fibres but are generally less than 1% for weakly guiding multi-mode fibres,[1] in which the core and cladding refractive indices are similar in value. Most of these modes attenuate as rapidly as 10^4dB/m, however modes with high angular momentum, have been calculated to propagate over many kilometres.[4,11] These waves are referred to as tunnelling rays, analogous to a particle confined in a potential barrier, these modes quantum mechanically tunnel through to follow one of the free space paths. In a typical multimode waveguide, if all guided and leaky modes are initially excited, after 1m of propagation 10-20% of the remaining power is predicted to reside in leaky modes. After 1km this fraction is reduced to 10-20%, therefore leaky modes are predicted to have a large influence on measurements of optical properties, especially in the near-field profile, which is made on a short (~1m) length of fibre[12,13]. The existence of leaky modes has been confirmed by measurements,[1,14,15] only the outermost modes were excited and the bound and leaky modes were determined. Table 2.3[16] gives the fraction

of bound, tunnelling and refracting rays at launch and distance z for step index multimode optical fibres.

Fibre	Symbol	CK40 POF	Caco PCS	Caco PCS	PCS
Core diameter (μm)	$2a$	980	1000	200	62.5
Numerical aperture	NA	0.50	0.40	0.40	0.40
Bound ray fraction	$P_b(0)$	0.25	0.160	0.160	0.160
Tunnelling ray fraction	$P_t(0)$	0.178	0.123	0.123	0.123
Refracting ray fraction	$P_r(0)$	0.572	0.717	0.717	0.717
Tunnelling ray losses due to radiation at distance z from launch	$\frac{P_t(z)}{P_t(0)}$	$\approx$0.6 for z = 107 m	$\approx$ 0.6 for z = 106m	$\approx$ 0.5 for 20m< z <63 m, $\approx$ 0.45 for z = 10 000 m	$\approx$ 0.4 for z = 106 m, $\approx$ 0.3 for z = 1000 m

Table 2.3 Fraction of bound, tunnelling and refracting rays at launch and distance z for step index multimode optical fibres[16]

2.4.1 Evanescent Field

Higher order modes have more core cladding reflections per unit length. At each of these reflections some light is absorbed into the evanescent field as they propagate down the optical fibre, resulting in an attenuated output signal. Evanescent field penetration of greater than 50% can be achieved in single-moded fibres but are generally less than 1% for weakly guiding multi-mode fibres,[1] in which the core and cladding refractive indices are similar in value. These are the very modes modulated in evanescent field optical fibre sensing, it is this affected by the measurand acting as the cladding.

As power loss due to an absorbing cladding is beyond the path of the light ray, geometric optics do not apply and is therefore regarded as a diffraction, or a wave effect, which is dependent on the wavelength of light propagating in the core. Treating the ray locally as a plane wave allows the power loss[2,17,18] at a reflection or turning point to be calculated, which in turn allows the attenuation of ray power along the fibre,

due to cladding absorption, to be calculated with knowledge of the density of reflection points, which is determined by geometric optics.

The local plane waves in the cladding material of an optical fibre become evanescent and decrease exponentially with radial distance. This *evanescent field* has a decay of e^{-1}, and is dependent upon properties of the materials of the core and cladding and the wavelength of light propagating in the fibre core. It is this short range sensing volume within which the evanescent field may interact with a measurand, acting as the fibre cladding, attenuating due to refractive index changes, absorption or scattering. Particular attention will be given to the evanescent field in this thesis as the project sensors are based on the attenuation of this field and the existence of tunnelling rays.

The evanescent field in the cladding medium is characterised by the penetration depth d_p[19], where the beam intensity drops to e^{-1} of its original magnitude may be calculated using formula 2.4:

$$d_p = \frac{\lambda}{2\pi n_1 \sqrt{\sin^2\theta - (n_2/n_1)}} \qquad \text{---2.4}$$

Where λ, is the wavelength of incident light, θ is the angle of incidence to the normal at the interface and n_1, and n_2 are the refractive indices of the core and surrounding media. Though d_p is typically less than λ, its value rises sharply as the angle of incidence approaches the critical angle $\theta_c = \sin^{-1}(n_2/n_1)$.

To evaluate the tunnelling ray loss a generalised fibre attenuation parameter G[17] (equation 2.5) shows that the tunnelling ray power decays to 50% of its initial value when $G = 0.03$. This means that the characteristic distance at which the power has decayed to half, $z_{50\%}$ may be calculated:

$$G = \frac{1}{V}\ln\left(2\theta_c \frac{z}{a}\right) \qquad \text{---2.5}$$

$$z_{50\%} = \frac{a}{2\theta_c}\exp(GV) \qquad \text{---2.6}$$

Where G is the attenuation parameter of fibre and $z_{50\%}$ represents the distance from fibre core at which the power of the tunnelling has decayed to half of its original value. The distance $z_{50\%}$ is dependent on the fibre diameter and refractive index profile. This shows that the attenuation of the tunnelling rays depends strongly on fibre diameter and that wide-core multi-mode fibres may well attenuate tunnelling rays much less than single-mode fibres.

The amount of light power available in the evanescent field to interact with the measurand is described by the fraction r of total guided power in the cladding region, where P_{clad} is the power in the cladding region and P_{tot}[20] is the total guided power in the medium.

$$r = \frac{P_{clad}}{P_{tot}} \qquad \text{---2.7}$$

The ratio r depends upon the normalised optical frequency or V-number[20], V, which determines the number of electromagnetic modes in the fibre:

$$V = \frac{2\pi a}{\lambda} NA \qquad \text{---2.8}$$

Where a is the radius of the fibre core and λ represents the source wavelength.

Optical fibres with V-numbers below ~2.405 support only one mode per polarisation direction. Multimode fibres can have much higher V-numbers, the number of modes supported in a step-index fibre may be calculated approximately[24] as

$$\text{Number of Modes} \approx \frac{4}{\pi^2} V^2 \qquad \text{---2.9}$$

A 1mm CK40 POF with NA= 0.5, a=980μm, source wavelength λ=650nm has a V-number of 4737 and supports 1 x 10^7 modes. In single-mode fibres V < 2.405, r > 50%, large diameter fibres are highly multimodal and are ideally suited for applications of evanescent wave sensing because of their ease of handling and higher power throughput. For weakly guiding fibres ($n_{co} \approx n_{cl}$) such as telecommunications multimode silica fibre, values of r < 1% are typical.[20] The guided power in the cladding, and hence the sensitivity of an evanescent field optical fibre sensors, is determined largely by the tunnelling rays. Table 2.3 shows that a greater fraction of tunnelling rays is launched as NA increases indicates in agreement with Chandy *et al.*[21]

The evanescent field can be maximised by exciting high order modes in order to optimise the penetration depth and increase the sensitivity of the sensor.[1] This can be achieved by tapering in the sensing region, by low order mode removal via masking at the launch optics into the fibre[22,23] using a mode filter, or by coupling the light from a parallel coherent laser beam off axis into a large diameter multimode fibre.

2.4.2 Tunnelling Rays

Tunnelling rays differ from refracted rays in the way they interact with the fibre cladding. Refracted rays propagate alternately between the core and cladding region crossing the interface by refracting each time. However in the case of tunnelling rays the transmitted part of the ray appears to tunnel a finite radial distance into the cladding and then radiate power outwards from the fibre.[24] Due to repeated refractions the tunnelling rays lose power each time they propagate across the core/cladding interface, losing optical power, even if the fibre were non-absorbing.

The attenuation of tunnelling rays has been shown to depend strongly on fibre diameter, thus wide core fibres may attenuate tunnelling rays much less than lower

mode fibres. The evidence for increased penetration depth of tunnelling rays in POF is described by Zemon and Fellows,[1] which further supports the use of large diameter POF. Most of these modes attenuate as rapidly as 10^4dB/m, however modes with high angular momentum, have been calculated to propagate over many kilometres.[11]

Figure 2.13[24] gives a visual representation of the three regions of space for an incident ray at point P of the core. *Bound ray* angles lie in the half cone $\theta_z \leq (\pi/2) - \alpha_c$, and *refracting rays* lie in the half cone $\alpha_i \leq \alpha_c$. The two half cones touch in the meridional plane. *Tunnelling rays* are incident in the two symmetric regions on either side of the meridional plane through P and exterior to the half cones.[25]

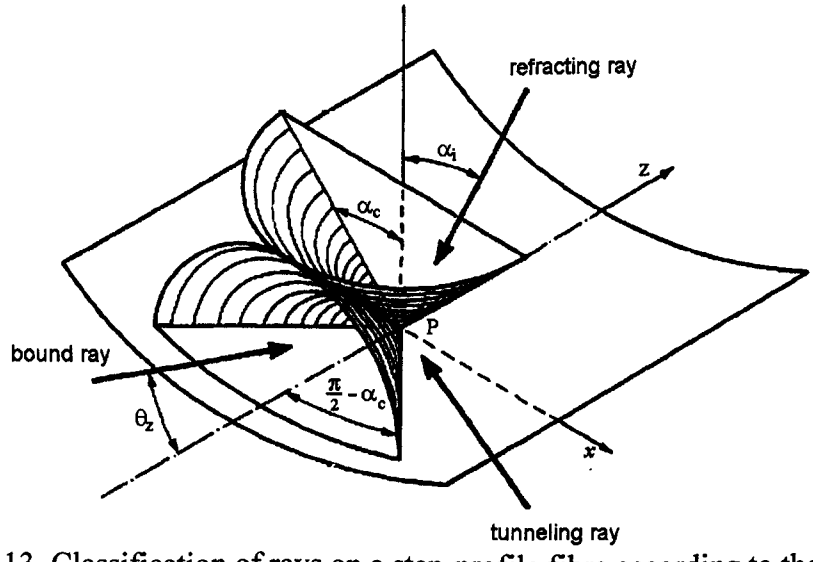

Figure 2.13 Classification of rays on a step-profile fibre according to the angle of incidence at the interface[24]

In a typical multimode waveguide, if all guided and leaky modes are initially excited, after 1m of propagation 10-20% of the remaining power is predicted to reside in leaky modes. After 1km this fraction is reduced to 10-20%, therefore leaky modes are predicted to have a large influence on measurements of optical properties. The optical radiation coupled out at the radiation caustic propagates along the optical path in the fibres cladding. Since light cannot be detected in the evanescent region, this transfer process is referred to as electromagnetic tunnelling or simply as tunnelling. Through

consideration of electromagnetic field profiles of tunnelling modes in the region of the core/cladding interface tunnelling rays have been shown to be an intermediate between bound and refracting rays[26]. In terms of light power propagation, tunnelling rays may be ignored for few-moded fibres. They cannot be ignored, however, for large multi-mode fibres, even over long distances. Total power coupled into a fibre, using an LED as the light source, has been defined as[24]:

$$P_{TOT} = \pi^2 a^2 I_o \qquad \text{---2.10}$$

where a represents the fibre radius; I_o is the maximum light intensity emitted.

The LED light source was assumed to be a Lambertian source, i.e. the angular distribution of light intensity is described by a cosine function:

$$I(\theta_o) = I_o \cos\theta_o \qquad \text{for} \quad 0 \le \theta_o \le \pi/2 \qquad \text{---2.11}$$

Total power launched into bound [$P_b(0)$] and tunnelling [$P_t(0)$] rays is defined as[24]:

$$\frac{P_b(0)}{P_{TOT}} = n_1^2 \sin^2\theta_c \qquad \text{---2.12}$$

$$\frac{P_t(0)}{P_{TOT}} = \left(1 - \frac{2\cot\theta_c}{\pi} + \frac{2\theta_c \cos 2\theta_c}{\pi \sin^2\theta_c}\right) n_1^2 \sin^2\theta_c \qquad \text{---2.13}$$

$$\text{where} \quad \theta_c = \frac{\pi}{2} - \sin^{-1}\left(\frac{n_2}{n_1}\right) \qquad \text{---2.14}$$

Subtracting the two components from total power (P_{TOT}) gives the power launched into refracting rays. The values of $P_b(0)$ and $P_t(0)$ clearly depend upon the refractive index of the fibre. It has been shown that the attenuation of tunnelling rays depended on fibre diameter, indicating that wide core fibres attenuate tunnelling rays much less than single mode fibres.[24]

A numerical evaluation of radiation loss on 1mm diameter POF and PCS supports claim that for fibres with a core diameter above 500mm the power contribution

from these tunnelling rays can be half that of bound rays along with the extended penetration depth indicates that in evanescent field based large core fibre sensors, tunnelling rays may participate in signal light modification and transmission, as bound rays do.

Disregarding tunnelling rays will lead to underestimation of the extent of light modulation due to a measurand in intimate contact with the fibre core acting as the cladding. Analytical results from planar waveguides indicated that the higher order modes have comparatively larger initial amplitude of evanescent field that decays slower than that of lower order modes. When all modes have equal power the evanescent field of the near-cut-off modes less than 1mm from the core surface is about the same as the evanescent field of the near-fundamental modes in the vicinity of 10s microns from the fibre surface, the latter was subsequently used for evanescent field sensing.

These results are qualitatively applicable to optical fibres. The theoretical feasibility of evanescent field based large core multimode fibre sensors to sense at locations sub-millimetres away from the core surface was confirmed.[30] The electromagnetic field of one fibre can be excited by means of evanescent field coupling when in its vicinity, i.e. a power transfer from the first fibre to the second will occur.

In terms of wave optics light sources in the fibre cladding interact with the evanescent field tails of the bound and tunnelling modes, transferring some power to the modes. The total power in the fibre core is a function of scattering particle concentration and increases as fibre core radius, NA and sensing length increases. When considering the light power change resulting from the evanescent effects, the contribution from the tunnelling modes may be as much as half that attributed to bound rays, since tunnelling modes also have evanescent fields in the cladding and about half

of them can propagate over distances as long as kilometres without much power attenuation.

Since mathematical models describing evanescent field effects in large core fibres remain a challenge to theoretical researchers in this area, only qualitative discussions of evanescent field effects are presented.

Experimentation by F H Zhang[30,31] demonstrated that considering only bound modes underestimated power attenuation in the transmitting fibre due to an attenuating cladding by up to 28%, indirectly confirming the attenuating contribution of tunnelling modes.

2.5 Attenuation of Propagated Light in Optical Fibres

The refractive index, absorption and scattering properties of the cladding directly affect the amount of light coupled into the evanescent field. It is this property that evanescent field sensors exploit.

Attenuation due to Absorption

The absorption and refractive index of the cladding directly affects the amount of light coupled into the evanescent field[27,28,29]. Evanescent field sensors exploit this property. What is seen as a disadvantage for data transmission purposes is exploited in a sensor. Energy is absorbed from the evanescent field due to certain mechanical and chemical medium in contact with the optical fibre core.

Attenuation due to Scattering

Light scattering occurs when a beam of light falls on a particle smaller than the wavelength of light incident. The light energy of the ray involved is redistributed to other surrounding rays, bound or leaky, resulting in a change in direction, phase or wavelength.

There are two types of scattering:

Linear, e.g. *Rayleigh* and *Mie* scattered wavelength unchanged from original.

non-linear, e.g. *Raman* and *Brillouin* scattered wavelength shifted from original.

Linear Scattering

The oscillating electromagnetic field of the incident light exerts a periodic force on each electronically charged particle causing it to oscillate sympathetically. As an oscillating charged particle radiates in all directions, except along the plane of travel, the intensity of radiation scattered is large in the direction of constructive interference and small in the direction of destructive interference. The induced oscillation charge distribution of each scatterer influences polarisation and angular distribution of the scattered energy.

The extent to which the radiation interferes constructively or destructively with the resultant scattered field is also affected by the position of the scatterers.

Rayleigh scattering involves randomly dispersed independent particles that are less than one tenth of the light wavelength. The total scattered intensity is simply the sum of scattered intensity due to each individual particle. The scattered light intensity is inversely proportional to the fourth power of the incident wavelength.

Mie scattering involves spherical particles of a size comparable to the incident light wavelength. The scattering pattern of a sphere depends on the size and refractive index of the scattering particle, which are normally very involved.

Non-linear Scattering

The effects of non-linear scattering depend on a high power of intensity, i.e. it is weak at low powers, but can become stronger when light reaches high intensities. Non-linearities in optical fibres are small but accumulate as light passes through many kilometres of fibre. As the sensors developed in this project use less than 1mW of power, this does not occur in this thesis, and therefore will not be reviewed.

Single and Multiple Scattering

Single scattering occurs where the optical depth of the medium is sufficiently small so that radiation scattered by a single particle escapes from the medium unhindered. Here the total scattered light intensity is proportional to the optical depth of the medium.

Optical depth, τ, is the product of particle number N, in a unit volume of a medium, the depth, l, of the medium through which incident light passes and the total energy attenuated σ_t, also defined as the extinction cross-section by many references, by a particle:

$$\tau = N\sigma_t l \qquad \text{--- 2.14}$$

Multiple scattering occurs where there is a dense population of scattering particles or the thickness of the medium is such that the radiation scattered by a particle may be further scattered by other particles before escaping the medium. Here the total scattered light intensity is less than for the single scattering case. There are no general analytical expressions presently to describe multiple scattering.

Interrogation of scattered light should reveal the number, size, structure and orientation of particles and their interactions, however the calculation are too involved. It would be necessary to solve Maxwell's equations with the boundary conditions for each individual scattering element, which only describe simple geometric shapes, spheres, spheroids and cylinders. However many applications involve multiple scattering, e.g. atmospheric and ocean optics, optical scattering by bodily tissue and scattering by stellar and interstellar media. Various methods have been developed in these areas based on different historical theoretical approximations peculiar to their field and are therefore highly specialised for their purpose.

Light scattering by aqueous particle suspensions was investigated[30] by F.H.Zheng.[31] An intrinsic passive optical fibre sensor was designed and configured to detect particulate matter suspended in liquid media and was characterised for measurement of yeast cell culture growth. A transmitting fibre was orientated alongside a receiving fibre, with a small gap between them where the measurand was introduced. It was demonstrated that the evanescent field in the vicinity of the transmitting fibre was disturbed in the presence of a receiving fibre. The transmitting fibre lost power to the surrounding measurand due to attenuation via absorption and scattering of the evanescent wave. Measurement of light power at the end of the receiving fibre as a function of yeast cell population density confirmed the excitation of modes in the receiving fibre due to the presence of the evanescent wave. Comparison between

experimental data derived from the evanescent wave absorption measurement and numerical simulation indicated that consideration of only bound modes underestimated the power attenuation in the transmitting fibre by up to 28%. The experimental observation of transmitted light pattern of the suspensions showed the occurrence of light scattering in the media.

It was proved that non-linear scattering may be ignored in the sensing process of the sensor and that linear scattering dominates. The characteristics of the liquid excluded the possibility of Rayleigh scattering; therefore the dominating scattering mechanism was attributed to Mie scattering. Measurement of the backscattering light in a length of 1mm POF indicated that linear light scattering in polymer fibres contributed substantially.

2.6 Summary

The main types of optical fibre readily available are manufactured for the telecommunications industry. POF has very low loss 150dB/km, i.e. 0.15dB/m at the wavelengths of light used by this project, is very easy to cut, polish and terminate with due to its physical size, and requires fairly simple procedures to be carried out on them to make them ready for sensing. The power loss is acceptable for the connections in the sensor: LD to optical fibre, single fibre to two fibres, reference and sensor, in Y-splitter, fibre to detector. From section 3.5 there was potentially 66μW available for sensing purposes after the Y-splitter.

The physics of light propagation and attenuation have been described and justifies the selection of 1mm diameter multimode POF. The design of step index optical fibre was described, as this is the fibre type used by the project in the production of the evanescent field sensor. Conditions for the coupling and propagation of light rays into a step profile optical fibre have been discussed, also the NA and critical angle, which are two very important properties of an optical fibre that give an indication of the proportion of light that may be coupled into a fibre and is dependant upon the refractive index of the optical fibre core. The larger the acceptance angle, and therefore larger the NA, the greater the proportion of light coupled into the fibre core. CK40 POF has core diameter, a=980μm, NA= 0.5, illuminated by a source wavelength λ=650nm has a V-number of 4737 and supports 1×10^7 modes.

The types of ray propagating in a fibre core have been described, meridional rays, which cross the fibre axis each time it is reflected and skew rays that exist in the outer part of the fibre core and propagate in a helical path, never crossing the optical fibre axis. The different modes in which rays may propagate along a fibre have been described, including fundamental and leaky modes. Leaky modes consist of evanescent

and tunnelling rays and are the rays that are modified by conditions in the cladding. The importance of leaky modes cannot be overemphasised since these are the modes that are modified by the measurand acting as the cladding to the sensing fibre. Evanescent field penetration of greater than 50% can be achieved in single-moded fibres but are generally less than 1% for weakly guiding multi-mode fibres[2], In a typical multimode waveguide after 1m of propagation 10-20% of the remaining power is predicted to reside in leaky modes, after 1km this fraction is reduced to 10-20%, therefore leaky modes are predicted to have a large influence on measurements of optical properties, especially in the near-field profile, on a short (~1m) length of fibre.[12,13] Leaky modes have been measured. [1,14,15]

The *evanescent field* has a decay of e^{-1} and is dependent upon properties of the materials of the core and cladding and the wavelength of light propagating in the fibre core. The evanescent field may be modified with a measurand, acting as the fibre cladding, due to refractive index changes, absorption or scattering. Particular attention is given to leaky modes in this thesis as the project sensors are based on the attenuation of the evanescent field and the existence of tunnelling rays.

Through consideration of electromagnetic field profiles of tunnelling modes in the region of the core/cladding interface tunnelling rays were shown to be an intermediate between bound and refracting rays.[26] For large multi-mode fibres, total power coupled into a fibre, using an LED as the light source, has been defined.[24] The evidence for increased penetration depth of tunnelling rays in POF has been described which further supports the use of large diameter POF.[1]

Scattering also contributes to signal attenuation, the mechanisms involved have been described. The scattering processes involved are linear; however they are multiple and are very difficult to describe. Measurement of the backscattering light in a length of

1mm POF indicated that linear light scattering in polymer fibres made a substantial contribution.[31]

References

[1] S Zemon, D Fellows, "Tunnelling Leaky Modes in a Parabolic Index Fibre" Appl. Opt. vol.15, No.8, pp1937-1941, 1975

[2] AW Snyder, "Leaky-ray Theory of Optical Waveguides of Circular Cross-section", App. Phys. vol.4, pp273-298, 1974

[3] AW Snyder, DJ Mitchell, "Leaky rays on circular optical fibers", J. Opt. Soc. Am., vol.64, p599, 1974

[4] AW Snyder, DJ Mitchell, C Pask, "Failure of geometric optics for analysis of circular optical fibers" J. Opt. Soc. Am., vol.64, p608, 1974

[5] KS Schneider, "Fiber Optic Communications for the Premises Environment" Chapter 2, www.telebyteusa.com/foprimer/foch2.htm accessed 4th December 2008

[6] Mrzeon, "Optical_fiber_types.svg". www.en.wikipedia.org/wiki/Image:Optical _fiber_types.svg accessed 4th December 2008

[7] J Hecht, "Understanding Fiber Optics", 4th ed. Prentice-Hall International UK Ltd, London, 2002.

[8] D Peitscher, G Schulte, H Muhlen, J Kauser, O Ziemann, " Correct Definition and Reproducible Measurement of Spectral Attenuation for Step Index Polymer Optical Fibers" 9th International POF conference, 2000

[9] R Paschotta, "Encyclopedia of Laser Physics and Technology", www.rp-photonics.com/modes.html accessed 4th December 2008

[10] C Pask, AW Snyder, DJ Mitchell, "Number of Modes on Optical-Waveguides" J. Opt. Soc. Am. vol.65, Issue 3 pp356-357, 1975

[11] JD Love, C Pask, "Universal curves for power attenuation in ideal multimode fibres", Electron Lett. vol.12, p254, 1976

[12] FME Sladen, DN Payne, MJ Adams, "Correction Factors for the Determination of Optical-Fibre Refractive-Index Profiles by the Near-Field Scanning Technique", Appl. Phys. Lett. 28, 255, 1975

[13] JA Arnaud, RM Derosier, "Uncertainties of the leaky mode correction for near-square-law optical fibres", Bell Syst. Tech. J, vol.55, p1489, 1976

[14] WJ Stewart, Optical Fiber Transmission (Digest of Technical Papers presented at Topical Meeting, Williamsburg, Virginia, 1975, pub. Optical Soc. of America, Washington, paper TUD8, 1975

[15] WJ Stewart, Digest of IEE European Conference on Optical Fibre Communication, London (Institute of Electrical Engineers, London WC2, 1975

[16] C Saunders and P J Scully, "Sensing Applications for POF and Hybrid Fibres using a Photon Counting OTDR", Meas. Sci. Technol. vol.18, pp615–622, 2007

[17] AW Snyder, JD Love, "Attenuation Coefficient for Rays in Graded Fibres with Absorbing Cladding", Electron. Lett., vol.12, pp255-257, 1976

[18] M Born, E Wolf, "Principles of Optics", Pergamon Press, Oxford, p40, 1970

[19] N. J. Harrick, Internal Reflection Spectroscopy, Wiley, Interscience, New York, 1967

[20] B D MacCraith, "Enhanced evanescent wave sensors based on sol-gel derived porous glass coatings", Sensors and Actuators B, vol.11, pp29-34, 1993

[21] R Philip-Chandy, P J Scully, P Elderidge, G Grapin, G Jonca, G D'Ambrosio and F Colin, "An Optical Fibre Sensor for Biofilm Measurement using Intensity Modulation and Image Analysis", IEEE J. Selected Topics in Quantum, vol.6, No.5, pp764-772, 2000

[22] V Ruddy, "An Effective Attenuation Coefficient for Evanescent Wave Spectroscopy using Multimode Fibre", Fibre Integrated Opt., vol.9, pp142-150, 1990

[23] BJC Deboux, E Lewis, PJ Scully, RJ Edwards, "A Novel Technique for Optical Fibre pH Sensing Based on Methylene Blue Adsorption", J. Lightwave Technol. vol.3, pp1407-1414, 1995

[24] AW Snyder, JD Love, "Optical Waveguide Theory", Chapman and Hall, 1983

[25] JD Love, C Winkler, "Attenuation and Tunneling Coefficients for Leaky Rays in Multilayered Optical Waveguides", J. Opt. Soc. Am., vol.67, No.12, pp1627-1633, 1977

[26] HG Ungar, "Planar Optical Waveguides and Fibres", Chapter 4, Clarendon Press, 1977

[27] V Ruddy, B MacCraith, JA Murphy, "Spectroscopy of Fluids using Evanescent Wave Absorption on Multimode Fibre", SPIE vol.1172, Chemical, Biological and Environmental Sensors pp83-92, 1989

[28] AG Mignani, R Falciai, L Ciaccheri, "Evanescent Wave Absorption Spectroscopy by Means of Bi-tapered Multimode Optical Fibres", Applied Spectropscopy, vol.52, No.4, pp546-551, 1998

[29] S Guo, S Albin, "Transmission Property and Evanescent Wave Absorption of Cladded Multimode Fibre Tapers", Optics Express vol.11, No.3, pp. 215-223, 2003

[30] FH Zhang, E Lewis, PJ Scully, "An Optical Fibre Sensor for Particle Concentration Measurement in Water Systems Based on Inter-fibre Light Coupling Between Polymer Optical Fibres", Transactions of the Institute of Measurement and Control, vol.22, No.5, pp413-430, 2000

[31] FH Zhang PhD thesis

CHAPTER THREE

Components of Evanescent Field Sensor

3.1 Introduction

The various instruments and components available for the design of the POF evanescent field biofilm sensor are presented in this chapter in order to make an informed and considered design.[1] Standard component should be used where possible to keep costs low, however custom components must be manufactured to optimise the sensor.

The sensor should be a compact on-line instrument to be used in situ. It also should be non-skilled user friendly and cheap to construct. The light source must be able to produce intense emissions in suitable wavelength bands; sufficient power must be coupled into the sensor to allow attenuation due to the measurand to be detected. The

light source should also have stable intensity over extended periods; require only simple power requirements with high efficiency and low replacement cost.

There is great difficulty in sourcing standard couplers and components for POF sensors as they are not commercially available for this purpose. Items had to be designed and manufactured especially for this project and are described in section 3.5.

The POF sensor designed in this project exploits modulation of the evanescent field, which utilises the higher modes of light propagating in the fibre. In order to make efficient use of light power available, light must be coupled off-axis into the POF. Background perturbations, such as temperature change, must be taken out of the sensor reading. 2x1 couplers for POF are not readily available and one was designed in-house by a previous researcher, which was made entirely from plastic and was not reliable for extended use. The plastic screws had been over tightened and the threads had been destroyed, as a result the previous researcher had resorted to using Blu-Tack© to hold the fibres and holder together, rendering the interrogating signal very unstable.

3.2 Why Plastic Optical Fibre?

Silica fibre was used initially but this proved to be unsuitable for biofouling sensor purposes, as biofilm refused to grow on the surface of the silica. This may have been due to the biofilm and silica fibre surface having the same negative charge, mutually repellent. POF surface has no charge[2] in water, whereas Silica has a negative surface charge.[3] Marine bacteria often show remarkable negative charge density,[4] which may explain the refusal of biofilm to attach itself to the silica.[5] The silica fibre was also much smaller diameter than the POF used; the radius of curvature may also have been too great for the biofilm to attach itself. Silica fibre has a smooth surface, an electron

microscope image of a declad POF reveal a surface with pits and grooves (figure 4.9), giving the biofilm a key in which to attach.

The transmission fibres were step index 1mm diameter PMMA core with a fluorinated polymer cladding sheathed with a 2.2mm black polyethylene jacket, Eska Premier™ from Mitsubishi*. The sensing region had its cladding removed and the core was exposed to the measurand, the process is described in more detail in section 4.4. The POF was least attenuated at the wavelength ranges 470nm – 620nm and 640nm – 670nm with losses below 200dB/km section 2.2, the light sources chosen must therefore fall within these ranges. The light sources presently used by this project are two laser diodes (LD) one emitting at 670nm, the other emits between 620-690nm, both with maximum output of <1mW, driven by 6V transformer. Recent spectral analysis work with biofilm carried out by the author of this thesis, section 5.4, suggests that there are peak absorption wavelengths associated with the particular biofilm used in experiments at 486nm and 656nm, both wavelengths are within low attenuation regions of POF. Further investigation into this would be very interesting to wavelength match sensor to measurand. With the fast improvements in LED manufacture, improvements in light power and wavelength boundaries being pushed it will become increasingly an option to be able to produce bespoke sensors for particular targeted detection. Cells have self fluorescence related to metabolism[6] and can also be encoded with quantum dots for precise tagging of molecule/cell structure.[7]

* Appendix iii

3.3 Evaluation of Light Sources

The chosen light source should provide light at wavelengths within the lowest attenuation windows for POF which is between the wavelength ranges 470nm – 620nm and 640nm – 670nm with losses below 200dB/km, section 2.2 and at a suitable intensity. They should also be of low voltage as the sensor is to be deployed in aqueous environment, the light emitted must be of a stable wavelength and intensity for a reasonable lifetime as the sensor is designed monitoring for extended periods of time. The light source must be fairly easy to couple into a POF without too much loss of light power. Lasers seemed an obvious choice at the start of the project; they produce monochromatic parallel and narrow beams of extremely intense light ranging from mWs to 10s mWs. They are, however, generally inefficient and require high voltage power supplies, and only produces a few discrete wavelengths, depending on the active laser medium. The lasers under consideration such as Helium Neon gas laser tended to be costly (£500 upwards) of relatively high power, 5-6mW therefore careful handling and through training would be necessary for the user, they were large, therefore not easily transportable and to set-up on site. They required high voltage to power them, not recommended in wet environment and had inherent ac fluctuations. Their glass tube construction is fragile and the high voltage required made them unsuitable for wet environments. Lasers power of a greater power than 1mW would require risk assessment and laser safety precautions.

Laser Diodes

At the beginning of this project, 1999-2000, LDs were becoming cheaper due to increasing everyday devices were developed for them, e.g. CD players, games consoles, DVD players all use semiconductor lasers. They also offer high intensity coherent light, have a very long life: some datasheets list expected lifetimes for LDs exceeding 100,000

hours - over 12 years of continuous operation, have high reliability, a small emitting area, and primarily designed to operate in the infra red and red regions of the spectrum, and in green and blue since the mid to late 2000s. Now they are relatively cheap compared to lasers (less than £10). LDs are small and compact and require low driving power, therefore safer for untrained users. This project uses Class I LD of wavelength 670nm and 620-690nm, with maximum power output <1 mW. Class 1 laser devices cannot produce damaging radiation levels to the eye even if viewed accidentally since the blink response protects the eye. Prolonged staring at the laser beam however, should be avoided as a matter of good industrial safety practice. These wavelengths were chosen principally due to safety, cost and availability. The aim was to produce cheap, disposable sensors that were robust and could be operated by unskilled personnel.

Suitability for use with POF

POF has minimum attenuation in the wavelength regions of 470nm – 605nm and 640nm – 660nm all of which have a loss of 200dB/km or below, section 2.2. Although losses are greater than for silica fibre, over the short lengths the sensor is designed to operate over, these losses were acceptable. The emission wavelengths of the lasers used fall within these desirable regions.

Stability

The light sources available to this project were monitored for stability. This was carried out by launching the light from the light source into a long length of POF and taking an intensity reading every hour using an Ando photodetector, figure 3.7. At the time, the research group wished to buy a relatively expensive stabilised LD; but this proved to be the most unstable when tested. The graph in figure 3.1 shows that the two most stable LDs in the stability test proved to be those previously selected by the research group

and was already in operation. These were class II LDs of wavelength 670nm with maximum output of <1mW.

Ultrabright Leds

The sensor operates well with the chosen LDs, however with the recent introduction of ultrabright LEDs costs can be reduced without compromising the quality of sensing. The author of this thesis measured the power of various ultrabright LEDs available at the time in order to ascertain their suitability for future use in the projects sensor. Table 3.1 gives the measured power of the LEDs tested. This was measured using a calibrated standard handheld light meter as used by the laser safety office at Liverpool John Moores University, the LEDs were shone directly into the light meter. The viability of the use of these ultrabright LEDs lay in the coupling of light power from these sources into 1 meter of POF with cladding and protective sleeving intact.

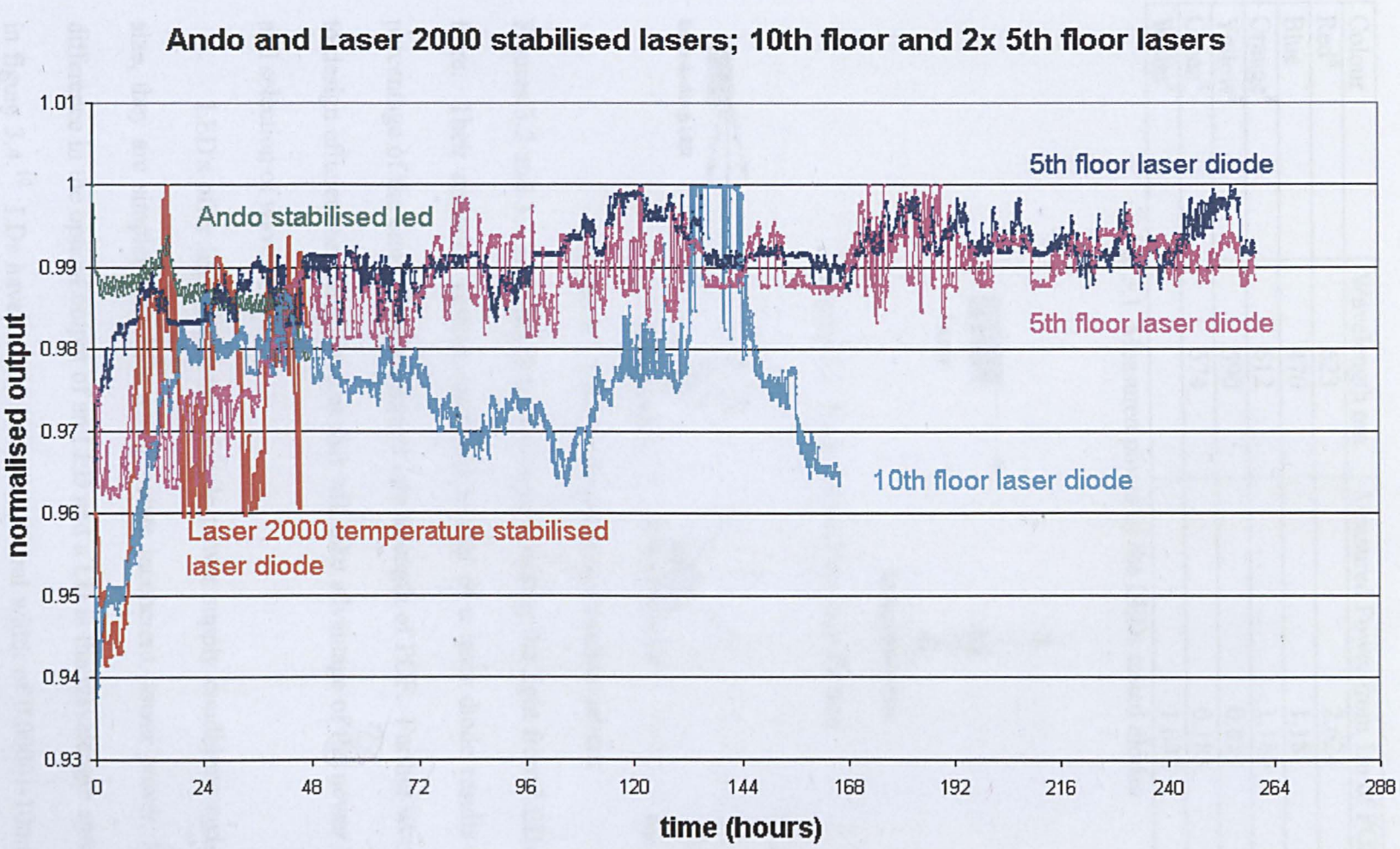

Figure 3.1 Comparison of the stability of various light sources available to project.

Colour	Wavelength nm	Measured Power from 1m of POF, mW
Red[8]	623	2.624
Blue	470	1.181
Orange[8]	612	1.180
Yellow[8]	590	0.859
Green[8]	574	0.183
White[9]		1.098

Table 3.1 Measured power of the LEDs tested diodes

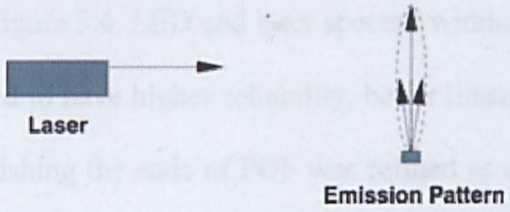

Figure 3.2 Laser Diode Emission Pattern

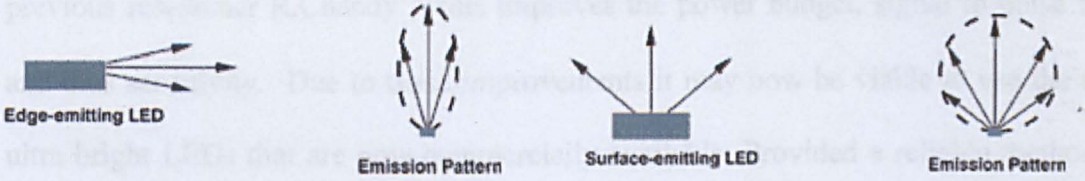

Figure 3.3 LED Structures and emission pattern

Figures 3.2 and 3.3 highlight the problem of coupling the light from LEDs into optical fibre. Their emission pattern compared to that of a laser diode results in a smaller percentage of the emitted light coupled into a length of POF. Further work is required to design efficient coupling devices that will take advantage of the newer LEDs power and selection of wavelengths.

LED's offer high efficiency, simple power supply conditions and are small in size, they are simpler than LDs and generate incoherent, lower power, light. A key difference in the optical output of an LED and a LD is the wavelength spread as shown in figure 3.4.[10] LDs have much narrower spectral width of 0.00001-10nm Full-Width Half-Maximum (FWHM) compared to that of an LED, 40-190nm FWHM.

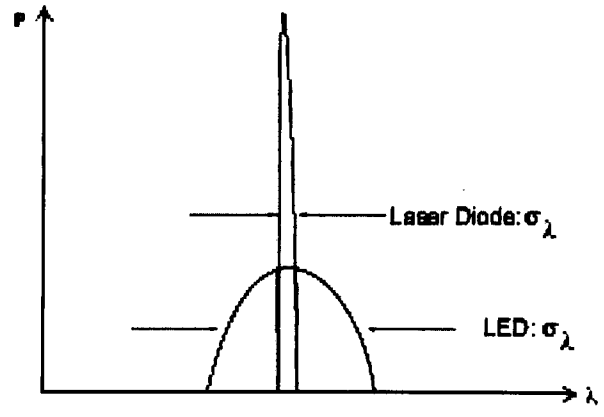

Figure 3.4 LED and laser spectral widths

In their favour LEDs tend to have higher reliability, better linearity and lower cost than LDs. The method of polishing the ends of POF was refined as detailed in chapter four, section 4.3.1, resulting in up to 10 times light coupled into the fibres compared with the previous researcher R.Chandy[11], this improves the power budget, signal to noise ratio and thus sensitivity. Due to these improvements it may now be viable to use the new ultra bright LEDs that are now commercially available. Provided a reliable method of coupling is arrived at, better than 50% of the available light guided into the POF for sensing purposes would be acceptable, given that the measured power of the blue ultrabright LED using the laser safety officers powermeter was in excess of 2mW. Careful use of lenses or the manufacture of customised couplers should be investigated. The pigtailing method of coupling light from the LED into a POF has been refined[12]. The polycarbonate dome of the LED has been chemically etched using concentrated sulphuric acid revealing the emitting area, however a method of physically holding the LED and POF in position needs to be developed. Polishing the polycarbonate dome has been precarious as was drilling into the dome.

Wavelength Matching to Measurand

The range of wavelengths now available enables the design bespoke sensors by matching light source with target measurand.[13] Spectral analysis work with biofilm described in section 5.4, indicates there are peak absorption wavelengths associated with the particular biofilm used in experiments at 486nm and 656nm. Both these wavelengths coincide with low attenuation regions of the POF transmission spectra. Matching the spectral identity to the wavelength of a light source could further improve detection. Figure 3.5 was obtained by the author of this thesis and shows the spectrum of various ultrabright LEDs, most noteworthy are the blue and red and orange, which have peak output coinciding with the peak absorption of the biofilm. The rapid improvements in LED manufacture, in terms of light power and wavelength emission boundaries are constantly being pushed, enhancing the possibility of producing bespoke sensors for targeted detection.

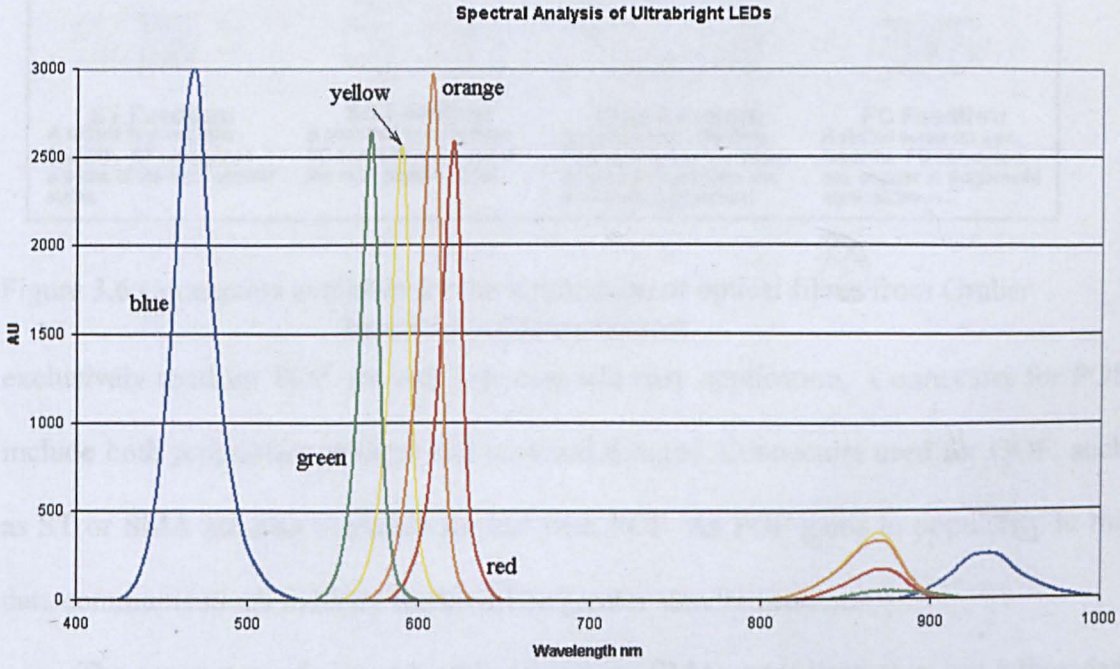

Figure 3.5 Spectral analysis of blue, red, green yellow and orange ultra bright LEDs

3.4 Commercially Available Components

Connectors

Most optical fibre connectors are made for the communications industry which generally uses GOF, these tend to be much smaller in diameter ~125μm compared with CK40 1mm diameter POF. Figure 3.6[14] show a variety of connectors available for the termination of optical fibre. Commercially available POF Cable Connectors are

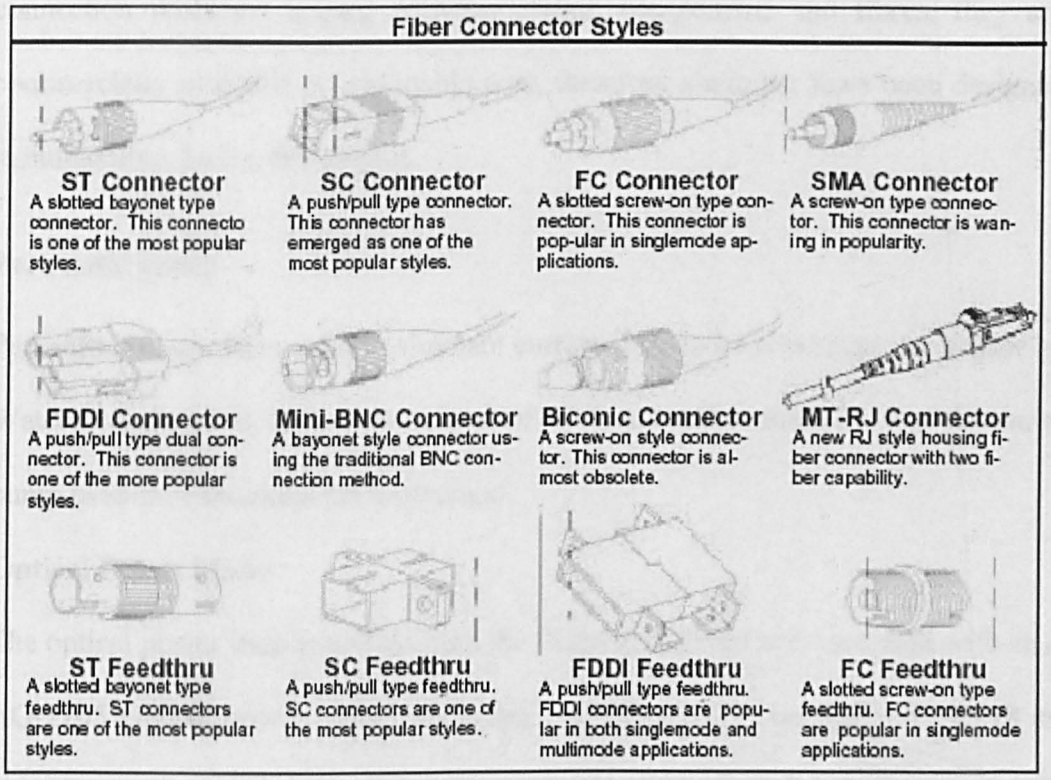

Figure 3.6 Connectors available for the termination of optical fibres from Gruber Industries cable connectors

exclusively used for POF are very low cost and easy application. Connectors for POF include both proprietary designs and standard designs. Connectors used for GOF, such as ST or SMA are also available for use with POF. As POF gains in popularity in the data communications industry there will be greater standardisation.

The connectors of choice by this project are SMA connectors, they use a threaded plug and socket. Devices and detectors used in this project had SMA plugs, but in addition they are compact and have exceptional mechanical durability. It is quick to

assemble as it requires no special tools, crimping or gluing and is suitable for 1mm polymer fibre with 2.2mm jacket. These connectors are being phased out due to communications industry advances as materials and components are standardised, which poses a problem to 1mm diameter POF sensor work, few suppliers now stock this type of connector, Harting[15] is one of the few reliable sources in the UK.

The novel use of commercially available components in this sensor results connection problems arising between certain components and fibres, they are not commercially available at reasonable cost, therefore a number have been designed and manufactured during this project.

Peristaltic pump

Peristaltic pumps were used to simulate current flow to be experience by sensor in use. Watson-Marlow Ltd, H.R. flow inducer of the type MHRE, manufactured the peristaltic pump used to re-circulate the measurand.

Optical Power Meter

The optical power transmitted through the fibres is detected and measured with an Ando AQ-2105 Optical power meter which has two channels. Two Ando AQ-2718 silicon photodetector sensors units operating between wavelengths 400-1150nm were used.

Figure 3.7 Ando AQ-215 Optical power meter

3.5 Components Designed During Project

The intrinsic POF Evanescent Field biofilm sensor was to be optimised. This includes lowering the cost by developing a light powermeter of acceptable sensitivity made from readily available components, ruggedisation of the sensor, ensuring that alignment within the sensor unit would stay true and would not require expert training to deploy and improving the experimental set-up to reflect the environment in which it was to be used.

3.5.1 Optical Powermeter

To optimise the sensor an optical powermeter that was sensitive, self-contained, low voltage with low noise and low cost was required. The project developed a transimpedence amplifier circuit, based on a design supplied by the manufacturer of the operational amplifier used. The optical powermeter needed to be made from readily available components; however a connector was required to couple light from the reference and sensor fibres to a photodiode. Due to the large NA of the wide diameter POF the light emerging from the end of the fibre is highly divergent, hence a wide diameter photodiode (0.5mm) was required to ensure that the maximum amount of the signal light was collected.

Figure 3.8 is a pre-existing transimpedence circuit designed for the CLOOPT project[11] and was presented to the author of this thesis near the end of the project.

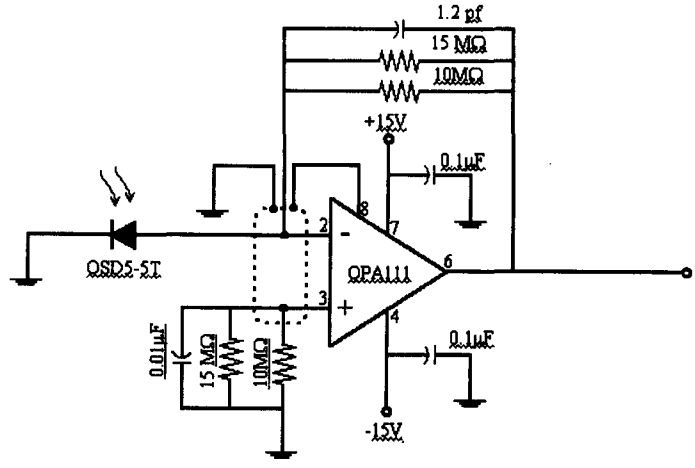

Figure 3.8 Transimpedence amplifier

It is based on the design in figure 3.9 from the Burr-Brown OPA111 specification sheet for a "sensitive Photodiode amplifier"

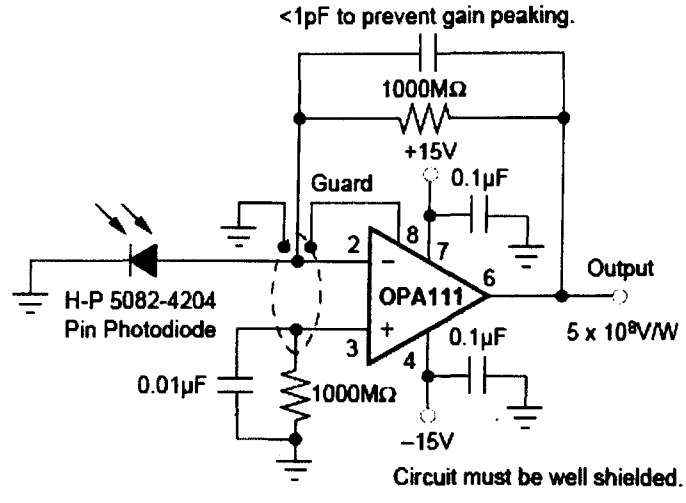

Figure 3.9 Sensitive Photodiode Amplifier circuit from the Burr-Brown OPA111 specification sheet

Incident light on the OSD5-5T silicone photodiode is transformed into a photocurrent which supplies the inputs of an OPA111 instrumentation-grade FET pre-amplifier. The amplifier provides the amplification and filters the high frequency components of the signal using the 1.2pF capacitor. The transimpedence amplifier converts a photocurrent into a voltage using a feedback loop. The optical and amplification module was constructed, based on commercial operational amplifiers.

Centronic OSD5-5T silicone photodiodes[16] (figure 3.10) are particularly suited to low light level applications from 430-900nm where the highest signal to noise ratio is important.

OSD5-5T
Active area = 5mm^2 2.52 diameter
Responsivity at 436nm = 0.18AW^{-1} min 0.21 AW^{-1} typical
Dark Current = 2 nA max 0.5 nA typical
Capacitance at V_r=0V 130pf max
Capacitance at V_r=12V 35pf max

Series 5T –Typical Spectral Response

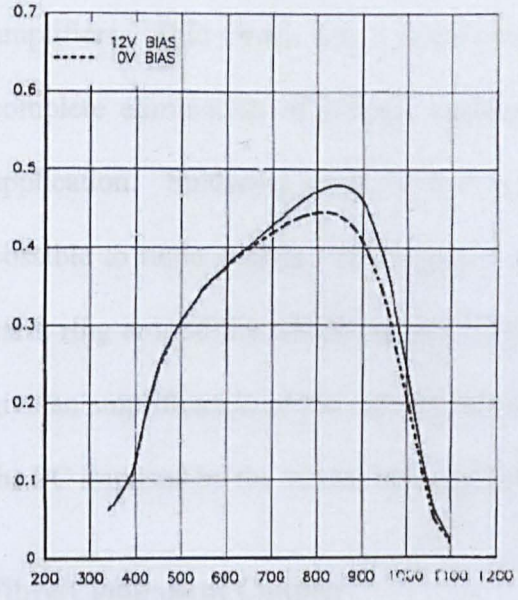

Series 5T – Typical Capacitance versus Bias Voltage for a given Detector Area

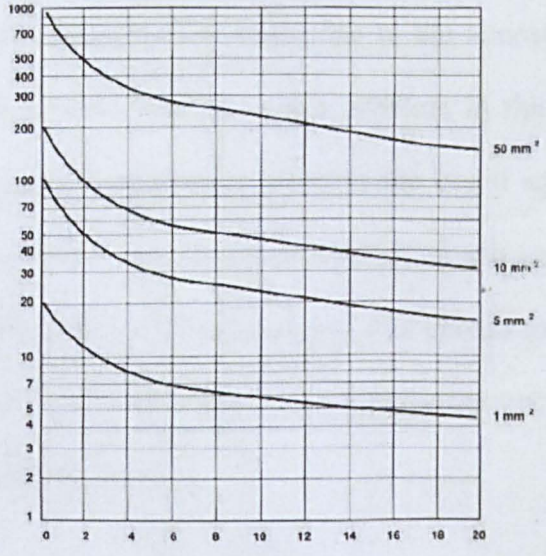

Figure 3.10 Centronic OSD5-5T silicone photodiode specifications

The photodiode has a large window which allows for simple butt-coupling, maximising light collection from the POF sensor and are simple to integrate into an amplifier circuit without specialist power supplies. The Ando powermeters also use silicone photodetectors and so the technology has been proven.

Best advantage may be taken of the photodiodes behaviour as an extremely linear current generator if it is operated into a very low resistance in comparison with the diode shunt resistance. The large diameter of the POF and therefore large

acceptance angle means that the light from the end of the POF diverges as it emerges. The large sensing area, 5mm^2, of the photodiode was required to ensure that all of the light from the optical fibre was collected. This is not a standard way to couple light from an optical fibre and so housing is not commercially available for optical fibre connection, hence one was designed, figure 3.11.

Burr-Brown OPA111 operational amplifiers[17] are precision monolithic dielectrically isolated FET operational amplifiers. Noise, bias current, voltage offset, drift, open-loop gain, common-mode rejection and power supply rejection are superior to BIFET amplifiers. This circuit has a linear response and gives low noise due to the almost complete elimination of leakage current but is slow which is not a problem in this application. Soldering must be kept neat and components as close to the board as possible to radio pickup. Mains noise was reduced with the use of capacitors and an earth ring around the whole circuit. The value of the feedback resistors was chosen to give an amplification of the signal to below 10V DC, which was the limit of the input to the PC imposed by the virtual instrument LabView© software.

Fibre/Component Coupler

The large sensing area of the photodiode, 5mm^2, was required to ensure that all of the light from the optical fibre was collected. As this is not a standard way to couple light from an optical fibre there is no commercially available housing for optical fibre connection and so one was designed.

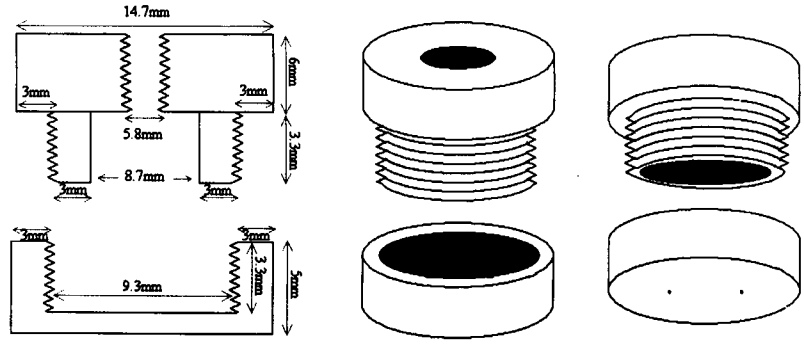

Figure 3.11 Design of fibre/component holder

Any changes in alignment between components due to inappropriate handling of the sensor set-up will result in erroneous readings. A fibre/photodiode holder was designed as shown in figure 3.11 to immobilise the ends of fibres in alignment with the photodiode used in the transimpedence circuit to achieve maximum fibre signal coupling to the photodiode. An SMA connector is screwed into the top of connector, the component is held in place via the holes in the base, which also insulates the contacts from each other. The optical fibre is then inserted into the SMA connector whilst the transimpedence circuit is operational and adjusted until a maximum output is detected. The SMA connector is then tightened holding the fibre in optimum orientation. The holder eliminates light that is not from the sensor, negating erroneous readings.

The module can be easily adapted to couple fibre to various components. Alignment in optical physics cannot be over-emphasised. The possibility of a change in the signal not due to sensor/measurand changes would render the sensor most inaccurate.

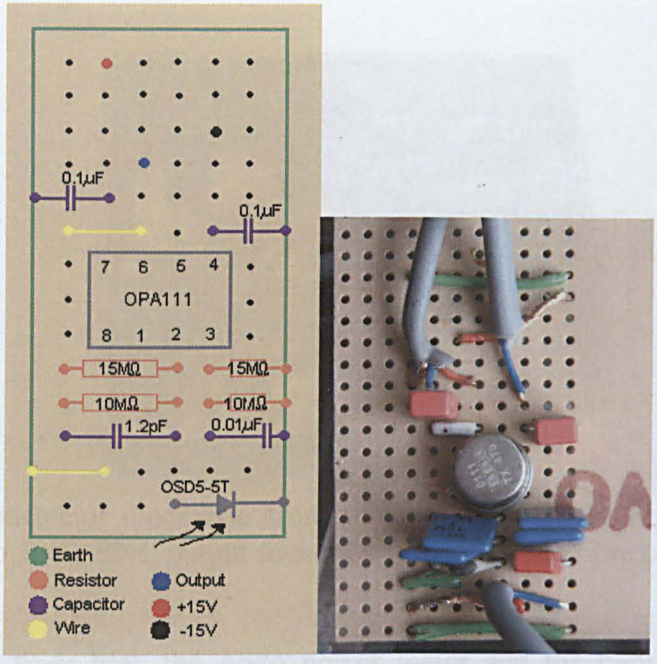

Figure 3.12 circuit board of transimpedence amplifier circuit

This fibre/component connector was incorporated into the transimpedence amplifier box and provided a secure connection to the detector. The circuit was trialled on the project board in figure 3.12 to confirm operation:

Figure 3.13 shows the optical powermeter built for this project using readily available components, excepting the photodiode/fibre connector specifically designed by the author to immobilise the reference and sensor fibres and to eliminate all other light. The box was earthed and provides a Faraday cage, filtering out radio noise, all Earths were connected. Perspex is placed in the bottom of the box to insulate the circuit from the earthed box. The circuit boards were fixed in position within the box to reduce movement. Figure 3.13 clearly shows the photodiode/fibre connectors secured to the optical powermeter housing.

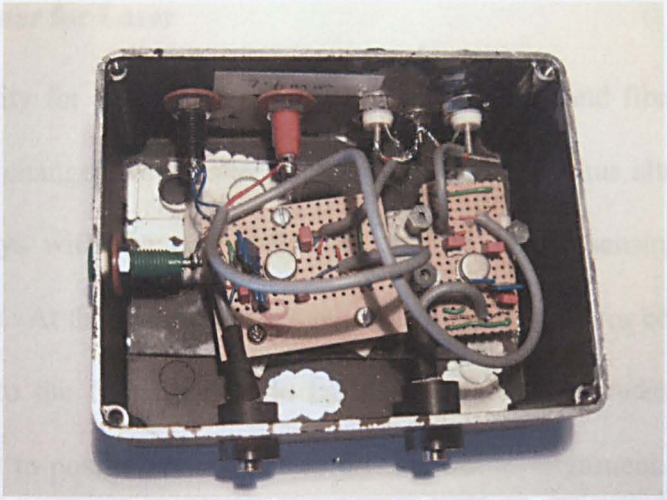

Figure 3.13 photodetector clockwise from the left wall, Earth, negative and positive power sockets, two 50Hz BNC output sockets, two photodiode/fibre connectors.

The signal from both the Ando power meter and the circuit was monitored (Figure 3.14) using the same lengths of fibre, laser diode light source and Y-splitter. Carried out on different days and location, revealed the Ando power meter with 0.9-0.1% noise and diurnal drift of 0.5%. The circuit yielded a steady 0.2% noise and diurnal drift of 0.35%, resulting with a circuit that cost less than £100 to build with comparable operating limits to a power meter costing £5,000.

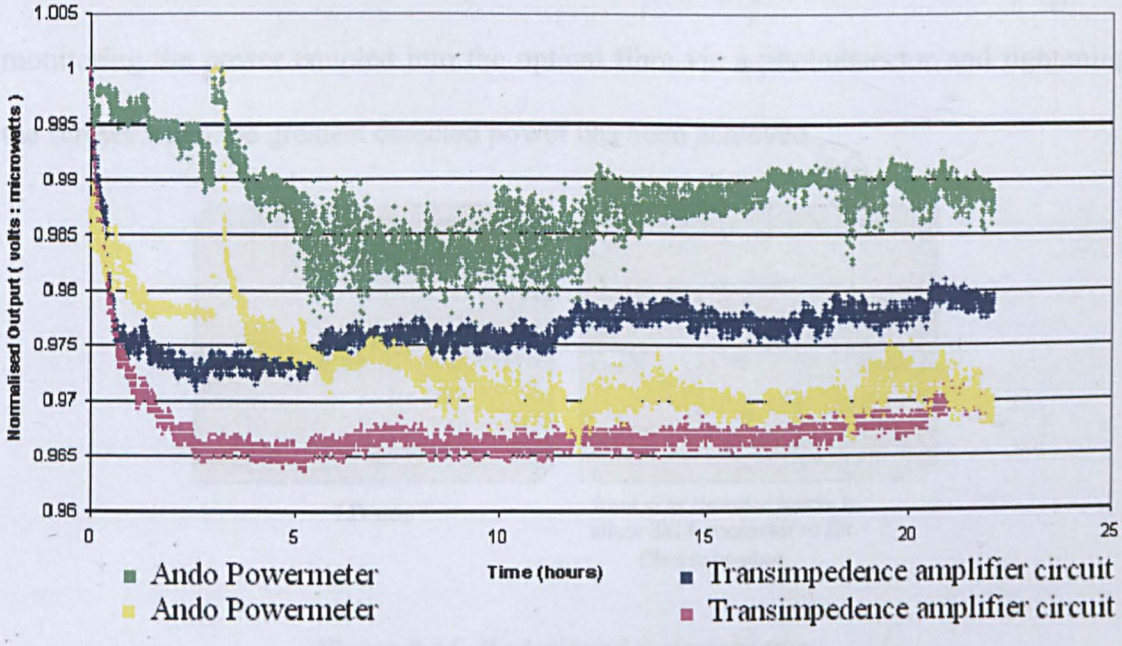

figure 3.14 stability test of Ando powermeter and photodetector built during this project from readily available components

3.5.2 X-Y Positioner for Laser

A high priority for optical fibre sensing is that the LD and fibre alignment does not change as any changes would alter geometry of the fibre, thus altering the incident angles of light rays with the core reflecting surface during sensing, giving rise to erroneous readings. At the start of the project, the original stage for coupling light from the laser diode into the fibre was made from plastic and was rudimentary and very imprecise, difficult to position and prone to drifting out of alignment. This resulted in inefficient coupling and the position of the fibre in relation to the laser diode would change yielding erroneous readings.

An improved x-y positioner was designed and made of brass for the LD housing (figure 3.16). The x-y positioner has slotted holes to allow horizontal and vertical positioning which can be immobilised in its final position by tightening the relevant pairs of screws. The x-y positioner has a threaded holder that allows an SMA connector to be fixed onto it, again immobilising the optical fibre. The optical fibre is fixed in position, the horizontal position of the x-y positioner is determined by monitoring the power coupled into the optical fibre via a photodetector and tightening the screws when the greatest detected power has been achieved.

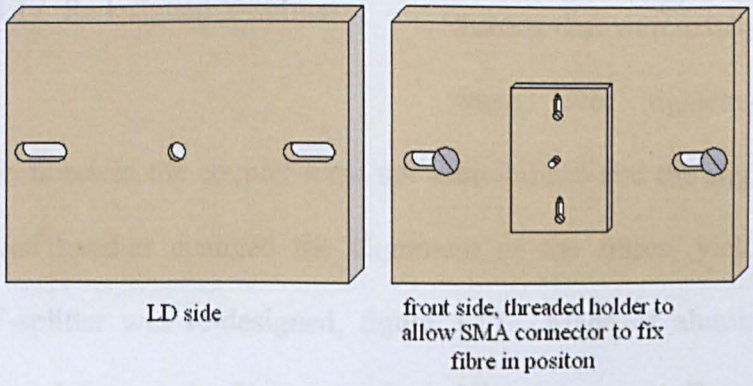

Figure 3.16 Redesigned x-y positioner

The same procedure is carried out for the vertical positioning. Optimal alignment of the POF with the LD was achieved, coupling the maximum power into the fibre thus improving the sensitivity of the sensor, and ensured the fibre did not drift from its position resulting in erroneous readings.

3.5.3 Y-Splitter

A Y-splitter divides light signal between the sensing fibre and a reference fibre for common mode signal rejection, coupling light into both fibres off-axis, which conveniently ensures the outer most modes are excited. It is the outermost modes that are attenuated most by the properties at the core/cladding interface of the evanescent field sensors developed by this project. The existing Y-splitter was made entirely of plastic parts held together with plastic screws, with threads that were easily compromised when over tightened and were ineffective. The fibres in the coupler were not immobilised and the slightest knock by an inexperienced handler changed the alignment of the fibres, yielding erroneous results. The Y-splitter was re-designed, figure 3.17. Made of aluminium and held together with metal screws, the fibres were immobilised once set. Determined tugging at the fibres did not dislodge them.

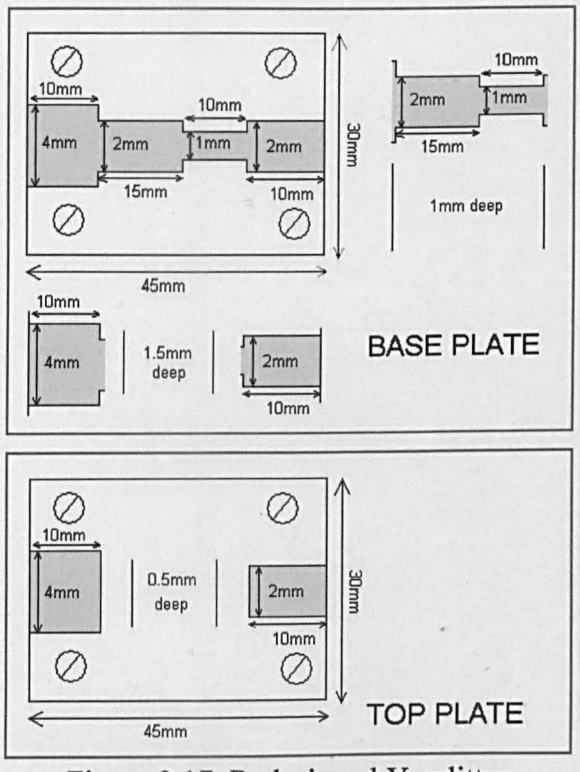

Figure 3.17 Redesigned Y-splitter

Other groups have used the Y-splitter and continue to do so in their research. Dr Kevin Kuang Singapore University (formerly Liverpool University) presently uses the Y-splitter in his on-going research developing strain gauges for uses in structurally health indicators e.g. strain; vibrations; impact damage; natural fatigue. Dr Patricia Scully of University of Manchester (formerly of Liverpool John Moores University) continues to use the Y-splitter with her on-going research into optical fibre sensors.

3.5.5 Flowchamber Redesign

Previous work by R. Chandy[11] was performed on an experimental configuration, which could be improved upon. Figure 3.11[11] shows the original design for the experiment.

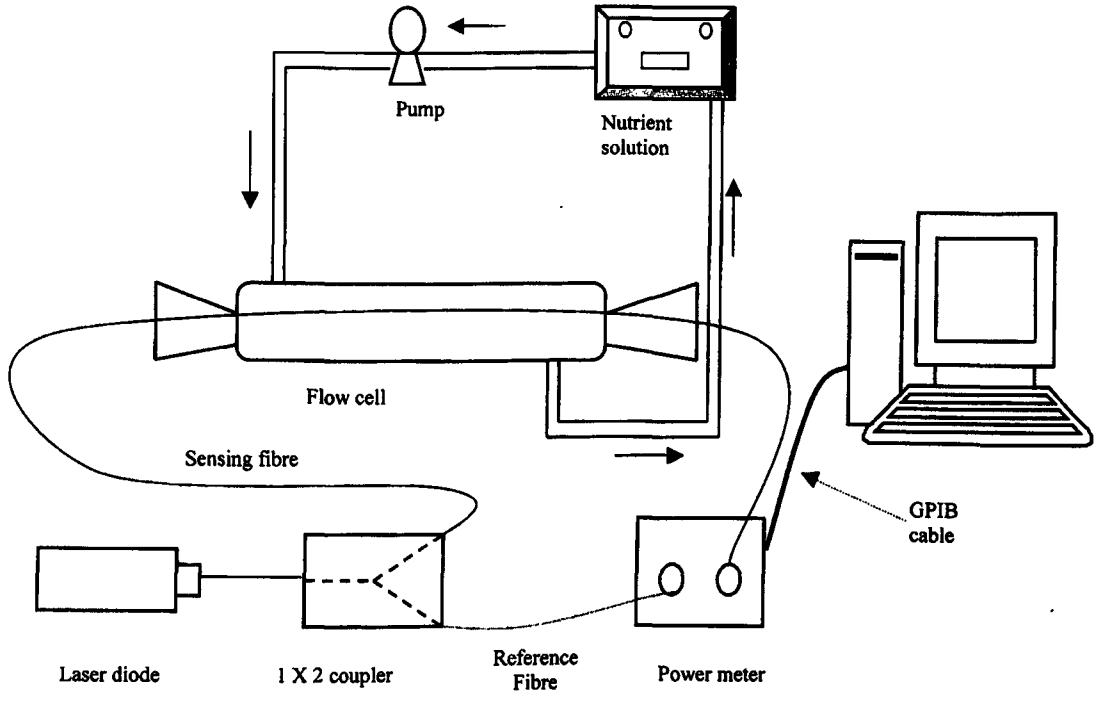

Figure 3.18 Original design of flowchamber.

This flowchamber design did not allow thorough drainage of the system, the measurand from the previous experimental run did not flush out efficiently without compromising sensor fibre alignment, giving rise to optical drift. The measurand was pumped through the system under pressure, which did not accurately mimic conditions that the sensor was to be ultimately implemented. The fibres themselves were clamped in place at both points of exit from the flowchamber to achieve a water-tight seal, causing the outermost modes of the light propagated in the fibre to be stripped out, the very modes required by an evanescent field sensor.

A new design was proposed. The placement of the drainage holes at one end of the flowchamber at its lowest point ensured complete removal of measurand. This was

possible without compromising the position of fibres; it was not necessary to touch the flowchamber during this process.

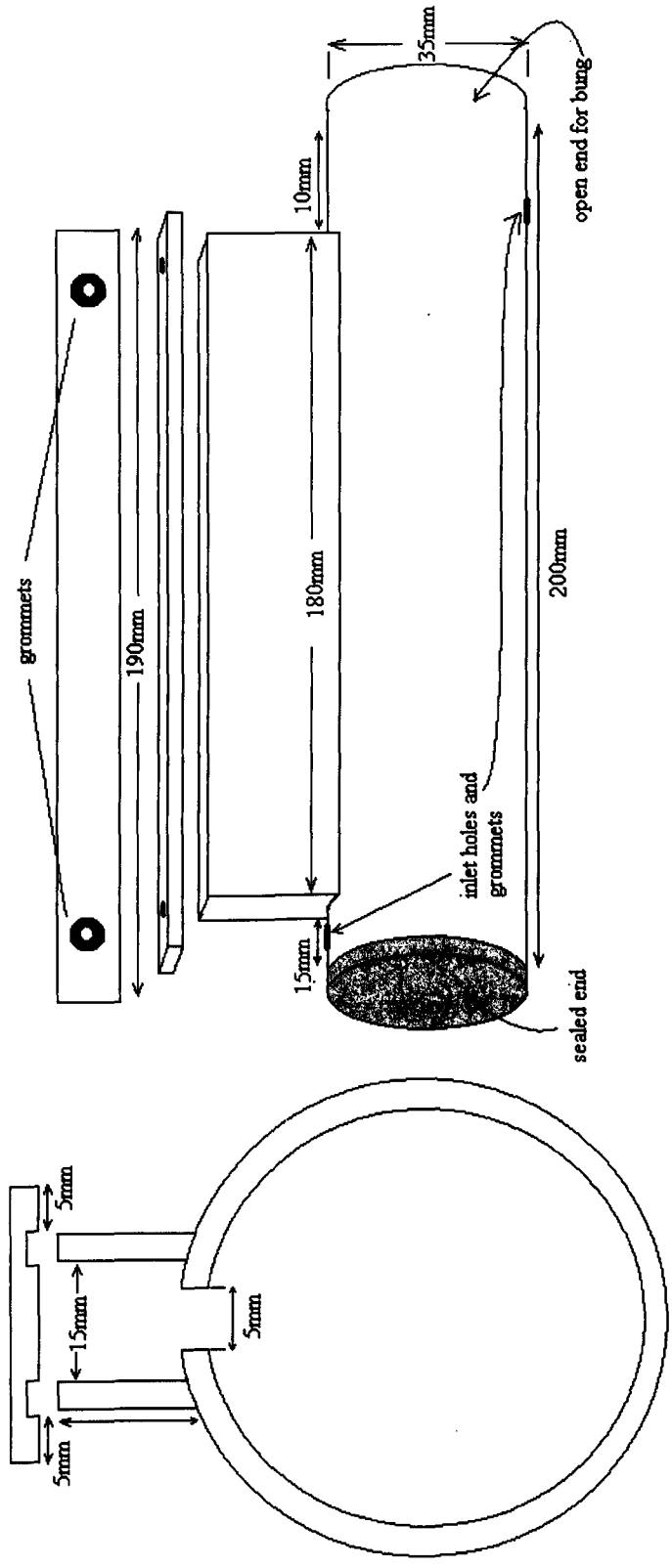

Figure 3.19 Redesign of experimental setup

The sensing fibre was held in position with SMA connectors in the lid of the flowchamber, which also reduced evaporation over long periods of sustained sensing.

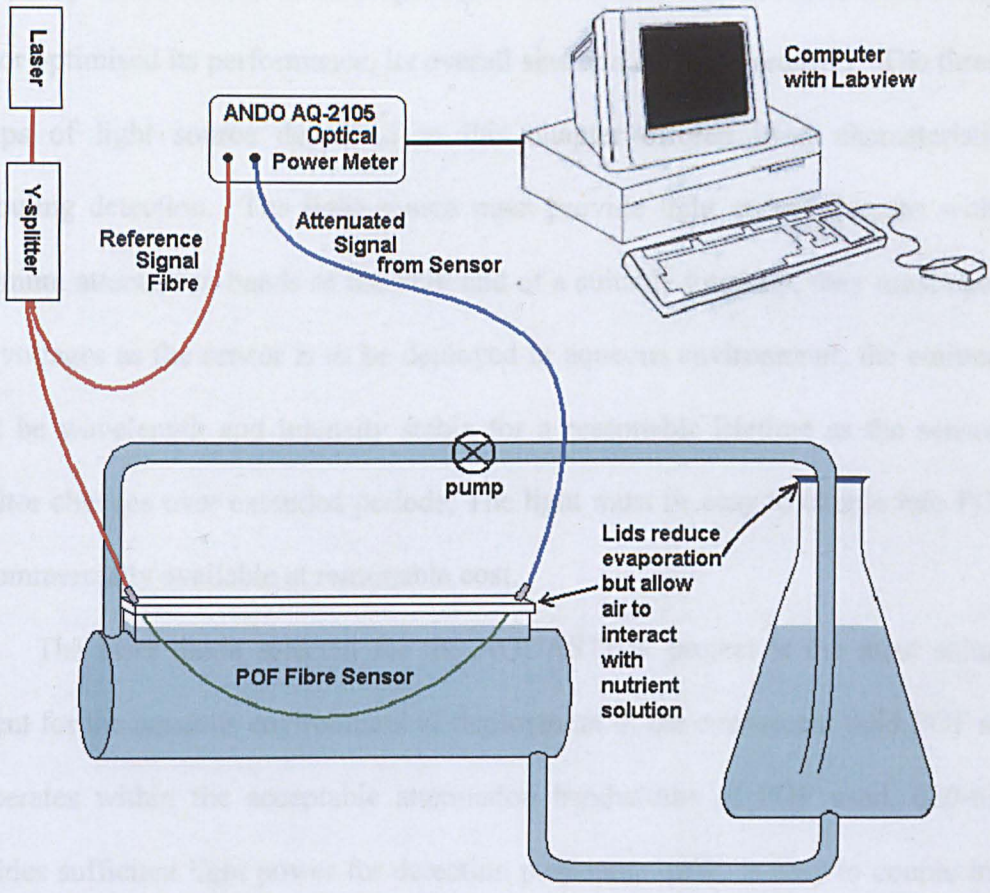

Figure 3.20 Operational configuration of POF evanescent field sensor.

There was no longer pressure on the fibre and the outermost modes could propagate unhindered. The measurand was no longer circulated under pressure in the system. The height of the liquid in the flowchamber was regulated by the height of the liquid in the reservoir and the system operated in normal atmospheric pressure similar to that of its intended use.

3.6 Summary

The components chosen and designed for the intrinsic evanescent field POF biofilm sensor optimised its performance, its overall size and cost was reduced. The three main groups of light source described in this chapter offered ideal characteristics for biofouling detection. The light source must provide light at wavelengths within the minimum attenuation bands of the POF and of a suitable intensity, they must operate at low voltages as the sensor is to be deployed in aqueous environment, the emitted light must be wavelength and intensity stable for a reasonable lifetime as the sensor is to monitor changes over extended periods, The light must be easy to couple into POF and be commercially available at reasonable cost.

The laser diode selected for the AQUASTEW project is the most suitable at present for the aqueous environment of deployment of the evanescent field POF sensor. It operates within the acceptable attenuation bandwidths of POF used, 620-690nm, provides sufficient light power for detection purposes, 1mW, is easy to couple into the sensor due to the narrow emission pattern.

Improvements in LEDs introduce high enough powered light sources, as feasible alternatives with the extra scope of wavelength matching to target measurand at much lower costs and enabling the development of throwaway devices. Coupling the available light power from LEDs is the main obstacle at present.

Connectors formed a crucial part of an optical fibre sensor link; they enabled light to be coupled into the fibre system, from fibre to fibre and finally to the detector. They had to provide reliable, stable alignment, must be robust, and easy to terminate fibres by cutting or polishing. SMA coaxial connectors with a screw type coupling mechanism, available from Gruber Industries Inc., is the connector of choice of this

project as devices such as power meters had SMA connectors and held the fibres firmly in place. These are being eased out by the telecommunications industry as they make advances in their field, moving towards bayonet style connectors (Figure 3.6 Gruber Industries Inc.). FC connectors were also considered, however they were not made to a high standard and had rough burrs inside that damaged the fibre, compromising mode stability.

Several components were custom designed for this project and have resulted in optimised performance of the sensor:

- A self contained powermeter made from commercially available components in a transimpedence amplifier that rivalled commercially available powermeter. The circuit was of a historical design but the author of this thesis has refined it to eliminate as much noise as possible by reducing pick-up by components through the use of a PCB and housing the circuitry in an isolating solid aluminium case. The resulting module is a much smaller and rugged package that will ultimately lead to miniaturisation and self-containment at reduce costs.
- A housing unit that immobilises fibre alignment to photodetector.
- Increase and stabilisation of power coupled into sensor due to x-y positioner which allows fine positioning of fibre to LD alignment.
- Stabilisation of reference signal and optimisation of sensing signal by off-axis coupling, ensuring that the high order modes utilised have the largest population due to the Y-splitter, and not removed by mode stripping.
- The redesigned flowchamber holds the optical fibre sensor in position without mechanical strain or perturbations, the system operates at normal atmospheric pressure, a closer approximation to its final intended deployment.

References

[1] MN Taib, R Narayanaswamy, "Solid-state Instruments for Optical Fibre Chemical Sensors A Review" Analyst, vol.120, pp1617- 1625, 1995

[2] NW Hayes, CJ Tremlett, PJ Melfi, DJ Sessler, AM Shaw, "Uranyl-specific Binding at a Functionalise Interface: A Chemophotonic Fibre Optic Sensor Platform", Analyst, No.133, pp616-620, 2008

[3] J Rayss, G Sudolski, "Ion Adsorption in the Porous Sol-gel Silica Layer in the Fibre Optic pH Sensor", Sensors and Actuators B, Chemical. vol.87, No.3, pp397-405, 2002

[4] S Leone, A Silipo, EL Nazarenko, R Lanzetta, M Parrilli, A Molinaro, "Molecular Structure of Endotoxins from Gram-negative Marine Bacteria: An Update", Mar Drugs, vol.5 No.3, pp85-112, 2007

[5] M Fletcher, GI Loeb, "Influence of Substratum Characteristics on the Attachment of a Marine Pseudomonad to Solid Surfaces", Appl Environ Microbiol, vol.37, pp67-72, 1979

[6] JC Pickup, F Jussain, ND Evans, OJ Rolinski, DJS Birch, "Fluorescence-based Glucose Sensors", Biosensors and Bioelectronics", vol.20, pp2555-2565, 2005

[7] P Jorge, MA Martins, T Trindade, JL Santos, F Farahi, "Optical Fiber Sensing Using Quantum Dots", Sensors, vol.7, pp3489-3534, 2007

[8] Toshiba LED Lamp InGaAlP: Red Light Emission TLSH180P, Orange Light Emission TLOH180P, Yellow Light Emission TLYH180P,Green Light Emission TLGE183P

[9] Nichia Ultra bright white LED,NSPW310A 20mA 3mm

[10] KS Schneider, "Fiber Optic Communications for the Premises Environment" Chapter 2, www.telebyteusa.com/foprimer/foch2.htm, accessed 4th December 2008

[11] R Philip-Chandy, PJ Scully, D Thomas, "A Novel Technique for On-line Measurement of Scale using a Multimode Optical Fibre Sensor for Industrial Applications", Sensors & Actuators B, vol.71, pp19-23, 2000

[12] MS Whalen, TH Wood, "Effectively Nonreciprocal Evanescent-wave Optical Fibre Directional Coupler", Electronic Letters, vol.21, No.5 pp175-176, 1985

[13] M Yokota, T Okada, I Yamaguchi, "An Optical Sensor for Analysis of Soil Nutrients by Using LED Light Sources", Measurement Science and Technology, vol.18, pp2197-2201, 2007

[14] Gruber Industries Inc., 21439N. 2nd Ave. Phoenix, Arazona, 85027 USA,www.gruber.com

[15] HARTING Ltd., Caswell Road, Brackmills Industrial Estate, Northampton, NN4 7PW, UK., Tel. +44 16 04 / 76 66 86, 82 75 00, Fax. +44 16 04 / 70 67 77, http://www.HARTING.co.uk

[16] Centronic Ltd, Centronic House King Henry's Drive, Croydon, Surrey, CR9 0BG, England

[17] Texas Instruments

CHAPTER FOUR

Preparing Plastic Optical Fibre for Sensing

4.1 Introduction

Optical fibres are manufactured to conform to data transmission specifications to be immune from their surroundings; electromagnetically, chemically and physically, to preserve launch conditions and minimise signal loss.

The nature of intrinsic optical fibre sensors is to allow target exterior conditions affect the launch signal; hence the optical fibre must be modified to make it sensitive to the external perturbation. The various methods of modification are described in this chapter.

Refractive index changes and any scattering properties[1] of the cladding contribute to the attenuation of light power propagating in the optical fibre core. A fraction of the light signal coupled into a 1mm fibre diameter optical sensor escapes into the cladding via leaky modes[2,3] to contribute to the evanescent field and as tunnelling rays. These leaky modes are utilised to monitor changes in the medium surrounding the core acting as an extended cladding.

The fraction of power propagating in the cladding of a single mode fibre with respect to total guided power is higher, greater than 50%, however multimode fibre have a higher proportion of tunnelling rays which exist much further away from the fibre core,[4] over many kilometres.[5,6]

The attenuation due to refractive index change of the cladding of a PMMA 1mm diameter optical fibre was characterised during this project and is described in chapter six. The ends of the POF must be terminated in such a way as to optimise the coupling of light power. Effective polishing is essential and a good working practice is described that consistently delivers required results.

The cladding layer of POF is designed to ensure maximum total internal reflection of light signal launched into it. This is desirable in telecommunications; however is a

distinct disadvantage in intrinsic evanescent field sensor technology where the signal launched must be able to interact with the surrounding measurand. The POF must be altered to achieve a sensitised area, via simple removal of the cladding and the reshaping of the fibre contour, which increases the ratio of light propagating in the evanescent field, further enhancing the sensitivity of the sensor.

Much research has gone into the efficient removal of the cladding of POF without compromising the core.[7] The revealed core must be undamaged and optically clear to allow efficient coupling of light into the evanescent field to be affected by the measurand.

The transmission fibre used in this project is Mitsubishi Eska Premier [Step index; NA 0.5; Refractive Index of core: 1.49] and the sensor fibre used is Raytela™ POF from Toray Industries PFU-FB1000,which has a 980 μm diameter core and 20 μm thick cladding.

Varying the diameter of the POF allows further manipulation of the modes within the core.[8] The penetration depth of the evanescent field and the proportion of power within this field in the smaller diameter section are increased.[8] The change in diameter is itself useful for use when fibres of different diameters are used within a system, in coupling fibres of different dimensions or interfacing fibres to devices. A length of fibre with gradually decreasing diameters is referred to as a tapered fibre. An end-taper is a fibre with the truncated end diameter diminishing, a mid-length tapered fibre has a diameter that gradually decreases and then gradually increases. These tapered fibres must also be undamaged and optically clear. Methods for achieving this in silica fibre are already well established[8,9] and usually involved heating a target area of the fibre and straining the fibre but were not immediately transferable to POF as the temperatures

required were much lower than for GOF. The method for achieving tapers in POF was achieved through many developmental stages and is presented in this chapter.

4.2 Plastic Optical Fibre Cable

Plastic optical fibre as supplied by manufacturers require further processing before they are suitable for sensor purposes. POF can be supplied with a protective jacket to protect the fibre core and cladding from damage. This is usually used for transmission purposes, not for sensing (Mitsubishi Eska Premier[χ] [Step index; NA 0.5; Refractive Index of core: 1.49; Transmission Loss 0.15dB/m; Bandwidth 40MHz/50m; operation temperature [55 ~85°C]). The fibre end must be revealed from this sleeve and well polished to achieve the most efficient coupling of light power into the optical fibre core. Simple procedures can minimise damage experienced by the fibre as any nicks or roughening along the fibre will result in loss of signal. POF is also supplied without the protective sleeve, just fibre core and cladding.[10] This type is used for sensing purposes; but has to be modified in order to be used as sensors.

The fibre cladding is removed in order to expose the fibre core to the measurand; thereby the measurand becomes the effective cladding allowing changes occurring at the fibre core/measurand interface to be detected. A reactive cladding may be coated onto the exposed core to optimise the reaction with the target measurand that would further facilitate detection of the specified measurand.

In order to make the sensor more sensitive a tapered fibre is desired. This chapter aims to describe how the procedure has been optimised through many stages of improvement culminating in an automated repeatable procedure resulting with optically

[χ] Appendix 3

clear consistent tapering. Tapered fibres can also be used to interface fibres of differing dimensions.[11]

4.3 Termination and Coupling

The aim of this section is to describe an optimum method of terminating and coupling fibres. This includes cutting, polishing, transferring light from one optical fibre core into other (one or more) optical fibre core with the least amount of loss. The POF is initially cut through the protective plastic jacket with either a fibre cutter or a razor blade. The protective plastic jacket must then be removed without damage to the core or cladding as this would result in signal loss and therefore reduce the sensitivity of the instrument. The traditional method of terminating fibres is to cut and polish.

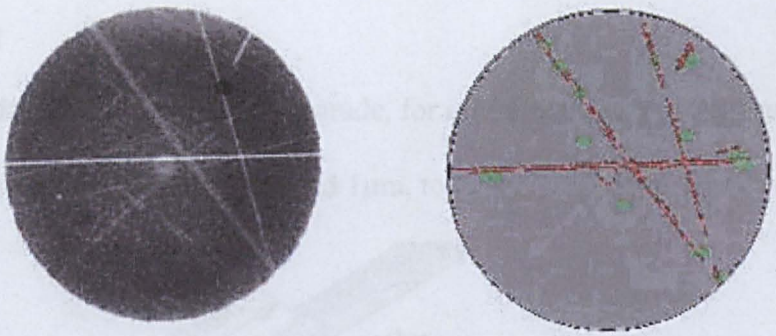

Figure 4.1 Image of a badly polished fibre end, the surface scratches scatter valuable sensing light signal, clearly shown on the illuminated right image

4.3.1 Polishing Ends of Fibre

The fibre ends must be finished to a mirror-like finish minimising scattering to ensure the most efficient coupling of light. Any defects on the surface of the fibre end will scatter the signal, resulting in less light available for sensing purposes, therefore loss in sensitivity of the instrument.

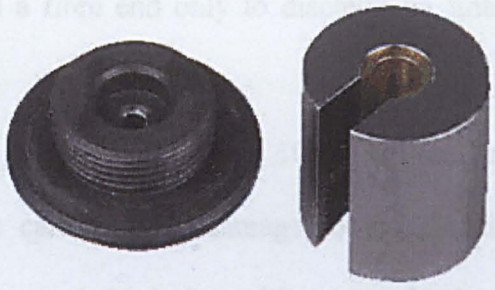

Figure 4.2 Polishing jig is spring loaded; POF is inserted into an SMA holder, which is held in place by the jig.

4.3.2 Equipment Required for Polishing:

- Spring loaded polishing jig, SMA POF holder that immobilises the fibre
- Sheet of plate glass to guarantee a smooth surface on which to carry out the polishing
- wet and dry abrasive paper, 1200 grade, for initial removal of rough material
- Lapping film 3M©: 30μm, 9μm and 1μm, to achieve the required mirror-like finish

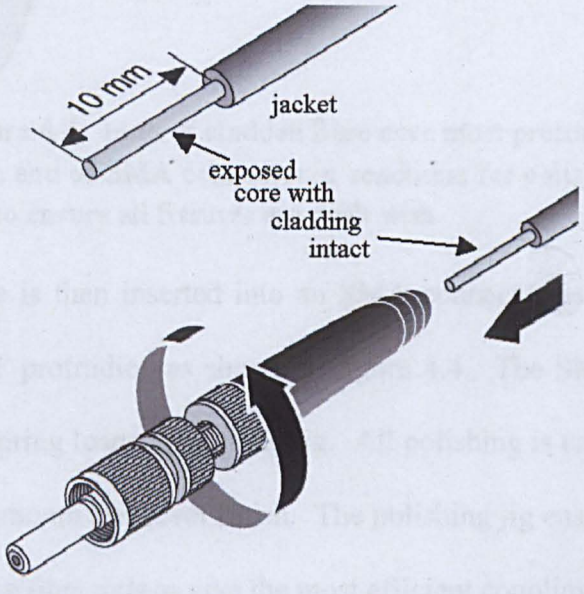

Figure 4.3 10mm fibre jacket stripped ready for insertion into SMA connector for polishing

4.3.3 Polishing Procedure:

The initial polishing is carried out to ensure that any mm deep fissures in the fibre due to cutting with a fibre cutter or razor blade is removed, it is deflating to have

meticulously polished a fibre end only to discover on final inspection a crack in the fibre.

1. If the fibre has protective sleeving, 10mm of the protective sleeving must be removed with great care without damage to the cladding. This is achieved by carefully nicking all round the jacket with a razor blade, stopping short of the fibre cladding. Using nose pliers, with insulation tape wound around each side to protect the fibre from the abrasive teeth, grip the sleeving and pull away from the fibre remove.

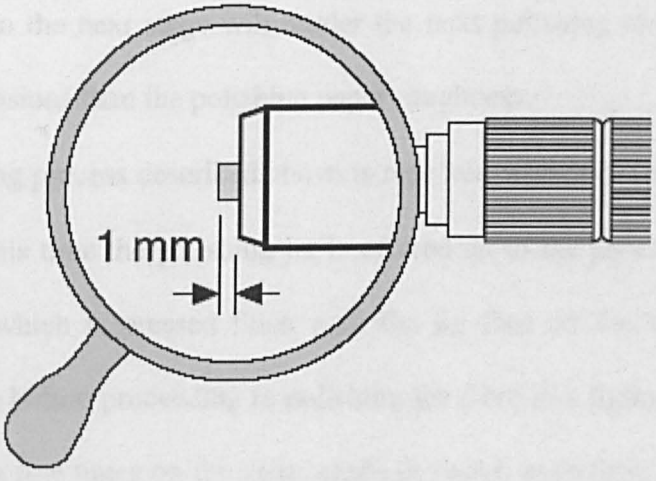

Figure 4.4 1mm of cladded fibre core must protrude from end of SMA connector in readiness for polishing off to ensure all fissures are dealt with

2. The exposed fibre is then inserted into an SMA connector as shown in figure 4.3 with 1mm of POF protruding as shown in figure 4.4. The SMA connector is then inserted into the spring loaded polishing jig. All polishing is carried out on the plate glass to ensure a smooth and level finish. The polishing jig ensures that the polished surface is 90^{o} to the fibre axis to give the most efficient coupling.
3. The 1mm free end of the POF is polished off using in a figure of eight for the equal distribution of polishing direction on wet and dry sandpaper 1200 grade generously wetted to assist the removal of excess material whilst polishing. The polishing jig

will eventually start to grip the abrasive paper; this is the indication that all the excess fibre has been polished off and is the stage to move onto the next grade of polishing film. This initial rough polishing ensures the complete removal of large scale fissures resulting from the initial cut with a blade or dedicated fibre cutter, that are greater than the roughness of the polishing paper.

4. The fibre and fibre jig in contact with the abrasive surface must be rinsed with copious amounts of water to remove all traces of debris; the fibre may be pushed through the holder to expose 1mm to aid complete removal of debris. Any debris carried on to the next stage will render the next polishing stage futile, since it has larger dimensions than the polishing paper roughness.
5. The polishing process described above is repeated with 30μm 3M© lapping diamond film, only this time the polishing jig is offered up to the paper with 0.5mm of fibre protruding which is pressed flush with the jig face on the wetted surface of the lapping film before proceeding to polishing the fibre in a figure of eight again. This is repeated a few times on the same grade of paper, each time, until the jig is felt to be 'gripping' the polishing paper, rinsing between each polish. When this stage is arrived at the jig and fibre end must again be copiously rinsed to ensure the remove all debris.
6. The process is repeated with 9μm diamond lapping film and then finishing with 1μm with minute backwards and forwards movements on the lapping film. The polished fibre end is then cleaned with alcohol to ensure it is grease free before it is inserted into a connector.

Care must be taken with the storage of lapping film. Different grades of lapping film must not be stored together as particles from the larger grades will contaminate the finer grades; measures must also be taken to protect them from the environment as particulate

matter and dust in the laboratory may settle on exposed lapping paper, compromising the finer grades.

4.3.4 Inspection of Polishing

The resulting polished surface may be inspected with proprietary inspection instruments. Better models of fibre inspection scopes have an internal light which give rise to a reflection from the surface of the fibre readily revealing any scratches or imperfections on the surface of the fibre end.

If a fibre inspection scope is not readily available a 20x microscope objective with the fibre end butted up to the lens and then tilted at an angle to the surface, may be used. The fibre must be orientated to cause light to be reflected off the polished surface, light should be excluded from the other end of the fibre for ease of viewing.

Improvements in polishing the fibre surface and in procedures in handling the fibres resulted in 10 times the power of light available to the experiment compared to previous readings by the research group.[12]

Another method of terminating a POF fibre involves using a hot knife and hot plate which gives very low coupling losses.[13]

4.3.5 Coupling

Alignment

Bad alignment when connecting fibre to fibre or fibre to equipment results in unnecessary loss of signal, lateral misalignment, angular misalignment, axial misalignment and poor finishing of the ends of fibres. Figure 4.7 shows several arrangements where this may occur. Good coupling efficiency is vital and is dependant upon the precise positioning of the fibre. Connectors are used where the length of fibre is expected to be replaced periodically. Each connector builds in a 4% attenuation of

the launched signal, so they are kept to a minimum. A good connector must be well centred to ensure the core may be aligned directly with a light source or another fibre within submillimetre accuracy.

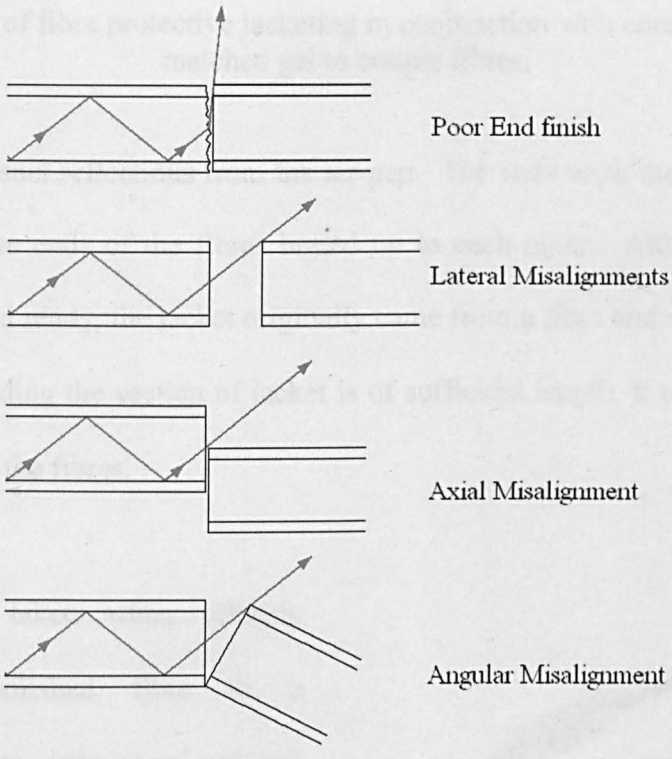

Figure 4.7 Signal losses due to fibre misalignment

Fibre Jacket

The simplest method of coupling the transmitting fibre to the sensing declad fibre was to use a short length of jacket previously stripped from the fibre itself. During the termination procedure a short length of fibre jacket is usually stripped in preparation for end polishing. This results in a snug tailor-made sleeving to the fibre lengths. The exposed polished ends of the fibres were inserted into a length of jacketing, ~ 2cm long, that fully enclosed the both exposed ends to at least 1cm either side as demonstrated in Figure 4.5. Core index matched gel was applied to the ends of the fibre to minimise

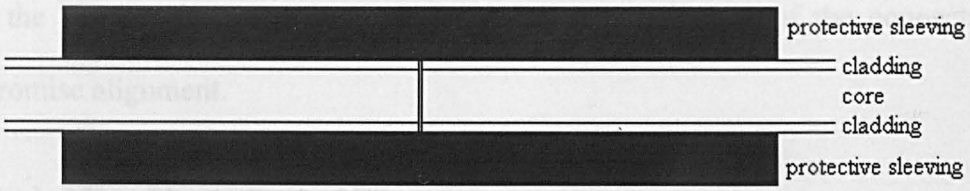

Figure 4.5 Use of fibre protective jacketing in conjunction with core refractive index matched gel to couple fibres.

losses due to Fresnel reflections from the air-gap. The ends were then inserted into the jacketing until the ends of the fibres butted up to each other. Although this method appears rough and ready, the jacket originally came from a fibre and so it absolutely fits the fibres. Providing the section of jacket is of sufficient length, it requires purposeful effort to separate the fibres.

Connectors

Care must be taken when offering painstakingly polished fibre to a connector. Some connectors are not made to exacting standards and can have abrasive burrs inside them that damage fibres and strip coupling modes reducing sensitivity. Insertion of a smooth ended bare metal wire into the connector will easily remedy this. The fibre end must be flush with the end of the connector tip. If the fibre end is inside the connector end there will be a resulting unacceptable loss of signal due to the air gap, 4% at each interface and scattering of the signal inside the connector tip. Figure 4.6 shows the connector of choice for this project from Gruber Industries, an SMA connector type, due to its entirely metallic construction and threaded parts which immobilise the POF. Care must be taken to ensure that the jacket of the POF is inserted into the threaded gripper part of the connector. Without the jacket to tighten the nut

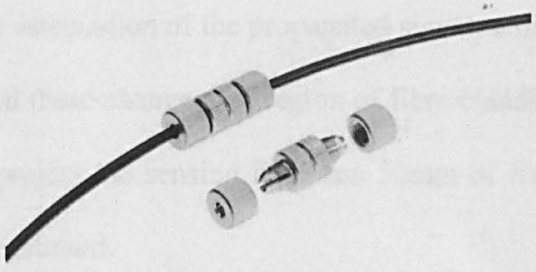

Figure 4.6 SMA connector

onto, the fibre is free to move, which would negate the use of the connector and compromise alignment.

4.4 Decladding Plastic Optical Fibre

The core of optical fibres must be able to interact with a measurand. The method of the removal of the doped Cytop cladding of POF[14] using acetone and water had already been demonstrated. The method described below was developed initially by our research team and extended the method to core tapering by modifying the solvent composition, exposure process and immersion times of Toray[χ] 1mm diameter unjacketed POF. The principle of operation of an evanescent field sensor is to allow a measurand to make contact with the fibre core, which then becomes the effective cladding. Changes in the properties of the measurand such as absorption, scattering, refractive index change, all contribute to the attenuation of the propagated signal, which may to be detected and interrogated to reveal these changes. A region of fibre cladding must be removed to achieve this. In this project the sensing fibre has 50mm of fibre cladding removed to expose the core to a measurand.

The area of the fibre to be declad is clamped in order to immobilise the region, as the fibre is susceptible to brittle stress fracture during the process. Neat acetone is dripped onto the target area until the cladding starts to wrinkle and detaches itself from the core. The cladding can then be removed using optical tissue soaked in 1:1 acetone/distilled water. This solution halts the dissolving action of the acetone whilst keeping the cladding pliable enough to complete its removal. The declad region of the fibre must be thoroughly rinsed with distilled water to remove all traces of acetone, and then wiped with isopropyl alcohol to leave a clean, grease-free fibre core ready for sensor purposes, figure 4.8 and 4.9.

[χ] Appendix 3

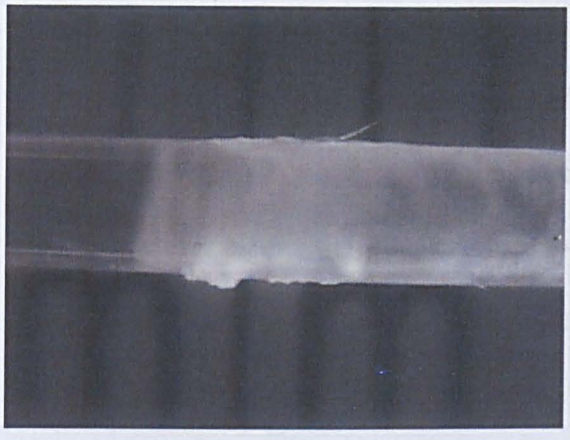

Figure 4.8 Declad fibre. Left of image is declad core, to the right fibre with cladding intact

Figure 4.9 2000x magnification of declad fibre surface

The 2000x magnification the images reveal pits and grooves on the surface of a declad fibre (figure 4.9). The pits may be attributed to the initial acetone attack on the fibre cladding, the grooves resulting from the mechanical removal of the cladding. These surface features conveniently provide a key,[15] which assists the attachment of measurand such as biofilm and any coatings[16] that may be considered.

4.5 Plastic Optical Fibre Tapering

The method of the removal of the doped Cytop cladding of POF[14] using acetone and water had already been demonstrated. The method described below was developed initially by our research team extended the method to core tapering by modifying the solvent composition, exposure process and immersion times of Toray 1mm diameter unjacketed POF. A fibre with a region of decreased radius has a greater proportion of light in the evanescent field.[9] Therefore a sensor with a reduced radius in the sensing region would be more sensitive to changes in the measurand. Tapering glass optical fibres is already an established procedure.[17,18] These are usually achieved either by mechanical or chemical means.

Producing taper in POF via the mechanical heat drawing method employed with silica fibre was difficult to control, due to the low melting temperature of PMMA (130-140°C). Previous researchers in the research group had already been proven[19] the principle of tapering POF using organic solvents but the procedure was not yet optimised or automated. In this project both end tapers and in-fibre tapers were investigated.

4.5.1 End Tapers

Figure 4.10 End taper with coupled light emerging from tip

End tapers were desirable to optimise POF sensors. The diminishing diameter results in more of the signal light coupled into the evanescent field for sensing purposes. The tapers must be readily produced with smooth profiles and optically clear. Tapers at the end of a POF were formed by immersing fibre ends into small glass receptacles of acetone and allowed to evaporate. This procedure revealed end tapers, figure 4.10, the dimensions of which could be controlled by varying the rate of evaporation of the acetone. This procedure was optimised by using glass receptacles of various combinations of surface area and volume, so that the evaporation rate could be controlled. Care was taken to ensure that the fibre did not touch the sides of the container which would result in tapers of uneven profile.

4.5.2 Mid-length Tapering

Decreasing the diameter of an optical fibre mid-length is desireable as it increases the ratio of evanescent field to launched signal, enhancing the sensitivity of the fibre[9].

4.5.2.1 Chemical Etching Stage 1 - Initial Confirmation of Tapering Process

Previous work by the research group confirmed the process of chemically tapering POF.[19] Mid-length POF tapers were initially formed by securing a loop of fibre in a minimum stress orientation, looped in the same curvature from the reel, as stress experienced by the fibre during the tapering process caused breakage figure 4.11. The tapering area was de-clad by rubbing an acetone soaked cleaning tissue along the area to be etched. This was then washed with water. The de-clad fibre area was then immersed

in a dish of etching solution with a large surface area to allow evaporation to take place giving rise to a change in solvent height; producing symmetric tapers; this created the taper in the fibre. Tapering was initially carried out in methylisobutylketone (MIBK):Acetone:water in a solution with the ratios of 3:1:1 A thin layer of material formed on the surface of the solution during tapering which had to be removed every 15 minutes. Different proportions of MIBK and acetone were investigated; higher concentrations of acetone caused the fibre to break, usually at the solution - air interface. Tapering rate decreased with lower concentrations of acetone. This method was originally a lengthy process taking 10-18 hours to produce a satisfactory taper. The etching solution had to be refreshed constantly resulting in uneven tapering.

This initial method was rough and ready; however it did prove the principle of producing a mid-tapered fibre. Tapers were formed, but the decrease in waist size was not uniform along the length of the taper due to the constant need to refresh the solvent. Decladding the fibre before tapering resulted in uneven tapering with conditions not easily reproduced. The fibre was held in place with adhesive tape that left residue on the cladding that needed removal before use. The evaporation rate of the solvent was not easily controlled as the process was carried out in the open laboratory, room temperature, humidity and air currents; all factors affecting evaporation rate were not easily controlled. Fumes from the volatile etching solvents were also problematic and unpleasant for researchers.

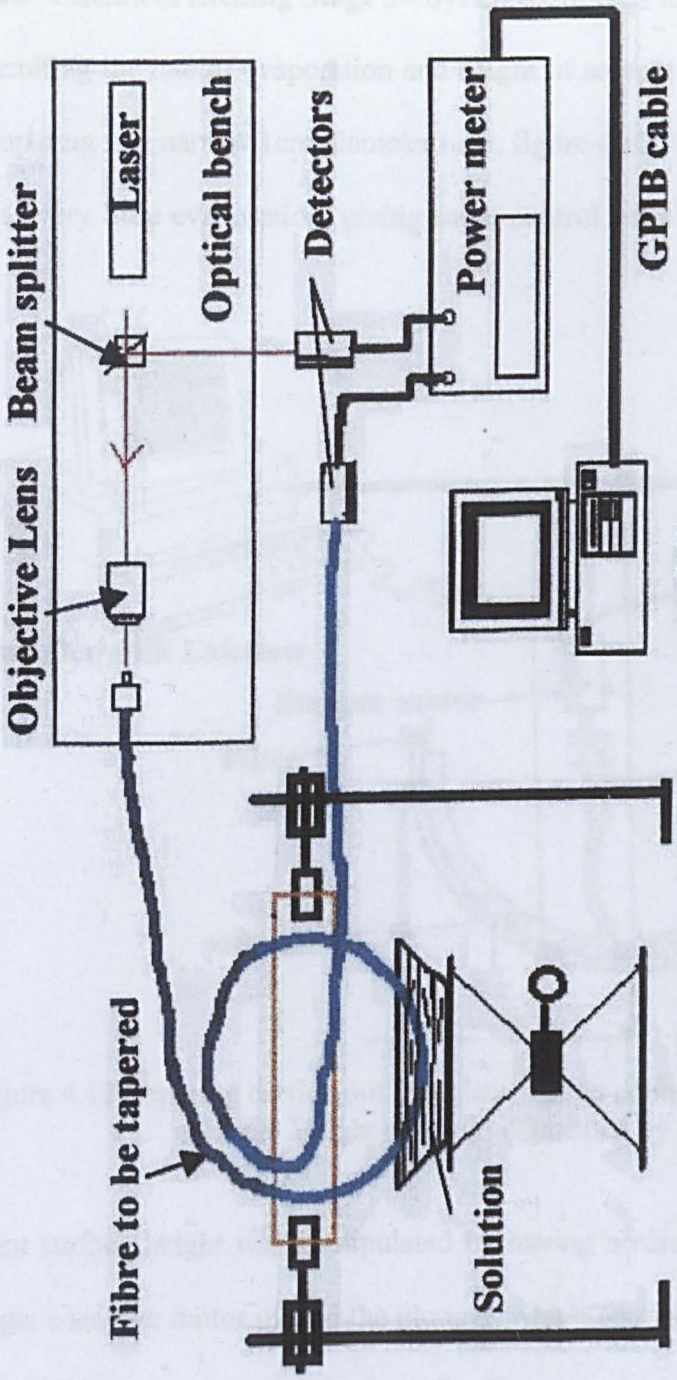

Figure 4.11 First stage in development of chemically tapered POF

4.5.2.2 Chemical Etching Stage 2 - Extractor Fan

The fumes from the evaporating solvent made an unpleasant working environment. The whole process was moved into a fume cupboard. However this caused the etching solution to evaporate at a much faster rate, requiring topping up every hour or so.

4.5.2.3 Chemical Etching Stage 3 - Syringe Injected into Tube

Controlling the rate of evaporation and height of solvent was attempted by carrying out the tapering in a narrow 1cm diameter tube, figure 4.12; the dimensions of the tube gave rise to very little evaporation, giving some control with the height of the etching. The

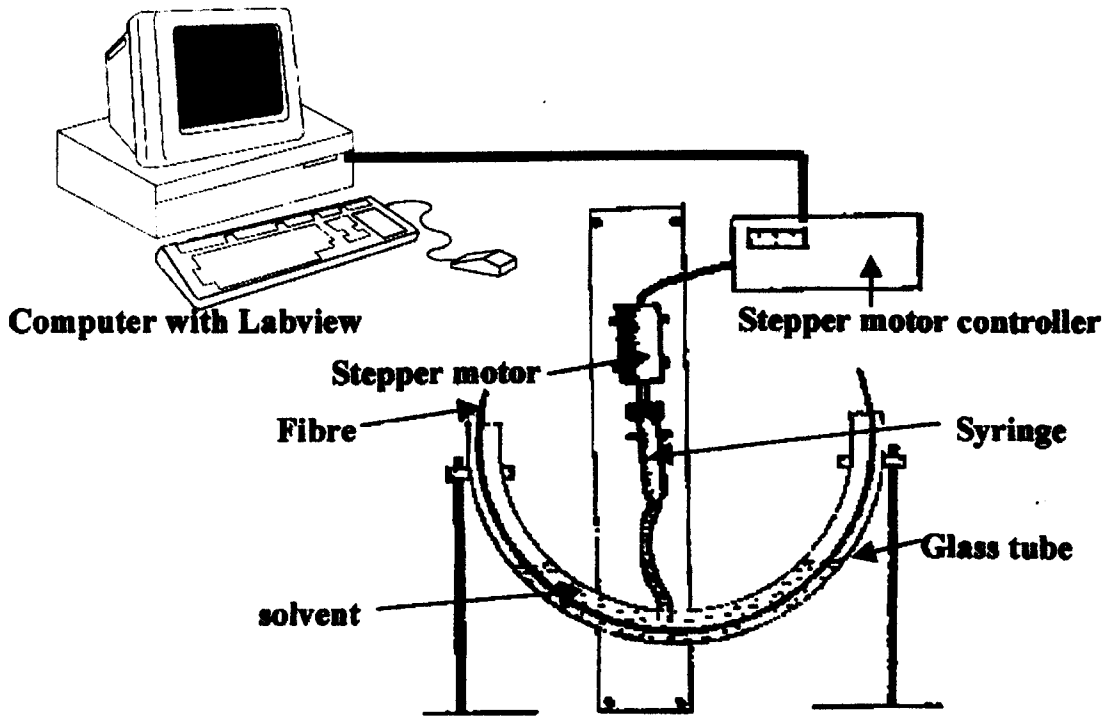

Figure 4.12 Tapering carried out in a glass tube to control evaporation of etching solvent. Height of liquid controlled by a syringe

solvent surface height was manipulated by having a reservoir of etching solution in a syringe; a stepper motor moved the plunger, which was in turn connected to a controller and LabView program running on a PC. The arrangement produced mid-length tapers but it proved impossible to remove the tapered fibre intact from the narrow tube. Attempts were made to produce a split tube but sealing became a new problem, as the solvent would attack the seal.

4.5.2.4 Chemical Etching Stage 4

Present Work - Automated Enclosed Mid-length Tapering [20]

In order to control evaporation the solvent was placed in a sealed container (figure 4.13). A glass tank was used in conjunction with an aluminium lid, which provided an efficient seal. Equilibrium within the tank was reached within 1.5 hours; the height of the etching solvent remained unchanged, indicating that the atmosphere was saturated.

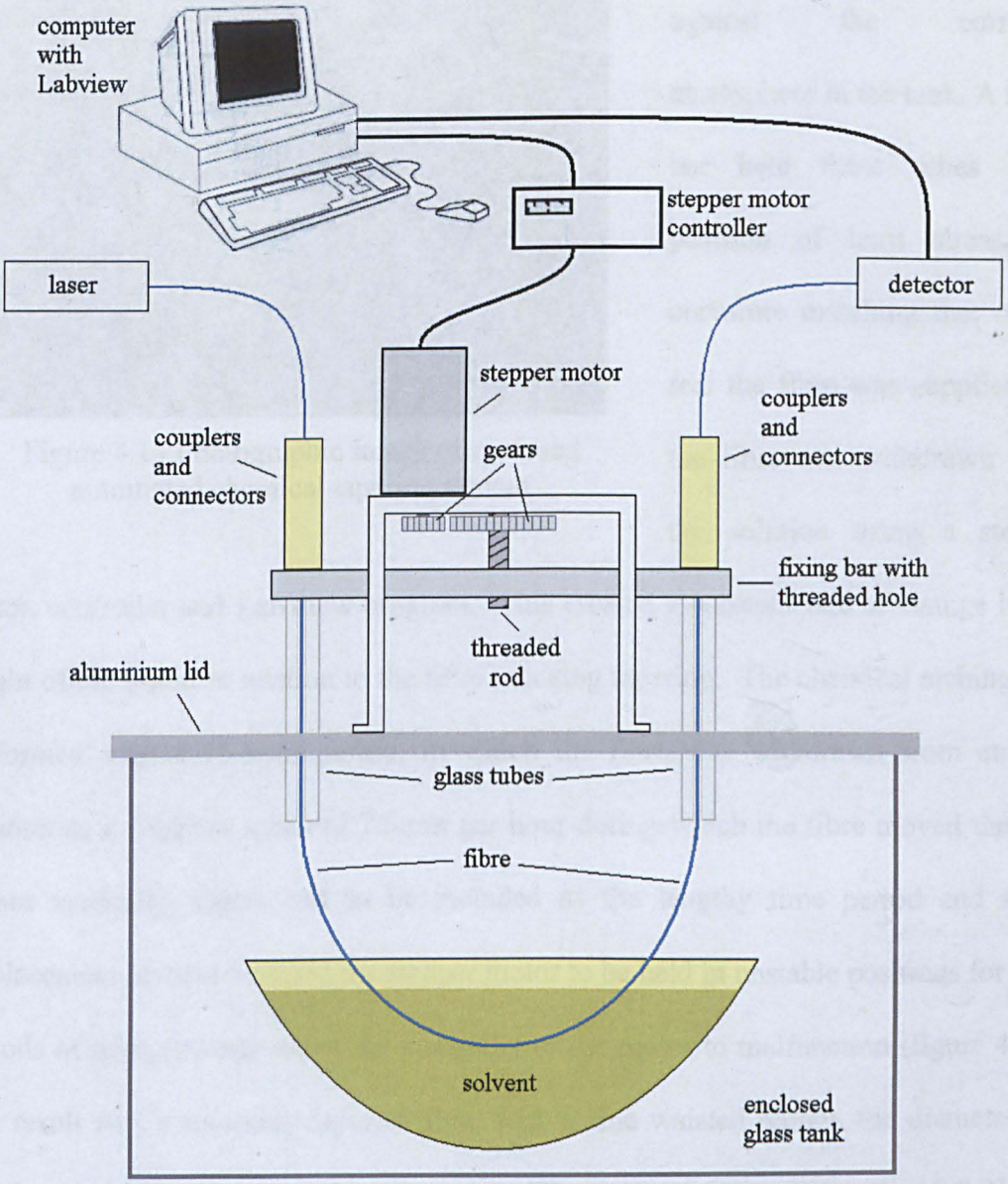

Figure 4.13 Automated chemical etching of POF. Evaporation is controlled by enclosing the wet end of the process in a glass tank.

Figure 4.14 Photographic image of enclosed automated chemical tapering system

As the depth of etching solution did not change, the position of the fibre relative to the etching solution was controlled. The fibre was inserted into inert glass tubes for protection against the corrosive atmosphere in the tank. A metal bar held these tubes in a position of least stress, the curvature matching that of the reel the fibre was supplied on; the fibre was withdrawn from the solution using a stepper motor, controller and LabView program. This created a constant rate of change in the height of the liquid in relation to the fibre inducing tapering. The chemical etching was performed over a 15-hour period, in which the fibre was withdrawn from etching solution as a constant speed of 2.5mm per hour during which the fibre moved through 40mm vertically. Gears had to be included as the lengthy time period and small displacement involved caused the stepper motor to be held in unstable positions for long periods of time, causing either the controller or the motor to malfunction (figure 4.14). The result was a smoothly tapered fibre, with a fine waisted region, the diameters of which were controlled by extraction rate. Fibres of minimum diameter of 0.21mm,

were achieved, figures 4.15 and 4.16, however the very slow extraction rate caused beads of partially dissolved matter to form along the tapered region.

4.5.2.4.1 Evolution of Etching Solution

Initially the etching solution used was three parts acetone to one part each of MIBK and distilled water. The target region of the fibre was declad first and then exposed to the etching solution.

This etching solution produced smooth tapers but with a few undesirable effects: a cloudy surface; partly dissolved cladding would collect on the surface of the etching solution and would clung to the taper; beads of material would collect along the taper. This needed to be cleaned away from the fibre by hand which resulted in a high percentage of destroyed tapers and inconsistent results. Many proportions of chemicals were experimented with and the most satisfactory formula was found to be 3:1 parts acetone to MIBK. This produced optically clear tapers; no beading whether fibre was

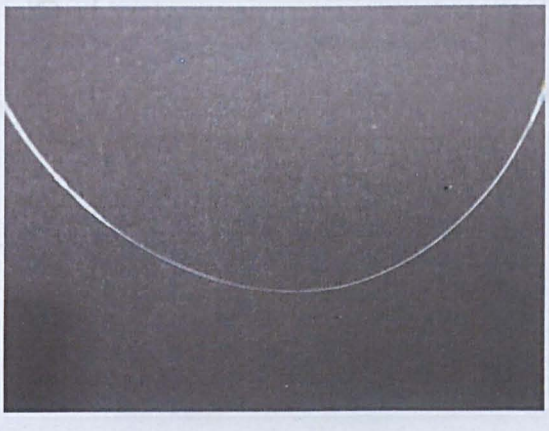

Figure 4.15 Optically clear tapered fibre

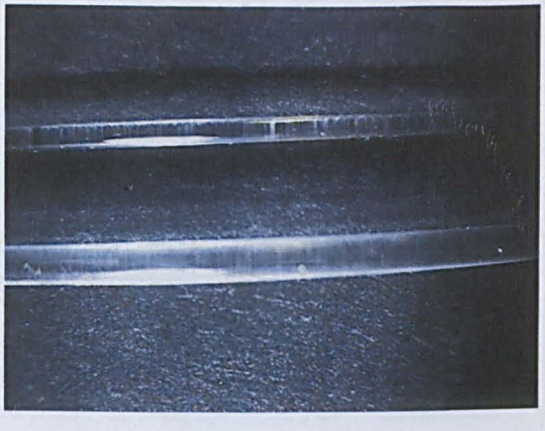

Figure 4.16 Tapered fibre above a fibre off the reel and with cladding intact

inserted or withdrawn from the etching solution; and the process was speeded up, taking only 5 hours to produce satisfactory tapers. The fibres did not need to be declad first. It appears that the water in the mix was preventing the PMMA dissolving fully. On-line monitoring was performed during the tapering process. The fibre was coupled to a

660nm laser diode and light was transmitted through the fibre to a detector. Light power was monitored using an Ando powermeter (figure 3.7).

The tapering process was monitored (figure 4.17) by measuring the light intensity through the POF whilst etching was performed.

The plot of fibre transmission intensity versus time enabled the repeatability of the tapering process to be measured; in that if the same length of fibre was tapered to the same diameter, using the same solution, then the plot exhibited a similar gradient.

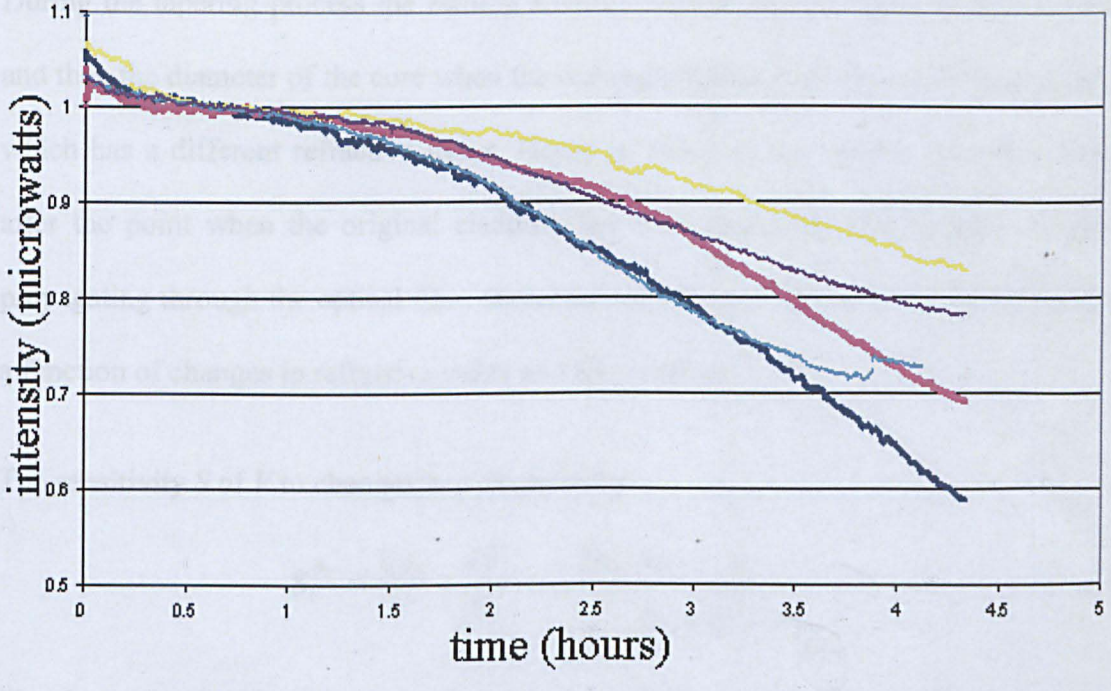

Figure 4.17 light intensity from POF as they are chemically tapered

4.5.2.4.2 Modelling of Process Parameter Changes[20]

Existing theoretical models for tapered fibre are either for single-mode fibre[21,22,23,24] or highly specific to an optimal configuration of multimode fibre,[25,26] neither of which can be readily adapted for the large diameter POF highly multimoded tapers and so a simple mathematical treatment has been developed which considers the effect of varying the fibre diameter and cladding refractive index on the *V*-number, to establish a relationship

between core radius, cladding refractive index and numerical aperture for dynamic prediction and compensation of optical parameters.

The sensitivity S of a function $f(x)$ to parameter changes can be represented as follows:

$$S_{a_i}^{f} = \frac{\Delta f(x)/f(x)}{\Delta a_i / a_i} \qquad \text{---4.1}$$

Where a_i = parameter of interest.

During the tapering process the etching solution reduces the thickness of the cladding and then the diameter of the core when the etching solution itself becomes the cladding, which has a different refractive index. Hence n_2 refers to the solvent refractive index after the point when the original cladding has been removed. The intensity of light propagating through the optical fibre decreases with time as shown in figure 4.17 and is a function of changes in refractive index and fibre radius.

The sensitivity S of V to changes in n_2 is given by

$$S_V^{n_2} = \frac{2n_2}{V} \times \frac{\partial V}{\partial n_2} = -\frac{2n_2}{V} \frac{\pi a}{\lambda_o} \frac{n_2}{\sqrt{n_1^2 - n_2^2}} \qquad \text{---4.2}$$

The change in V, defined in equation 2.8, as a result of a change in n_2 is given by

$$\Delta V = -\frac{2a\pi}{\lambda_o} \times \frac{n_2^2}{\sqrt{n_1^2 - n_2^2}} \times \frac{\Delta n_2}{n_2} \qquad \text{---4.3}$$

The effect of changes in the fibre radius a on the number of modes propagating into a fibre is given by

$$\frac{\partial V}{\partial a} = +\frac{\pi}{\lambda_o} \sqrt{n_1^2 - n_2^2} \Big|_{\lim_{\Delta a \to 0}} \qquad \text{---4.4}$$

with

$$S_V^a = +\frac{a}{V} \times \frac{\pi}{\lambda_o} \sqrt{n_1^2 - n_2^2} \qquad \text{---4.5}$$

From equations 4.1 and 2.8,

$$\Delta V = +\frac{2\pi}{\lambda_o}\sqrt{n_1^2 - n_2^2} \times \Delta a \qquad \text{---4.6}$$

The negative sign in equation 4.2 shows that an increase in the solvent refractive index, n_2, results in a decrease in the number of modes to be propagated into a fibre. The positive sign in equation 4.6 shows that a decrease in the radius of the core yields a decrease in the number of modes and hence a consequent decrease in the transmission.

From equations 4.2 and 4.4,

$$\frac{\partial V}{\partial n_2} = -\frac{an_2}{n_1^2 - n_2^2}\frac{\partial V}{\partial a} \qquad \text{---4.7}$$

Equation 4.7 shows that the rate of change of V with n_2 and a are equal, they have a linear relationship. With reference to equation 2.8, if $n_2 < n_1$, V is real and the wave is able to propagate along the guide. If, however, $n_2 > n_1$, V will be an imaginary quantity and this means that no propagation of modes takes place. Therefore, for equation 4.7 to be valid an increase in $(n_2 + \Delta n_2)$ must not exceed n_1:

$$\Delta V = \Delta a - \Delta n_2 \qquad \text{---4.8}$$

From equations 4.3 and 4.6

$$\Delta a = -\frac{an_2}{n_1^2 - n_2^2}\Delta n_2\Big|_{\Delta V \to 0} \qquad \text{---4.9}$$

From equations 4.3 and 4.6, the changes in the refractive index of the solvent, n_2 and core radius a, counteract each other. When the rate of change in light intensity is zero, i.e., when the gradient of the graph in figure 4.17 is zero, then

$$\left|\frac{an_2}{n_1^2 - n_2^2} = 1\right|_{\Delta V \to 0} \qquad \text{---4.10}$$

with

$$a = \frac{n_1^2 - n_2^2}{n_2} \qquad \text{---4.11}$$

or

$$an_2 = \mathrm{NA}^2 \qquad \text{---4.12}$$

Thus the product of the fibre radius and solvent refractive index forms a constant that is the square of the numerical aperture, and hence is a measure of the light propagating property of the fibre.

4.5.2.4.3 Discussion of Modelling

Core diameter and refractive index are two parameters that affect the propagation of modes in an optical fibre, and hence the intensity of the transmitted light. R Chandy et al[27] showed that fluctuations in the value of cladding refractive index cause changes in the critical angle that in turn determines the propagation of higher modes in the fibre. Mathematically, equation 4.3 shows an increase in the sensitivity of V (fibre V-factor) to variations in the refractive index, and hence a reduction in the number of higher modes propagating into the fibre. It is also shown that changes in either parameter a (core radius) or parameter n_2 (solvent refractive index) are directly reflected in V and thus the light transmitted through the fibre. An interesting point is that the sensitivity of V to changes in a and n_2 has positive and negative signs respectively. It is therefore possible that changes in both parameters will counteract each other, at some stage during the tapering process, conserving the number of modes guided in the fibre. Equation 4.9 estimates a relationship between the fluctuations necessary for both a and n_2 to maintain constant light intensity in the presence of parameter changes. This is a possible explanation for the flat region in the graph in figure 4.17 where changes in the light intensity diminish to zero. Equation 4.12 uses this assumption to relate the product of

the core radius and the solvent refractive index to the square of the numerical aperture. Another explanation could be the solvent dissolving the 20 μm thick cladding, in which the evanescent field decreases exponentially. Thus, the evanescent field is not significantly affected by the solvent until the last few microns of the cladding are dissolved away and the solvent begins to replace the cladding with a consequent change in refractive index, whilst the core diameter remains intact, with the result that the number of guided modes remains constant. The solvent dissolves the core with a consequential increased rate of roll-off of fibre transmission, and the taper becomes non-adiabatic. Figure 4.17a* shows a plot of the diameter of the POF as a function of time after being immersed in the solvent. The graph is l linear with a constant gradient of about 2 μm min^{-1}. The flat portion of the graph in figure 4.17 is between 20 and 60 min, so over this time period, the diameter of the fibre would have changed by 80 μm from 0.95 to 0.875 mm, which is more than the thickness of the cladding (40 μm). In this time period, the refractive index of the solvent surrounding the dissolving fibre was measured, using an Abbe refractometer, as 1.3665 ± 0.0005 or 0.04%. Minute changes in the solvent within the evanescent field of the fibre core could not be measured due to the sampling procedure requiring a few millilitres of the liquid to be drawn off with a pipette. Equation 4.12 can be used for dynamic prediction of parameters. For instance, knowing the core radius and the NA, it is possible to predict the refractive index of the solvent material and vice versa. The NA can be measured on-line using a CCD camera to monitor the spatial output of a multimode optical fibre.[27] Other parameters can be predicted such as critical angle, acceptance angle and spatial parameters of the light source. By tuning these parameters to their appropriate values, it is possible for an automated optical system (e.g. an optical communication system) to operate in the

* Appendix 11

presence of parameter fluctuation, while maintaining acceptable performance. In order for equation 4.12 to be valid, a change in the solvent material refractive index n_2 $(n_2+\Delta n_2)$ must not exceed n_1. Otherwise, V is an imaginary quantity and no guiding takes place.

4.5.4 Short Length Heat Drawn Mid-length Tapers

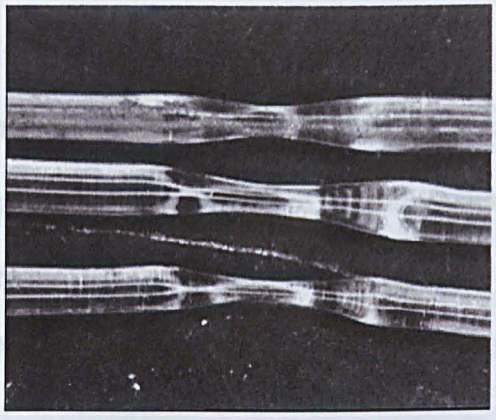

Figure 4.18 Heat drawn cladded POF midtaper produced by Dr K. Kuang

Initial attempts by the research team to produce mid-length tapers by heat drawing was unsuccessful due to the inability to control the heating temperature. Dr Kevin Kuang, formerly of Liverpool University, now of National University of Singapore, has produced millimetre long mid tapers in POF (figure 4.18). The target area of the POF was heated and a load was applied. These fibres have their cladding intact and appear symmetrical. These have been evaluated for strain measurements.[28,29] When the orientation of an optical fibre is changed the light propagated changes due to the alteration of the angle at which the rays would have been incident upon the fibre core. These changes reveal the extent of the deflection. POF are more elastic than GOF and have much smaller bend radius, thus are more suited to applications involving large deflections where GOF would shatter.

4.5.5 Chemical Tapering versus Heat Drawn Tapering

Chemical tapering produces long length tapers, it removes the cladding in the process, which makes it sensitive to external perturbations, as required for this type of sensor. The long length increases the surface area exposed to a measurand, increasing its sensitivity. The exposed fibre core may be coated with a reagent to further optimise the sensor.

Heat drawing produces much shorter lengths of taper with their cladding still intact. These are not suited for chemical and biochemical sensing as the cladding prevents interaction with external measurand but are ideally suited for strain measurements. The tapered region of the fibre is more sensitive to changes in orientation of the fibre which has the effect of altering the incident angle of rays at the fibre core/cladding interface, which has an affect on whether a ray is refracted into the cladding or not.

4.6 Summary

Termination and Coupling

The procedures involved in terminating fibre ends were described which refine and establish good working practice to consistently improve the proportion of available light coupled into fibres. Improvements in polishing the fibre surface and in procedures in handling the fibres resulted in an improvement of 10 times the power of light available to the sensor.

Sensitising Lengths of Plastic Optical Fibre for Sensing

Optical fibres are usually supplied with a cladding of lower refractive index material than the core and must be removed and the core exposed for evanescent field attenuation to occur.

Decreasing the diameter of POF results in more of the outer modes of the light signal available for sensing, but only with optically clear tapers. This was achieved for both end and mid-length tapers via chemical etching and short mid-length taper via heat drawing. The processes involved in developing the automated chemical etching have been described.

Decladding Plastic Optical Fibre: A simple and efficient method of removing the cladding of POF and exposing the evanescent field has been achieved. Target areas had their cladding stripped cleanly, efficiently with consistent and reproducible results. Electron microscope images reveal a smooth surface, however the images do reveal pits and grooves on the surface. These surface features may well to assist the attachment of measurand such as biofilm or optical coatings containing analytes. POF is now available without cladding on special order from Luceat.[30]

End Tapers: These were readily produced with the evaporation method. Taper geometry was easily controlled via surface area/volume ratio of chemical container used. They could be easily produced with the enclosed mid-length tapering method with minimal adaptation of the setup.

Enclosed Mid-length Tapering: The method went through many stages of development, but the enclosed tank method described in section 4.5.3.5 produced consistently good results: smoothly tapered fibre, with a fine waisted region; optically clear without the need for mechanical removal of the fibre cladding. The setup provided safe operation without the need of a fume cupboard and minimal loss of etching solution through evaporation, cutting down running costs. The process was theoretically modelled[20] revealing that the product of the fibre radius and solvent refractive index forms a constant that is the square of the numerical aperture, and hence is a measure of the light propagating property of the fibre.

Evolution of Etching Solution: The etching solution arrived at produces optically clear tapering without residue. The removal of the fibre cladding before tapering is no longer necessary, eliminating the possible inconsistencies this extra process brings.

Heating and Pulling method of Producing Mid-length Tapers: This readily produces successful tapers of a few millimetres in length with the cladding still intact as required for the strain sensor. The process could be further improved with automated mechanical manipulation and a controlled targeted heat source.

References

[1] BD MacCraith, "Enhanced Evanescent Wave Sensors Bassed on Sol-gel Derived Porous Glass Coatings", Sensors & Actuators B, vol.11, pp29-34, 1993

[2] AW Snyder, DJ Mitchell, "Leaky rays on circular optical fibers", J. Opt. Soc. Am., vol.64, p599, 1974

[3] AW Snyder, DJ Mitchell, C Pask, "Failure of geometric optics for analysis of circular optical fibers" J. Opt. Soc. Am., vol.64, p608, 1974

[4] FH Zhang, E Lewis, PJ Scully, "An Optical Fibre Sensor for Particle Concentration Measurement in Water Systems Based on Inter-fibre Light Coupling Between Polymer Optical Fibres", Transactions of the Institute of Measurement and Control, vol.22, No.5 pp413-430, 2000

[5] AW Snyder, DJ Mitchell, C Pask, "Failure of geometric optics for analysis of circular optical fibers" J. Opt. Soc. Am., vol.64, pp608

[6] JD Love, C Pask, "Universal curves for power attenuation in ideal multimode fibres", Electron Lett. vol.12, p254, 1976

[7] DF Merchant, PJ Scully, NF Schmitt, "Chemical Tapering of Polymer Optical Fibre", Sensors & Actuators No.76 pp365-371, 1999

[8] S Lacroix, R Bourbonnais, F Gonthier J Bures, "Tapered Monomode, Optical Fibers: Understanding Large Power Transfer", Applied Optics, vol.24, No.23, pp4421-4425, 1986

[9] AG Mignani, R Falciai, L Ciacceri, "Evanescent Wave Absorption Spectroscopy by Means of Bi-tapered Multimode Optical Fibers", Applied Spectroscopy, vol.52, No.4, pp546-551, 1998

[10] Toray Plastic Optical Fiber, Toray International UK Ltd

[11] K Lai, A Witkowska, SG Leon-Saval, WJ Wadsworth, TA Birks, "Fibre Core Shape Transitions for Optical Interfacing", Optical Society of America

[12] R Philip-Chandy, PJ Scully, P Eldridge, HJ Kadim, MG Grapin, MG Jonca, MG D'Ambrosio, and F Colin, "An Optical Fiber Sensor for Biofilm Measurement Using Intensity Modulation and Image Analysis", IEEE Journal on Selected Topics in Quantum Electronics, vol.6, No.5, pp764-772, 2000

[13] R Bockstaele, A van Hove, T Coosemans, C Sys, I Moerman, B Dhoedt, R Baets, P van Daele, J van Koetsem L van der Torren, "Microcavity LED-based Parrallel Data Link Using Small-diameter (125μm) Plastic Optical Fibres", J.Opt. A, vol.1 pp233-236, 1999

[14] J Bayle, J Mateo, Plastic optical fibre sensor of refractive index, based on evanescent field. Proceedings of POF 96, Sensors vol.1, pp220–227

[15] WG Characklis, GA McFeters, KC Marshall, Physiological ecology in biofilm systems. In: Characklis WG, Marshall KC, editors. Biofilms. New York: John Wiley & Sons; pp. 341-394, 1990

[16] CJ Brinker, AJ Hurd, "Fundamentals of sol-gel dip-coating" J. Phys. Ill Fiance 4 pp1231-1242, 1994

[17] P Hoffman, B Dutoit, RP Salath, "Comparison of Mechanically Drawn and Protection Layer Chemically Etched Optical Fiber Tip", Ultramicroscopy, vol.61, pp165-170, 1995

[18] S Mononobe, T Saiki, T Suzukin, S Koshihara, M Ohtsu, "Fabrication of a Triple Tapered Probe for Near-Field Optical Spectroscopy in UV Region Based on Selective Etching of a Multistep Index Fiber" Optics Communications vol.146, pp45-48, 1998

[19] DF Merchant, PJ Scully, NF Schmitt, "Chemical Tapering of Polymer Optical Fibre", Sensors and Actuators vol.76, pp365–371, 1999

[20] YM Wong, PJ Scully, HJ Kadim, V Alexiou, RJ Bartlett, "Automation and Dynamic Characterization of Light Intensity with Applications to Tapered Plastic Optical Fibre", J. Opt. A: Pure Appl. Opt. vol.5, pp51–58, 2003

[21] TA Birks, YW Li, "The Shape of Fiber Tapers", J. Lightwave Technol. vol.10, pp432–8, 1992

[22] JD Love, WM Henry, "Quantifying Loss Minimisation in Single-mode Fibre Tapers", Electron. Lett. vol.5, pp912–914, 1985

[23] WJ Stewart, JD Love, "Design Limitation on Tapers and Couplers in Single-mode Fibre Tapers", Proc. ECOC'85 pp559–562, 1985

[24] AW Snyder, JD Love, "Optical Waveguide Theory", (London: Chapman and Hall), 1982

[25] S Guo, S Albin, "Transmission Property and Evanescent Wave Absorption of Cladded Multimode Fiber Taper", Opt. Express, vol.11, pp215–23, 2003

[26] AM Mignani, R Falcial, L Ciaccheri, "Evanescent Wave Absorption Spectroscopy by Means of Tapered Multimode Optical Fibers", Appl. Spectrosc. vol.52, pp546–551, 1998

[27] R Philip-Chandy, PJ Scully, P Eldridge, HJ Kadim, G Grapin, G Jonca, G D'Ambrosio, F Colin, "An Optical Fiber Sensor for Biofilm Measurement using Intensity Modulation and Image Analysis", IEEE J. Sel. Top. Quantum Electron. vol.6, pp764–772, 2000

[28] YM Wong, PJ Scully, RJ Bartlett, KSC Kuang, WJ Cantwell, "Plastic Optical Fibre Sensors for Environmental Monitoring: Biofouling and Strain Applications", Strain, vol.39, pp115-119, 2003
[29] KSC Kuang, WJ Cantwell, PJ Scully, "An Evaluation of a Novel Plastic Optical Fibre Sensor for Axial Strain and Bend Measurements", Meas. Sci. Technol. vol.13 pp1523–1534, 2002
[30] Luceat S.p.A Viale F. Marconi 31, Dello (BS), Italy

CHAPTER FIVE

Plastic Optical Fibre Evanescent Field Biofilm Sensor

5.1 Introduction

Low cost, rugged sensors were developed in this project using 1mm diameter POF with a 5 cm declad area for environmental, chemical and biological monitoring, applications such as biofouling and scaling, algal growth, pH, particle concentration, turbidity, fluid flow, strain and water toxicity. This project was part of a European Commission funded research investigating biofouling and scaling in closed loop water systems Closed Loop Optimisation (CLOOPT),[*1,2] contract number ENV 4-CT97-0634, fourth RTD

[*] Appendix 4

Framework Programme in the area of "Environment and Climate". The project developed and evaluated on-line instrumentation and measuring techniques for fouling in closed loop water recycling loops to limit water consumption and reduce discharge of pollutants.[1]

The same sensor formed part of another European Commission RTD Project Water Quality Surveillance Techniques for Early Warning by Interface Sensors (AQUA-STEW)†, Contract No. EVK1-CT-2000-00066 Fifth Framework Programme (FP5) in the area of "Sustainable Management and Quality of Water", to design, construct and test new real-time measurement techniques and methods for water quality. The approach was to fingerprint natural water characteristics; to detect the presence of complex species and to measure accurately trace levels of priority pollutants.

5.2 Biofilms

A biofilm is a structure composed of microbial cells that can occur at either a solid-liquid interface, or a solid-gas interface and which cannot be easily removed by gentle rinsing. Biofilms are enclosed in a matrix of primarily polysaccharide material and can contain other organic substances: bacteria, fungi and algae, as well as inorganic substances entrapped in the film from the surrounding environment. It is a structure filled with water and consequently, it has similar optical properties to water.[3, 4] A pure biofilm is transparent and has a slightly higher refractive index than water. In real water systems, fouling and scaling may take place as well as simple biofilm formation, where coloured (absorbent) and scattering matter such as slime, chlorophyll, and limescale may also contribute to the attenuation process. Figures 5.1 and 5.2 show examples of damaging and costly effects of untreated biofilm.[5]

† Appendix 5

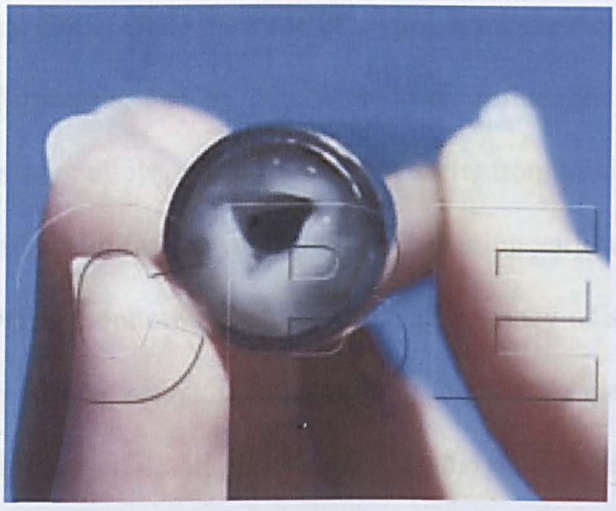

Figure 5.1 Cross sectional view of a stainless steel tube coated with a thick, healthy biofilm. Courtesy, N. Zelver

Figure 5.1 shows the cross section of a stainless steel tube clearly showing a thick layer of biofilm growing on the inside surface. The layer of biofilm has the effect of reducing the working diameter of the tube to a third, restricting fluid flow, reducing efficiency and contaminating the fluid carried in the tube.

Figure 5.2 Badly corroded pipe from a water distribution system, Courtesy, C. Abernathy, A. Camper

Figure 5.2 shows a badly corroded pipe from a water distribution system, an example of the costly consequences of microbial colonisation on metal surfaces, Microbially

Influenced Corrosion, (MIC). The presence of microorganisms modifies deposition and dissolution rates of minerals, and by this mechanism, influences the electrochemical properties of the metals or alloys, pitting corrosion results from this activity.[6]

Efforts to monitor biofilm growth have included using various coupon systems[7, 8] where biofilm growth is monitored via the weight discrepancy of a coupon before and after deployment, as well as scraping and weighing the sample biofilm from a known surface area of cooling towers.[9] All of which disturb the biofilm itself. Other methods include indirect methods incorporating changes in heat transfer resistance,[10,11,12] fluid frictional resistance[13,14,15] and electrochemical monitoring of biofilm accumulation..[16,17] It has also been desirable to be able to monitor the removal and inhibition of biofilm growth on-line to be able to ascertain the effectiveness of treatment. Continuous on-line monitoring techniques have provided the most reliable data in the water industry. The POF evanescent field sensor developed in this project provides on-line, real-time monitoring of biofilm growth. The refractive index, absorption and scattering characteristics of the biofilm matrix changed as biofilm grow. A POF evanescent field sensor can detect these changes since these mechanisms affect attenuation of the propagating light. The sensor operation has been demonstrated during this project.[18,19,20]

5.2.1 Characteristics of the Aqueous Medium

Conditions of the aqueous medium such as pH, nutrient levels, ionic strength, and temperature, may play a role in the rate of microbial attachment to a surface. Several studies have shown a seasonal effect on bacterial attachment and biofilm formation in different aqueous systems.[21, 22] This effect may be due to water temperature or to other unmeasured, seasonally affected parameters. A laboratory study[23] has shown that an

increase in nutrient concentration correlated with an increase in the number of attached bacterial cells. This project has derived a method of biofilm culture with the use of 0.1% yeast extract and tapwater from the mains at LJMU as this contained a small microbial colony and trace minerals that would allow biofilm to grow.[24] Distilled water is condensed steam from boiling water; the process kills microbes and removes the water's natural minerals.[25] Providing the distilled water is kept in sterilised containers distilled water does not contain bacteria or minerals and so would not support biofilm growth.

5.2.2 Biofilm Structure

Biofilms are composed primarily of microbial cells and exopolysaccharide (EPS), which may account for 50% to 90% of the total organic carbon of biofilms[26] and can be considered the primary matrix material of the biofilm. Biofilms are not a homogenous monolayer surface deposit, they are very heterogeneous, containing microcolonies of bacterial cells encased in an EPS matrix and separated from other microcolonies by water channels.[27] The structure and composition of biofilms is dependant upon the types and relative abundance of organisms present as well as physical and chemical factors in their environment.

5.2.3 Resistance to Antimicrobial Agents

Biofilm is very costly to industry,[28] for example, a biofilm can retard the speed of a ship by 20% or reduce the flow in a thin pipe by 50%.[29] Biofilms can also form an insulation layer that increases the heat transfer resistance in heat exchangers.[30] Biofilm can also be dangerous to human health in the water treatment industry.[31] Sensor fouling was a major factor in the failure of in-situ control instrumentation in potable water

treatment.[32] Errors in measurements and increased sensor response time were attributed to fouling, which occurred at all stages of the water treatment process. Potable water treatment processes were examined[33] and the types of sensor used for control purposes at each stage to determine that fouling occurred in all areas of the water treatment processes examined and may be attributed to the attachment of micro-organisms on sensor surfaces, deposition of particulate materials or the formation of precipitates. pH electrodes, turbidity cells, dissolved oxygen cells, conductivity cells, ammonia sensors, nitrate sensors, aluminium and iron analysers, water colour monitors and residual chlorine monitors were all examined. Biofouling caused increase in electrode response times ranging from 10 seconds when clean to several minutes when a fouling by a 1mm layer of "slime" was noted.[33] A localised shift in pH was caused by the fouling layer, especially in the case of lime precipitation fouling.[33]

5.2.4 Surface Conditions

The extent of biofiouling appears to increase with surface roughness.[34] Shear forces are reduced, providing micro-climates, and there is a greater surface area on rougher surfaces. Physical and chemical properties of the surface may also have a strong influence on rate and extent of attachment. Most investigators have found that microorganisms attach more rapidly to hydrophobic, non-polar surfaces such as Teflon and other plastics than to hydrophilic materials such as glass or metals.[35,36,37] These observations were confirmed by this research group since initial attempts of biofilm sensing were impossible with silica fibre. Rouxhet et al of UCL[38] investigated initial surface conditioning of the declad fibre PMMA core and reported that the fibre surface changed during exposure to water from being hydrophobic (negatively charged) to hydrophilic (positively charged) before biofilm formation.[38] X-ray Photoelectron

Spectroscopy, (XPS) analysis indicated that the organic macromolecules adsorbed on the fibre surface changed its wettability. Biofilm are negatively charged[39] and thus were attracted to the fibre. It is expected that these changes and conditioning would be detected during the initial changes. It was observed that during initial exposure of the declad fibre to the water and nutrient solution a rapid decrease in intensity occurred during the first few hours before a steady state value was achieved. This initial change had been discarded because it was thought to be spurious and due to initial instabilities in the light source, lie of fibre etc, but recent opinion[38] indicates that these changes may signal the initial conditioning of the fibres and the change in surfacic conditions from hydrophobic to hydrophilic determined by the presence of the organic macromolecules and leading to biofilm formation. The study of PMMA surface conditions is very important as this informs the work of coating the core surface. This is a rapidly growing research area as the ability to coat an optical fibre with a reagent optimises the performance of an optical fibre sensor.[40]

5.3 Detection and Removal of Biofilm

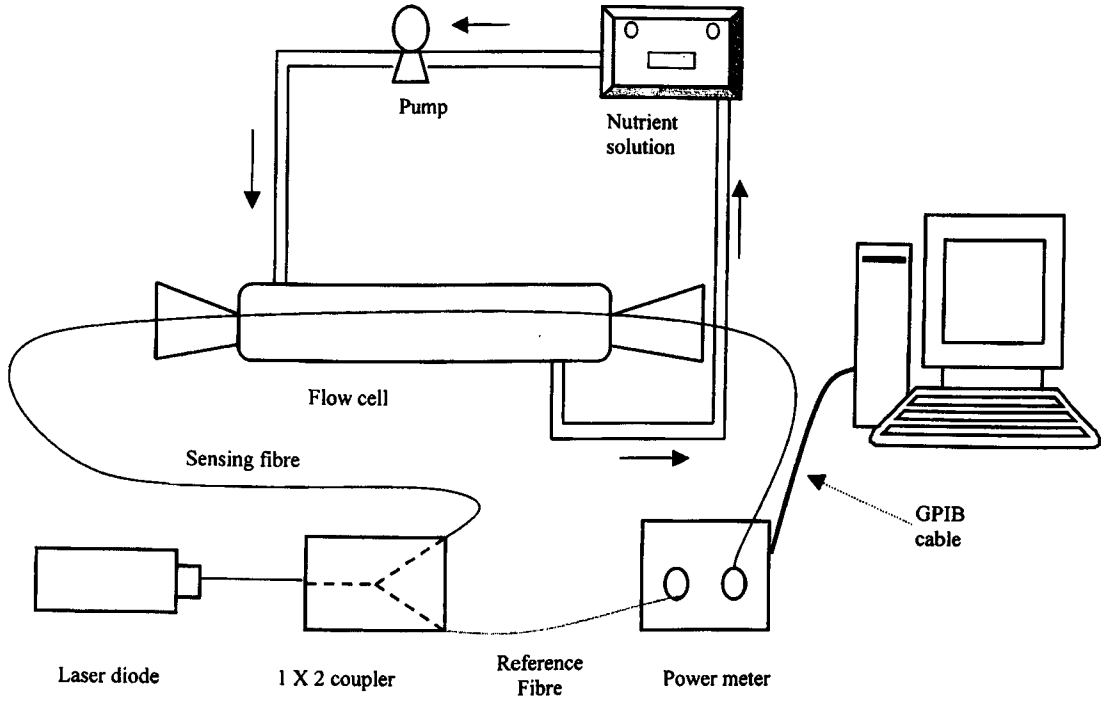

Figure 5.3 Experimental configuration of Evanescent Field POF Biofilm sensor.

The evanescent field POF sensor developed by the research group has been demonstrated to detect the early onset of biofilm growth.[Error! Bookmark not defined.]

A nutrient consisting of 1% yeast extract solution made up using tap water from the mains at LJMU which contains trace minerals, to encourage bacterial growth, was circulated through the system. The experiments would run over 7 days with one reading taken every hour. Initial difficulties included sealing the system to prevent evaporation. Initial results showed the output signal dropping indicating biofilm growth on the fibre surface, changing the refractive index of the fibre cladding as it grew, coupling an increasing proportion of light out of the fibre core.

Figure 5.4 shows the result of biofilm monitoring with the sensor carried out by R Chandy.[Error! Bookmark not defined.] It is postulated that this is due to the evanescent field energy being entirely attenuated by the biofilm growth, thus providing a maximum

range for the sensor. The biofilm grown under laboratory conditions reached equilibrium at a maximum of 2mm thickness, at which a constant biomass has been established, although evanescent field attenuation would not be able to measure biofilm growth greater than 1 mm from the core-cladding interface.[19] The refractive index of the biofilm was 1.336 at around four days growth, which is 2 x10-3 refractive index unit or a 0.15% increase compared to the surrounding water medium (1.334).[19]

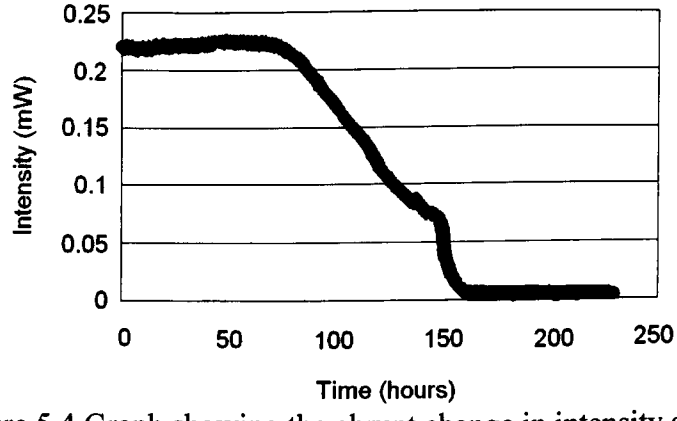

figure 5.4 Graph showing the abrupt change in intensity after 150 h of exposure to nutrient solution[4]

Biofilm growth was confirmed through electron microscope images in figures 5.5 to 5.7. Declad optical fibres were immersed in nutrient solution and removed after a period of time and air dried. These fibres were then gold sputter coated and then imaged using an electron microscope.

Figure 5.5 is a 1000x and shows clumps of biofilm attached to the PMMA core surface, the characteristic grooves and pits from the process of cladding removal are clear to see. These pits and grooves may well assist in biofilm attachment to the PMMA core surface by providing a keyed surface.

Figure 5.6 is a 2000x magnification and clearly shows a layer of biofilm. The cracking due to drying conveniently shows the planar nature of biofilm growth. Free-

floating bacteria form clumps and attach themselves to a submerged surface. They begin to produce slimy extracellular polymeric substances (EPS) and colonise the surface. EPS production allows the emerging biofilm community to develop a complex, three-dimensional structure.[41]

Figure 5.7 at 2000x magnification clearly shows individual bacteria clumped in islands similar to figure 5.4. The difference this time is that the clumps have formed on a biofilm surface, the POF core is completely covered by a layer of biofilm.

Figure 5.8 shows the absence of bacteria on the fibre core after exposure to contact lens protein removal tablet solution. Biofilms are highly resistant to most antimicrobial agents and disinfectants.[42] It was found that tablets used to remove protein deposits on contact lenses, one Trizyme[43] tablet dissolved in 10 cm^3 of a sterile buffered isotonic solution, also removed biofilm.

Figure 5.9 is the result of a 24 hour experimental run in which the evanescent field POF sensor developed by this project was immersed in a 1% yeast extract nutrient solution and shows the subsequent modulation of the propagating signal of a 37% drop in intensity due to biofilm growth, the change in refractive index absorption and scattering. The biofilm reached an optimum thickness of about 1mm, beyond which the propagating signal remains unchanged. The system was drained of the cloudy solution and flushed through with water after 9 hours; a protein removal solution was then introduced into the system. The propagated signal increased as the biofilm was killed, settling to a steady signal, ready for sensing again.

Figure 5.5 1000x magnification. Clumps of microbes on declad POF core after 6 hours exposure to nutrient solution

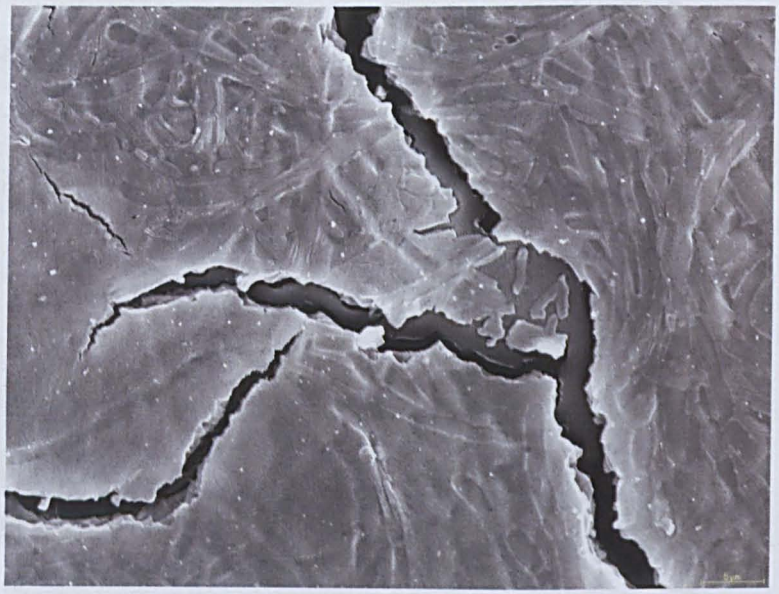

Figure 5.6 2000x magnification. Layer of biofilm on declad POF core 12 hours exposure to nutrient

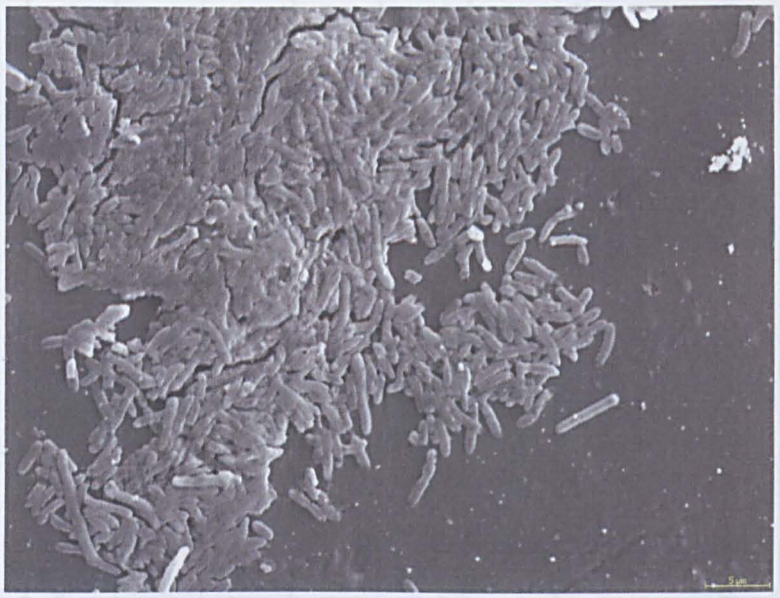

Figure 5.7 2000x magnification. Three days of bacterial growth

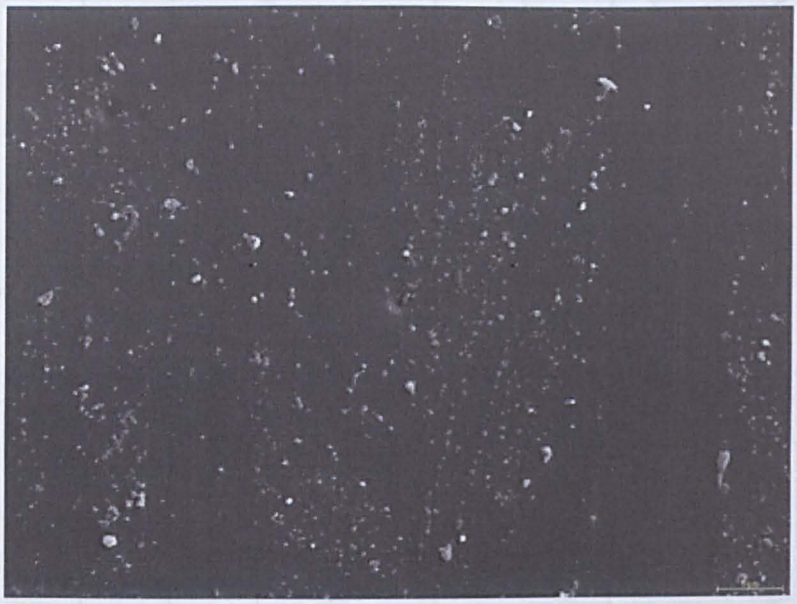

Figure 5.8 Electron microscope image at 2000 x magnification of the surface of POF after cleaning with protein tablet

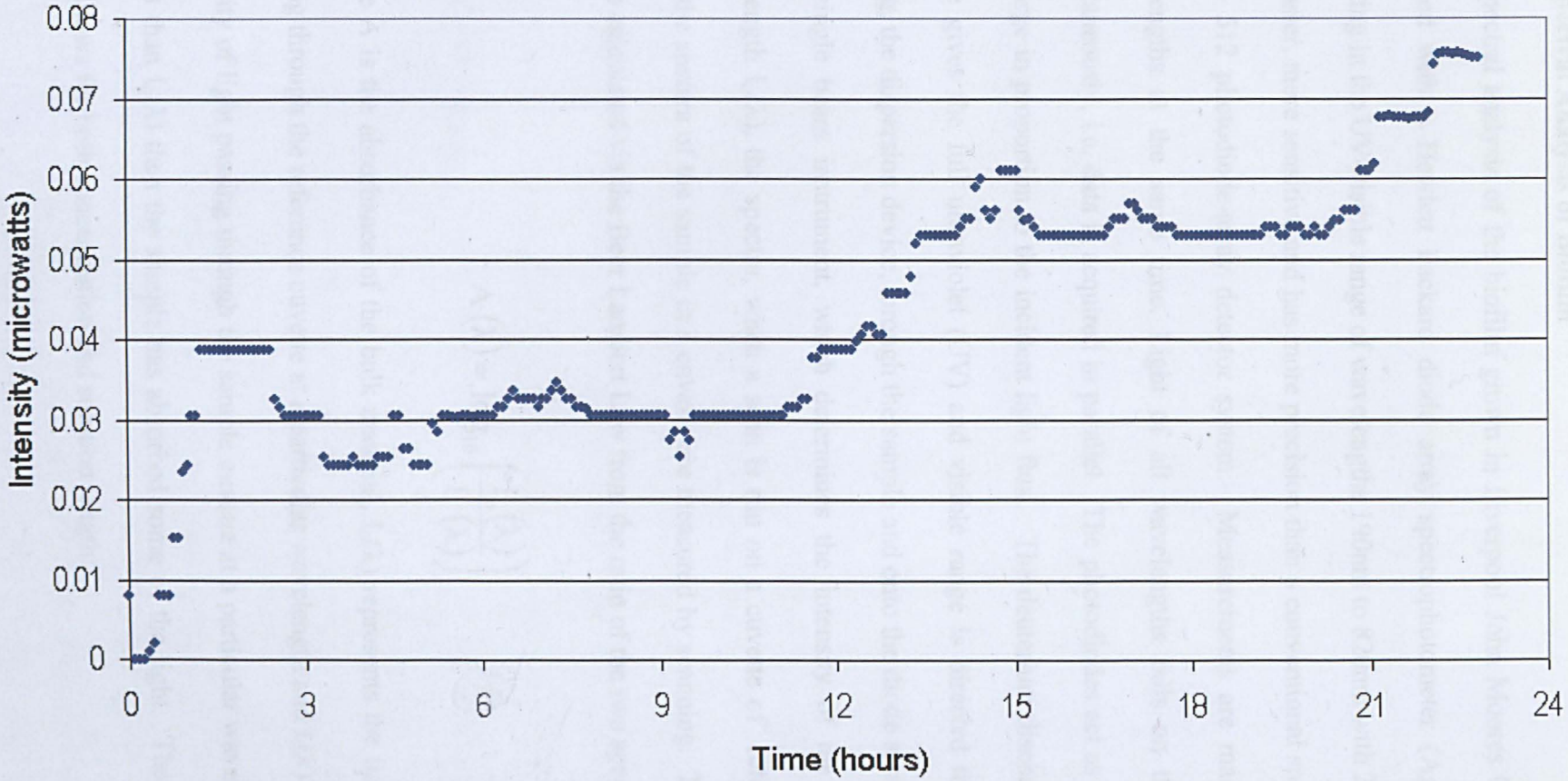

Figure 5.9 Graph showing signal change due to immersion in a nutrient solution and subsequent soaking in protein removal solution

5.4 Spectral Analysis of Biofilm

The spectral analysis of the biofilm grown in Liverpool John Moores University was obtained with a Hewlett Packard diode array spectrophotometer (Agilent) 8452A, operating in the UV-visible range of wavelengths 190nm to 820nm with 2nm resolution. It is faster, more sensitive and has more precision than a conventional spectrometer due to the 512 photodiode-array detector system. Measurements are made at different wavelengths at the same time. Light of all wavelengths falls on the diode-array simultaneously, i.e. data is acquired in parallel. The photodiodes act as capacitors that discharge in proportion to the incident light flux. The deuterium discharge lamp light source gives the full ultraviolet (UV) and visible range is directed through a fixed grating, the dispersion device, through the sample and onto the diode array. The system is a single beam instrument, which determines the intensity of the lamp at each wavelength $I_o(\lambda)$, the spectra, when a scan is run on a cuvette of reference sample. Then the spectra of the sample in a cuvette are measured by scanning. The absorbance is then calculated via the Beer Lambert Law from the ratio of the two spectra:

$$A(\lambda) = \log_{10}\left(\frac{I_o(\lambda)}{I_t(\lambda)}\right) \qquad \text{---5.1}$$

Where A is the absorbance of the bulk material, $I_o(\lambda)$ represents the intensity of light passing through the reference cuvette at a particular wavelength and $I_t(\lambda)$ represents the intensity of light passing through the sample cuvette at a particular wavelength. If $I_t(\lambda)$ is less than $I_o(\lambda)$ then the sample has absorbed some of the light. The Beer-Lambert Law allows for both concentration and solution length:

$$\log_{10}\left(\frac{I_o(\lambda)}{I(\lambda)}\right) = \varepsilon\, l\, c \qquad \text{---5.2}$$

ε is the molar absorption coefficient of the bulk material, l is the length of solution the light has passed through in centimetres and c is the concentration of the solution. We can therefore equate equations 5.1 and 5.2.

$$A(\lambda) = \log_{10}\left(\frac{I_o(\lambda)}{I_t(\lambda)}\right) = \varepsilon\, l\, c \qquad \text{---5.3}$$

Which means that the molar absorbance coefficient of the bio-culture in the water may be calculated using the rearranged formula:

$$\varepsilon = \frac{A}{l\ c} \qquad \text{---5.4}$$

A freshly made nutrient solution was used as a reference to ensure that we only measured any changes due to biofilm growth. This concentration was kept constant throughout. The lower limit was set to 350nm to obtain detailed analysis. The biofilm at various stages of growth were compared: typically 18, 32, 104, 126, 150, 174 hours. Figure 5.10 shows the result of the spectral analysis carried out on the bacteria grown for different lengths of time in the nutrient solution. The results consistently revealed peaks at 486nm and most strongly at 656nm. This indicated that the detection of different types of biofilm bacteria could be targeted with the use of wavelength matched light sources.

There are two sets of readings that are significantly lower than that of other timings, 104 hours and 174 hours. This may well be due to the clumping nature of bacterial growth. At these times the clumps of bacteria may be dispersed non-uniformly and the samples obtained at these times were less populated.

I have since discovered that the deuterium lamp has several sharp peaks in its spectrum, including a major emission line at 656nm and is so bright that the diodes at this wavelength are masked. The peaks detected through the spectral analysis of the biofilm may well to due to this and so the process needs to be repeated with the spectrophotometer recalibrated.

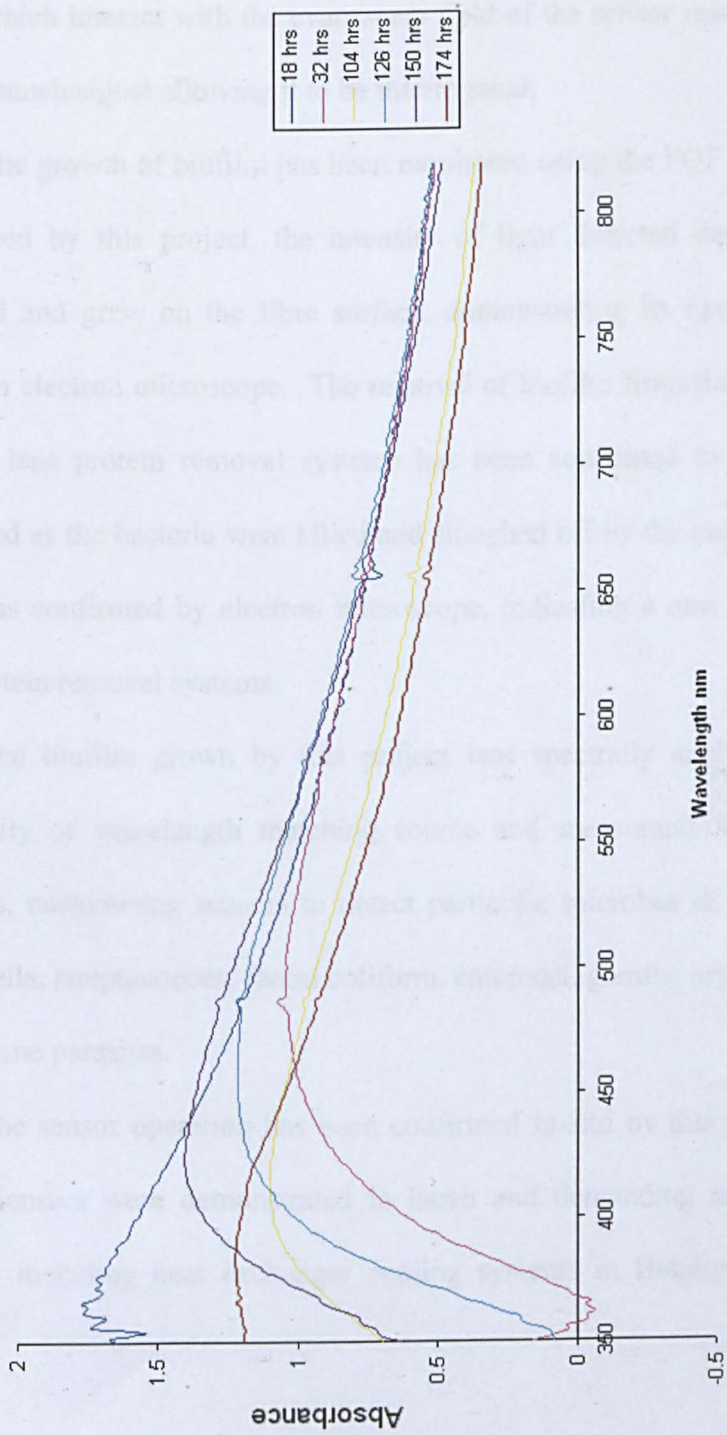

Figure 5.10 Graph of the raw data showing the absorbance of the biofilm grown at Liverpool John Moores at wavelengths 350nm to 820nm showing peaks at 486nm and 656nm

5.5 Summary

Evanescent field sensors were developed by this project for detecting biofilm growth. The conditions required for the formation of biofilm were investigated, the structure of biofilm lends itself to optical monitoring techniques. It is optically transmissive and its refractive index alters during its adhesion, growth and subsequent increase of thickness, all of which interact with the evanescent field of the sensor resulting in the attenuation of the launch signal allowing it to be interrogated.

The growth of biofilm has been monitored using the POF evanescent field sensor developed by this project, the intensity of light detected decreased as the biofilm attached and grew on the fibre surface, demonstrating its operation and by imaging using an electron microscope. The removal of biofilm from the sensor with the use of contact lens protein removal systems has been confirmed by the sensor, the signal increased as the bacteria were killed and sloughed off by the current of fluid circulated. This was confirmed by electron microscope, indicating a new application for contact lens protein removal systems.

The biofilm grown by this project was spectrally analysed and indicates the possibility of wavelength matching source and measurand for particular microbial colonies, customising sensors to detect particular microbes of interest such as e-coli, salmonella, streptococcus, faecal coliform, enterocci, giardia, cryptosporidium and other waterborne parasites.

The sensor operation has been confirmed in-situ by this project.**Error! Bookmark not defined.** Sensors were demonstrated in harsh and demanding industrial water process systems including heat exchanger cooling systems in Belgium and a paper mill in

France, and could sense the very early formation of biofilm, and biofouling removal and control by biocides.[44]

References

[1] European Commission project CONTRACT N° ENV 4-CT97-0634, partners: IRH Environnement, G Grapin, G D'Ambrosio, G Jonca; Liverpool John Moores University (LJMU): PJ Scully, RJ Chandy, YM Wong; University of Southampton: J Atkinson; Laborelec, L Duvivier, R Vanmaele, C Goffin, N Deridder; Université Catholique de Louvain: P Rouxhet, V Toniazzo, "On-line Measurement for Preventing Fouling When Closing Industrial Process Water Circuit", 1 February 1998- 31 July 2000

[2] CLOOPT European Commission Project, Contract No. ENV 4-CT97-0634, "On Line Measurement for Preventing Fouling when Closing Industrial Process Water Circuit [CLOOPT]" 1/2/1998 – 31/7/2000

[3] L Jain, "Evanescent Field Absorption (Refractive Index) Based Optical Fibre Sensor and its Application in Detection of Biofilms," M.Sc. thesis, Liverpool John Moores Univ., Liverpool, U.K., 1996

[4] R Philip-Chandy, PJ Scully, "On-Line Measurement for Preventing Fouling When Closing Industrial Process Water Circuit," IRH Environ., Nancy, France, EC Progress Rep., July 1998, Jan. 1999

[5] Montana State University Center for Biofilm Engineering: www.erc.montana.edu/default.htm accessed 4th December 2008

[6] Z Lewandowski, R Avci, M Geiser, X Shi, K Braughton, N Yurt, "Biofouling and Corrosion of Stainless Steels in Natural Waters", Wat. Scie. Tech.:Wat. Sup., vol.2, No.4, pp65-72, 2002

[7] HV Rege, W Sand, "Mini Plant for Simulation of Metal Corrosion and Biofouling for Evaluation of Countermeasures", Proc. NACE Int. Conf. Corrosion, Paper 306, Houston TX, 1999

[8] RD Kane, P Surinach, "A Field Study of Microbiological Growth and Reservoir Souring", Proc. NACE Int. Conf. Corrosion, Houston TX, 1997

[9] WF McCoy, ES Lashen, "Evaluation of Industrial Biocides in Laboratory Model Cooling Towers", Cooling Tower Inst. Annu. Conf., Paper TP-86-17, Houston , TX, 1986

[10] "Standard Recommended Practice On-Line Monitoring of Cooling Waters NACE Store - RP0189-2002

[11] WG Charcklis, H Turakhia, N Zelver, "Biofouling of Heat Transfer Surfaces Pat 2", Corrosion and Maintenance, vol.7, pp. 213-228, 1984

[12] M Turakhia, WG Characklis, N Zelver, "Fouling of Heat Exchanger Surface: Measurement and Diagnosis", Heat Transfer Eng., vol.5, No. 1-2, pp93-101, 1984

[13] HE Crandall, "Microbiological Test Methods in Association with Cooling Towers", Cooling Tower Inst. Annu. Conf., Paper TP-86-7, Houston, TX, 1986

[14] WH Dickenson, "Biofouling Assessment using an On-line Monitor", TAPP199 Papermakers Conference Proceedings Atlanta, GA, pp449-457, 1999

[15] HJ Lee, DG Han, SH Lee, JW Yoo, SH Baek , EK Lee, "On-line Monitoring and Quantitative Analysis of Biofouling in Low Velocity Cooling Water System", Korean J. Chemical Engineering, vol.15, pp71-77, 1998

[16] JS Smart, T Pickthall, A Carlile, "Using On-line Monitoring to Solve Bacterial Corrosion Problems in the Field", Proc. NACE Int. Conf. Corrosion paper 212, Houston TX, 1997

[17] GJ Licina, G Nekoksa, "An Electrochemical Method for On-line Monitoring of Biofilm Activity", Proc. NACE Int. Conf. Corrosion Paper 403, Houston TX, 1993

[18] R Philip-Chandy, PJ Scully, D Thomas, "A Novel Technique for On-line Measurement of Scale using a Multimode Optical Fibre Sensor for Industrial Applications", Sensors & Actuators B, vol.71, pp19-23, 2000

[19] R Philip-Chandy, PJ Scully, P Eldrige, G Grapin, G D'Ambrosio, F Colin, "An Optical Fibre Sensor for Biofilm Measurement using Intensity Modulation and Image Analysis", IEEE Journal of Selected Topics in Quantum Electronics vol.6, No.5, pp764-772 – JSTQE Optical Sensors Special Issue, 2000

[20] PJ Scully, R Philip-Chandy, YM Wong, R Bartlett, G Grapin, G Jonca, G D'Ambrosio, F Colin, N McMillan, M O'Neill, P Rouxhet, "On-line Measurement of Biofouling at Water Interfaces using Plastic Optical Fibre", Sensors & Their Applications XI/ISMCR 2001

[21] RM Donlan, WO Pipes, TL Yohe "Biofilm Formation on Cast Iron Substrata in Water Distribution Systems", Water Res vol.28, pp1497-1503, 1994

[22] P Fera, MA Siebel, WG Characklis, D Prieur, "Seasonal Variations in Bacterial Colonization of Stainless Steel, Aluminum, and Polycarbonate Surfaces in a Seawater Flow System", Biofouling 1989, vol.1, pp251-261, 1989

[23] MM Cowan, TM Warren, M Fletcher, "Mixed Species Colonization of Solid Surfaces in Laboratory Biofilms". Biofouling 1991, vol.3, pp23-34, 1991

[24] WH Kimratul-Aznita, AR Fathilah, "The Potential use of Chlorhexidine (CHX) and Hexetidine-containing Mouth Rinse in Maintaining Toothbrush Sterility", J. Med. Sci., vol.6, No.1, pp59-62, 2006
[25] Environment Protection Agency, www.epa.gov
[26] HC Flemming, J Wingender, C Griegbe, C Mayer, "Physico-chemical properties of biofilms". In: Evans LV, editor. "Biofilms: recent advances in their study and control", Amsterdam: Harwood Academic Publishers, pp19-34. 2000
[27] Z Lewandowski, "Structure and Function of Biofilms", In: Evans LV, editor, "Biofilms: recent advances in their study and control", Amsterdam: Harwood Academic Publishers, pp1-17, 2000
[28] WA Hamilton, "Industrial Problems due to Biofilms", British Biofilm Club Meeting, pp40, 1995
[29] R Lewin, "Microbial adhesion is a sticky problem," Science, vol.224, pp375–377, 1984.
[30] WG Characklis, "Process analysis in microbial systems: Biofilms as a case study," in Mathematics and Microbiology, M Bazin, Ed. London, U.K., Academic, pp171–234, 1983
[31] GA Gagnon, JL Rand, KC O'Leary, AC Rygel, C Chauret, RC Andrews, " Disinfectant Efficacy of Chlorite and Chlorine Dioxide in Drinking Water Biofilms", Water Research vol.39, pp1809–1817, 2005
[32] J Sedor, SG Mulholland, "Hospital Acquired Urinary Tract Infections Associated with the In-dwelling Catheter", Urol Clin North Am, vol.26, pp821-828, 1999
[33]RM Donlan, "Biofilm Control in Industrial Water Systems: Approaching an Old Problem in New Ways" LVEvans, editor, "Biofilms: Recent Advances in their Study and Control", Amsterdam: Harwood Academic Publishers, pp333-360, 2000
[34] WG Characklis, GA McFeters, KC Marshall: editors, "Physiological Ecology in Biofilm Systems", Biofilms, New Yourk, John Wiley and Sons; p341-394, 1990
[35] M Fletcher, GI Loeb, "Influence of Substratum Characteristics on the Attachment of a Marine Pseudomonad to Solid Surfaces". Appl Environ Microbiol 1979; vol.37, pp67-72, 1979
[36] B Bendinger, HHM Rijnaarts, K Altendorf, AJB Zehnder, "Physicochemical Cell Surface and Adhesive Properties of Coryneform Bacteria Related to the Presence and Chain Length of Mycolic Acids", Appl Environ Microbiol, vol.59, pp3973-3977, 1993
[37] JH Pringle, M Fletcher, "Influence of Substratum Wettability on Attachment of Freshwater Bacteria to Solid Surfaces", Appl Environ Microbiol 1983, vol.45, pp811-817, 1983
[38] CLOOPT report August 2000 - internal report
[39]F Gotz, T Bannerman K Schleifer, "The Genera Staphylococcus and Macrococcus", editors: M Dworkin, S Falkow, E Rosenberg, K Schleifer, E Stackebrandt, "The Prokaryotes", chapter 1.2.1, p44, Springer
[40] SR Cordero, H Mukamal, A Low, M Beshay, D Ruiz, RA Lieberman, "Fiber Optic Sensor Coatings with Enhanced Sensitivity and Longevity", Progress in Biomedical Optics and Imaging, vol.7 ,No.41, 2006
[41] H Helle, P Vuoriranta, H Valimaki, J Lekkala, V Aaltonen, "Monitoring of Biofilm Growth with Thickness-shear Mode Quartz Resonators in Different Flow and Nutrition Conditions", Sensors and Actuators B: Chemical, vol.71, issues 1-2, pp47-54, 2000
[42] RM Donlan, "Role of Biofilms in Antimicrobial Resistance", ASAIO J 2000;46:S47-S52.
[43] Trizyme, Sauflon Pharmaceuticals
[44] YM Wong, PJ Scully, RJ Bartlett, KSC Kuang, WJ Cantwell, "Plastic Optical Fibre Sensors for Environmental Monitoring: Biofouling and Strain Applications", Strain, vol.39, No.3, pp115-119, 2003

CHAPTER SIX

Characterisation of Evanescent Field Sensor

6.1 Introduction

The evanescent field sensor detects refractive index changes at the core-cladding interface, where the cladding consists of the surrounding measurand. Losses due to absorption and scattering effects also contribute to the attenuation of the launch signal and are discussed in more detail in section 2.5 of this thesis. These changes must be characterised to facilitate understanding of the modulated intensity of sensing light signal due to the measurand.

The aim of this chapter is to describe the procedures involved in profiling the change in intensity of light propagating in declad and tapered fibres due to refractive index change of their cladding.

6.2 Refractive Index Medium[1]

A range of clear, colourless, non-reactive liquids were required to ensure that attenutation was due to refractive index change not absorption or scattering. This is because the initial growth of biofilm manifests itself as a change in refractive index. Pure biofilm is colourless and clear, and therefore no absorption or scattering. Surfacic conditioning takes place before bacteria start to adhere and the sensor may be able to detect these initial changes at the core-cladding interfaces.

Since the experiment required 125 ml of liquid, commercial immersion oils were prohibitive ($800 for a full set of 91 different liquids with refractive indices over the range from 1.460 to 1.640, with each bottle containing 0.25 fl oz (7.393 ml)). Thus a set of refractive index solutions over the range 1.33–1.492 were formulated using different concentrations of distilled water and sucrose solutions to yield refractive indices up to 1.46. Above this value, baby oil[2] (non-oxidizing, optically clear mineral oil with refractive index 1.463) and Fractoil (cheap, colourless, synthetic immersion oil with a refractive index of 1.517) were mixed to obtain refractive indices of values up to above the fibre core (1.492). Table 6.1 gives the proportions required to achieve the refractive index liquid required.

Formulations for Achieving Optically Clear Liquid of Various Refractive Indices		
Refractive index	Distilled water (ml)	Sucrose (g)
1.332	200	0
1.340	200	9
1.350	200	27
1.360	200	44
1.370	200	63
1.380	200	80
1.390	200	102
1.400	200	132
1.410	200	160
1.420	200	180
1.430	180	210
1.440	145	180
1.450	120	190
1.462	100	200
	Immersion oil ml	Baby oil ml
1.462	0	200
1.470	20	180
1.480	100	190
*1.490	140	100
1.500	150	45
1.510	220	20
1.517	200	0

Table 6.1 Proportions required to achieve refractive index required.
*refractive index of PMMA core

The refractive indices of the test solutions were determined using an Abbe refractometer, a bench-top refractometer that offers the highest precision of the different types of refractometers. An Abbe refractometer uses a pair of right angled prisms of high refractive index glass (1.75), higher than most liquids. A drop of the liquid whose refractive index is to be measured is sandwiched between the hypotenuses of both prisms. The light entering the prism/fluid sandwich is refracted by the first prism, the fluid then the second prism. The light emerging from the second prism is parallel to the

incident light, however it will be off-set. How much it is off-set is a measure of the refractive index of the fluid.

A set of test solutions of different refractive indices was made up in advance and kept in glass stoppered bottles. The sucrose samples were prone to airborne contamination by microorganisms such as, microfungi, dust, allergens from mites dogs and cats, and as a result did not keep well in the laboratory.[3] Refrigeration would have resulted in crystallisation of the sugar molecules. This meant that a new batch of sucrose based refractive index liquids had to be made for each set of experiments if they were to be carried out over several days. The oils were not prone to fungal or bacterial growth.

6.3 Characterisation Procedure

The system shown in Figure 6.1 was used to characterise the declad fibre, it consisted of a flow chamber which was a Perspex tube capped at both ends, with an inlet at the top of one end and an outlet at the bottom of the opposite end. The flow chamber had a slot cut along length of the top to allow the insertion of the fibre to be characterised. The sensor was oriented in its least stress state to avoid twisting or creep of the fibre to avoid signal drift, this was the same curvature as supplied, dictated by the reel upon which it was wound. The refractive index liquid was held in a reservoir and circulated through the flow chamber with a peristaltic pump. The declad fibre to be characterised was held within the flow chamber by an arrangement of couplers and connectors in the lid of the flow chamber. The refractive index liquid was allowed to pump for 10 minutes before measurements were taken to ensure that the liquid was homogeneous. A laser diode emitting at a wavelength of 660nm was coupled via a Y-splitter into the end of the declad fibre to be characterised and into an unaltered reference fibre for common

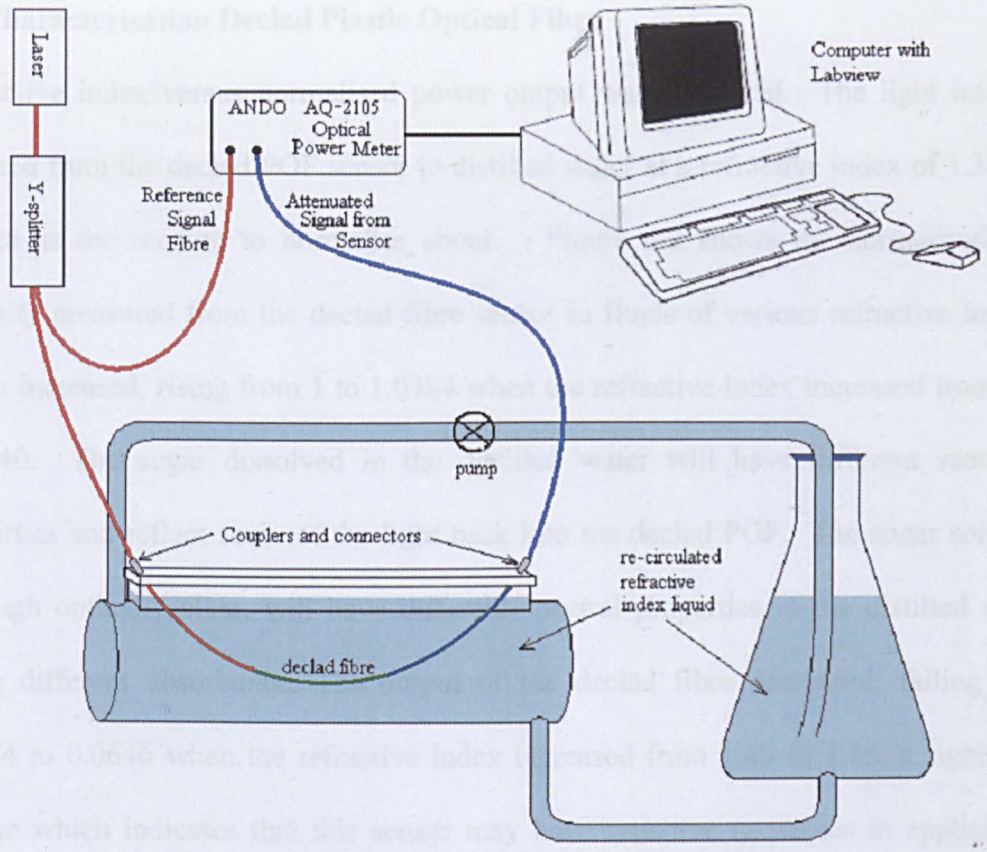

Figure 6.1 Apparatus used to characterise the sensor including sensitised POF with 5cm of cladding removed

mode rejection. This ensures that attenuation due to perturbations other than that being measured, e.g. temperature and is common to both is subtracted from the signal from the sensor, i.e. we only measure the attenuation due to refractive index change. The signal from both fibres is detected using an ANDO AQ-2105 Optical Power Meter and is collated by a computer using Labview data collection software.

The power output was measured over a short time period and an average was taken, then normalised about the average reading initially for distilled water. This procedure was repeated with liquids of increasing refractive index, as the lower refractive index liquids were less viscous than the higher and readily mixed with the higher refractive index liquids, reaching homogeneity quickly, the reverse was not true. Starting with high refractive index liquids lead to difficulty in achieving homogeneity and uncertainty of refractive index of material at the core surface.

6.4 Characterisation Declad Plastic Optical Fibre

Refractive index versus normalised power output was measured. The light intensity detected from the declad POF sensor in distilled water at a refractive index of 1.33 was chosen as the reading to normalise about. Figure 6.2 shows the normalised light intensity measured from the declad fibre sensor in fluids of various refractive indices, which increased, rising from 1 to 1.0384 when the refractive index increased from 1.33 to 1.40. The sugar dissolved in the distilled water will have different scattering properties and reflect some of the light back into the declad POF. The sugar solution, although optically clear, will have different spectral properties to the distilled water, hence different absorbance. The output of the declad fibre decreased, falling from 1.0384 to 0.0646 when the refractive index increased from 1.40 to 1.46, a significant change which indicates that this sensor may have sensitive responses in applications connected with quality control in oil which has higher refractive indices. The declad sensor was characterised with sensitivity ±0.007 refractive index units (to 2 standard deviations) or 0.5% below n=1.4 and ±0.002 refractive index units (2 standard deviations) or 0.15% above n=1.4. From 95% confidence limits, the accuracy of the POF was ±0.006 refractive index units (to 2 standard deviations) or 0.4% above 1.4.

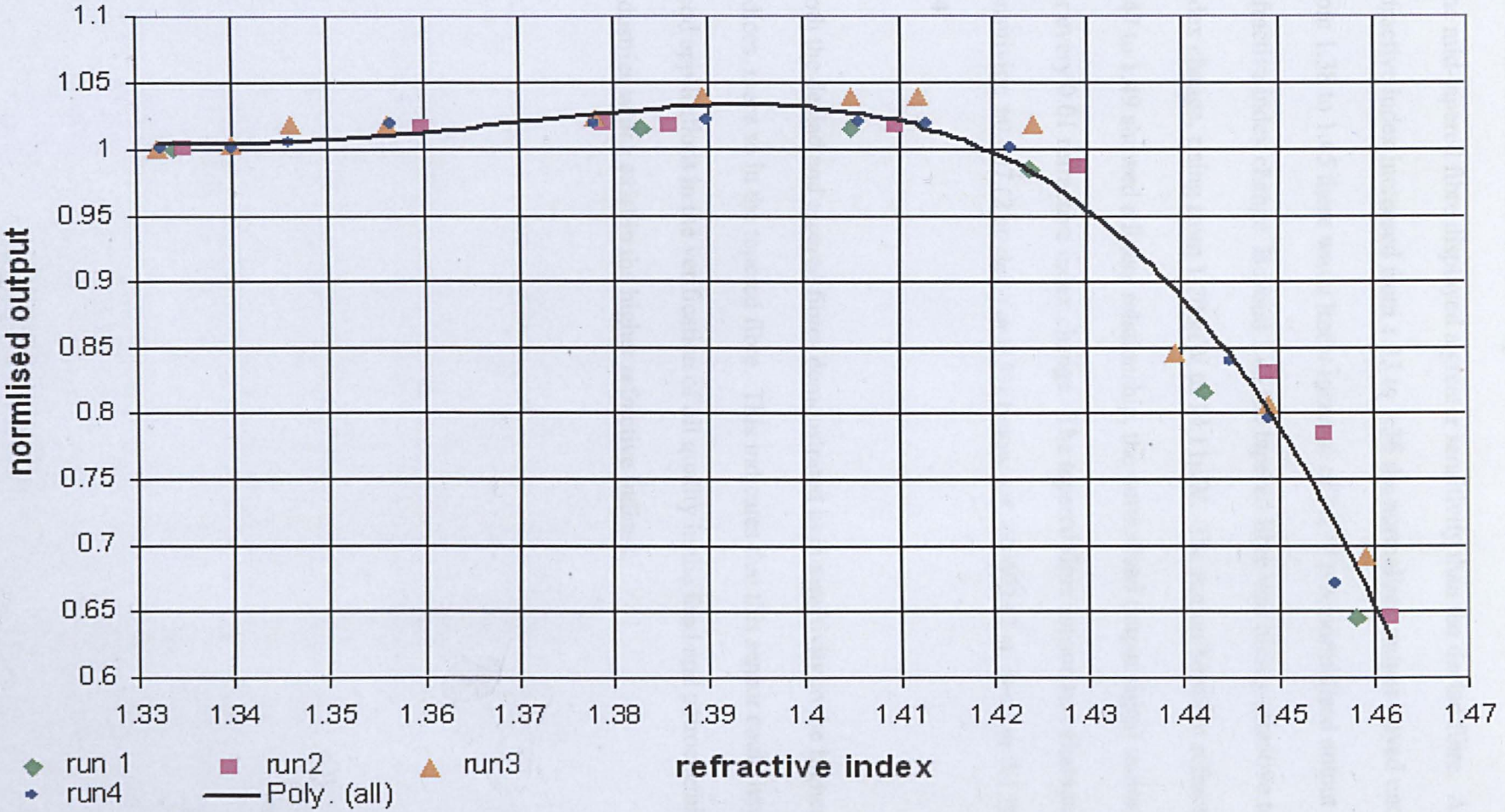

Figure 6.2 Graph showing the normalised intensity of modulated light power of the declad fibres sensor due to absorption/refractive index changes of the cladding.

6.5 Characterisation of Mid- tapered POF

The mid-tapered fibre displayed a greater sensitivity than the declad fibre. As the refractive index increased from 1.33 to 1.36 the normalised output stayed unchanged, from 1.38 to 1.45 there was a linear increase of 0.274 μW normalised output per 0.01 refractive index change. Beyond 1.45 the tapered fibre was highly sensitive to refractive index change, rising from 1.706μW to 14.11μW. The region between refractive indexes 1.47 to 1.49 showed a linear relationship, the normalised output signal increased 0.5μW for every 0.01 refractive index change. The tapered fibre sensor was characterised with sensitivity: ±0.007 (2 st. dev.) or 0.5% below 1.4. ±0.002 (2 st. dev.) or 0.15% above 1.4.

Both the declad and tapered fibres demonstrated high sensitivity in the higher refractive indices, more so in the tapered fibre. This indicates that this sensor could have very good applications in the verification of oil quality in the food and petrochemical industries which exist in the higher refractive indices.

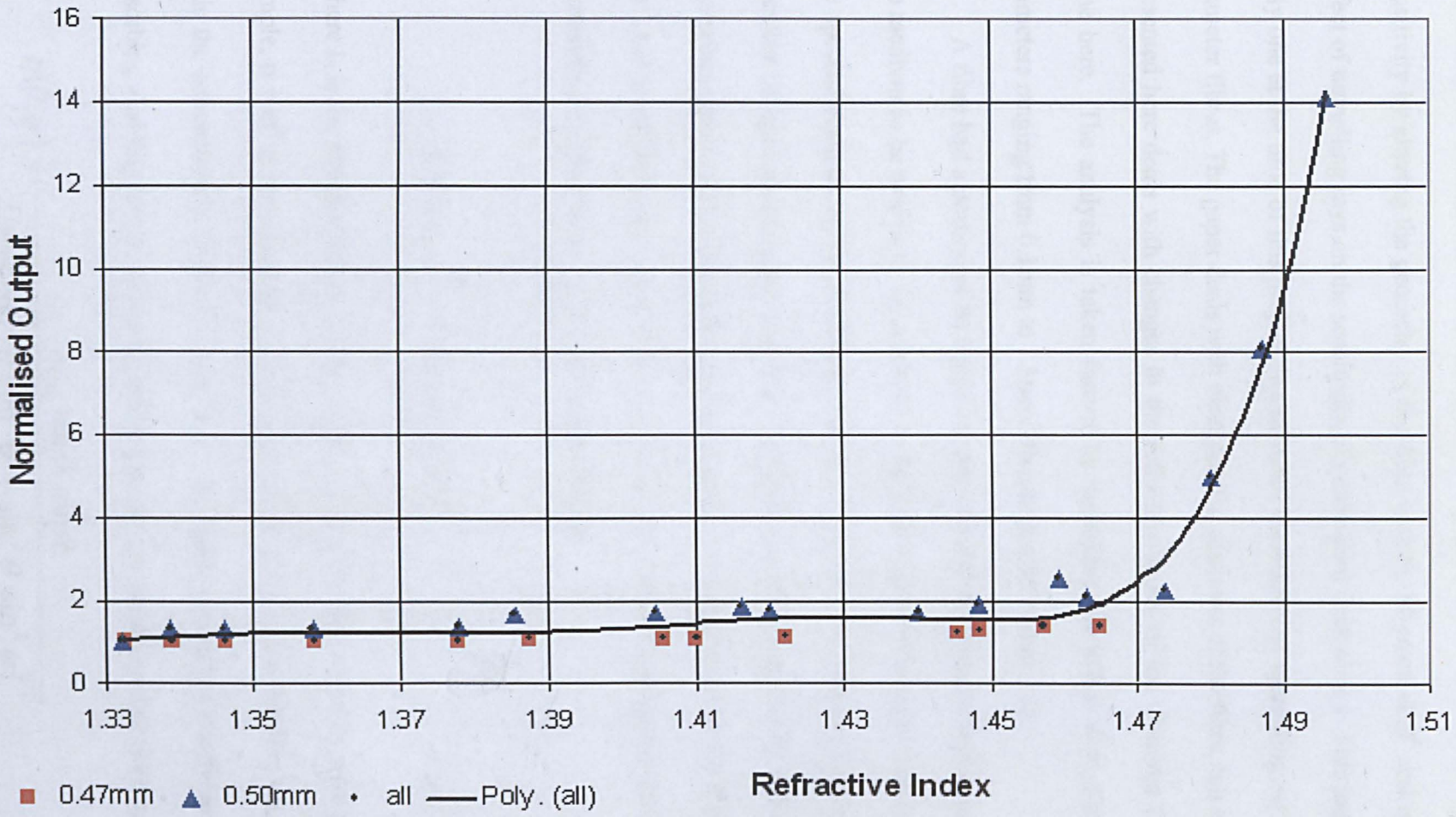

Figure 6.3 Graph showing the normalised intensity of modulated light power of the tapered fibre sensor due to absorption/refractive index changes of the cladding.

6.6 Evanescent Wave Absorption Theory in Optical Fibres

The theory of evanescent wave absorption was discussed with a view to improving sensitivity by altering the geometry of the fibre core by Mignani et al[4] and includes the effect of tunnelling rays on the sensitivity of evanescent field sensor. This paper was the only one at the time of this project that included the effects of tunnelling rays and large diameter fibres. The paper deals with changing the diameter of the fibre, but the analysis presented here deals with changes in the refractive index of the cladding for the first time here. The analysis is taken further by modelling the effect with different fibre diameters ranging from 0.1mm to 1.1mm, illuminated by 660nm LD.

A fibre had a portion of its cladding removed and the stripped region immersed in the medium to be analysed. In section 5.4 the Beer-Lambert law was used in obtaining the spectral analysis of the biofilm grown at Liverpool John Moores University. The intensity of light propagating in a fibre is due to the losses caused by the evanescent wave absorption in the surrounding medium and can be expressed as the Beer-Lambert law[4], but modified with η, to give the fraction of light power propagating in the medium surrounding the fibre core, i.e. the modified cladding

$$A = \log_{10} \frac{I_o}{I_t} = \varepsilon C L \eta = \alpha L \eta \qquad \text{---6.1}$$

Where I_o is the intensity of the incident light and I_t is the light intensity after passing the sample, $\alpha = \varepsilon C$ is the absorbance coefficient of the medium surrounding the fibre core; C is the concentration of the medium and ε its molar absorption coefficient. L is the absorbing cladding length. By considering a single ray, meridional or skew $\eta(\theta,\varphi)$

$$\eta(\theta,\varphi) = \frac{\lambda n_{ex} \tan\theta \ \sin\theta}{2\pi r_o n_{co}^2 \sin^2\theta_c \left(\sin^2\theta_c - \sin^2\theta \ \sin^2\varphi\right)^{1/2}} \qquad \text{---6.2}$$

Where λ is the illuminating wavelength of light, n_{ex} is the refractive index of the surrounding medium and $\theta_c=\arccos(n_{ex}/n_{co})$, the complementary of the critical angle, where n_{ex} is lower than n_{co}. θ is the angle between the ray and fibre axis and φ is the skewness angle.[5] Taking into account the intensity angular distribution, P (θ,φ); the fraction of power propagating in the modified cladding in the evanescent wave,η, may be expressed as:

$$\eta = \frac{\int_0^{\theta_f}\int_0^{\pi/2}\eta(\theta,\varphi)P(\theta,\varphi)d\theta d\varphi}{\int_0^{\theta_f}\int_0^{\pi/2}P(\theta,\varphi)d\theta d\varphi} \qquad \text{--- 6.3}$$

Where $\theta_f = \arccos(n_{cl}/n_{co})$ and is the complementary of the critical angle in the clad fibre, which is lower than θ_c. When a Lambertian light source is used the equation becomes:

$$\eta = \frac{\int_0^{\theta_f}\int_0^{\pi/2}\frac{\lambda n_{ex}\sin^3\theta\ \sin^2\varphi}{2\pi r_0 n_{co}^2\sin^2\theta_c\left(\sin^2\theta_c-\sin^2\theta\ \sin^2\varphi\right)^{1/2}}d\theta\, d\varphi}{\int_0^{\theta_f}\int_0^{\pi/2}\sin\theta\ \cos\theta\ \sin^2\varphi\, d\theta\, d\varphi} \qquad \text{---6.4}$$

The values of parameters of experimental components used by the research group were substituted into equation 6.4: Toray PFUFB1000 unjacketed optical fibre of radius (r_o) 0.5mm, illuminated by as laser diode emitting at (λ) 660nm and core refractive index (n_{co}) of 1.492; The effective cladding is the surrounding liquid (n_{cl}) and a range of values from 1.33 (distilled water) to 1.50 were substituted to discover the effects of refractive index change on the percentage of power in the evanescent field. Although θ_f

$= a\cos\left(\frac{n_{cl}}{n_{co}}\right)$ the cladding has been removed and replaced with n_{ex} $\therefore$ θ_f is replaced by θ_c in the first integrals of the equation. This yielded a graph, figure 6.6, which reflects the result of the characterisation experiments described in section 6.4.

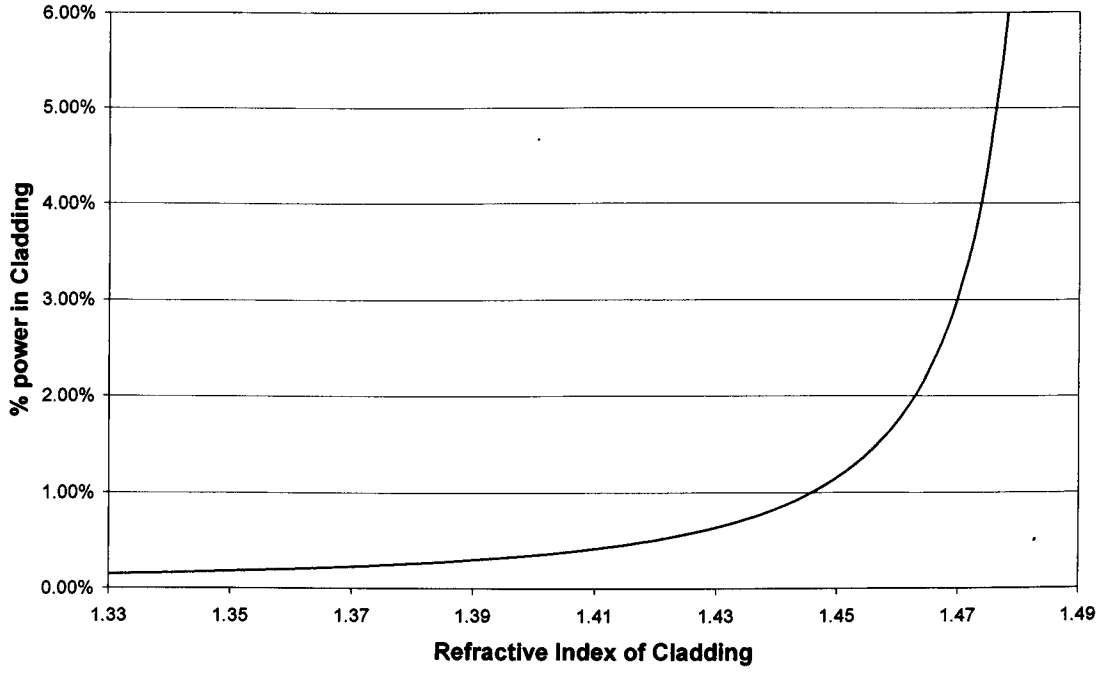

Figure 6.6 Percentage of launched power coupled into evanescent field due to refractive index change of cladding

The analysis predicted that the fraction of power guided into the surrounding medium would increased as the refractive index of the surrounding medium increased, tending towards infinity as the refractive index tended to that of the core, i.e. all light would be coupled out of the fibre as the cladding refractive index matched the refractive index of the core. This is in agreement with the characterisation procedure described in section 6.4 where the light intensity was detected in the declad POF sensor as the refractive index of the surrounding material, was changed. As the refractive index of the cladding approached that of the POF core the light intensity decreased exponentially.

Analysis of the percentage of light in the evanescent field due to core diameter has been carried out, the result of which is shown in shown in figure 6.7. More modes

are guided in the larger diameter core resulting in proportionally less power guided out. Decreasing the core diameter resulted in a higher fraction of light power coupled into the modified cladding as fewer modes are guided in narrower diameter core. This indicates the justification for producing a fibre with a region of narrower radius.
The larger 1mm POF is easier to use, coupling, terminating etc., tapering a mid length of a fibre would result in this ease of coupling together with a greater proportion of this light available for evanescent field attenuation.

The Skew Rays that give rise to tunnelling rays were taken into account by considering a PCS fibre 200μm core diameter ($n_{cl} \cong 1.4$), and n_{ex} in the 1.33 - 1.38 range, with a Lambertian illumination source, they arrive at a resulting average η value that is in the $6x10^{-3}$ to $8x10^{-3}$ range, which is an order of magnitude higher than the η value previously evaluated for the uniform fibre.

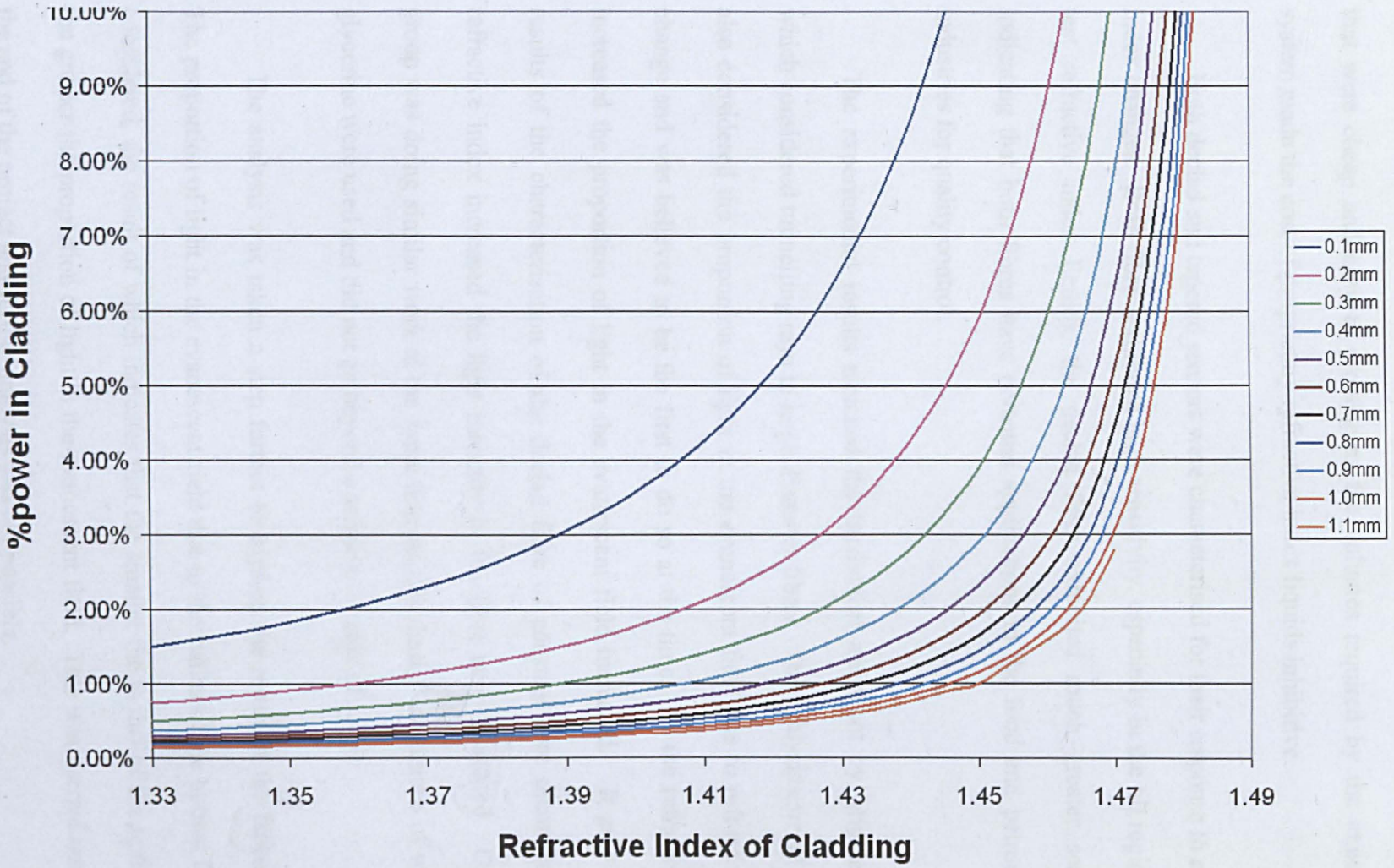

Figure 6.7 Percentage of launched power in evanescent field due to refractive index change of surrounding material for optical fibre diameters 0.1mm to 1.1mm

6.7 Summary

A range of optically clear and colourless refractive index liquids were developed that were cheap and easy to produce as the volumes required by the experimental system made the cost of proprietary refractive index liquids inhibitive.

Both declad and tapered sensors were characterised for their response to refractive index changes. Both fibres exhibited high sensitivity, especially in the oil region of the test refractive index liquids, the declad fibre exhibited much greater sensitivity, indicating that both fibres have potential applications in the food and petrochemical industries for quality control.

The experimental results matched the theoretical treatment by Mignani et al[4] which considered tunnelling rays in large diameter fibres. The analysis carried out here also considered the proportion of light in the evanescent field due to refractive index change and was believed to be the first to do so at the time. As the refractive index increased the proportion of light in the evanescent field increased. It predicted the results of the characterisation of the declad fibre of constant core diameter, as the refractive index increased the light intensity in the fibre core decreased. One other group was doing similar work at the same time as this thesis.[6] Solutions of water and glycerine were used and did not go beyond a refractive index of 1.410.

The analysis was taken a step further to explain the result of the tapered fibre. The proportion of light in the evanescent field due to the radius of the optical fibre was considered, the result of which indicates that the smaller the radius of the optical fibre the greater the proportion of light in the evanescent field. This was carried out right at the end of the project and further analysis was not possible.

By taking tunnelling rays into account, Mignani et al[4] found that the same fibre had η value within the range of $6x10^{-3}$ to $8x10^{-3}$ an order or magnitude higher than the previously evaluated, which supports the operation of the biofilm sensor developed. Mignani et al also found that reducing the core radius enhanced the fibre absorbance in agreement with our findings.

As far as we were aware, at the time of this research there was no other work published on intensity attenuation due to refractive index change, we were the only group to characterise POF in this way. Subsequently we have found one other group was doing similar work at the same time as this thesis.[6] They used solutions of water and glycerine but did not go beyond a refractive index of 1.410. No other research group has characterised the POF sensors above refractive indices above 1.410. The work in this chapter has informed four other papers.[7,8,9,10]

References

[1] YM Wong, PJ Scully, HJ Kadim, V Alexiou, RJ Bartlett , "Automation and dynamic characterization of light intensity with applications to tapered plastic optical fibre", Journal of Optics A: Pure and Applied Optics vol.5, pp51–58, 2003

[2] Asda own label baby oil purchased in 2002

[3] L Molhave, T Schneider, SK Kjaergaard, L Larsen, S Norn, O Jorgensen, "House Dust in Seven Danish Offices", Atmospheric Environment, vol.34, No. 28, pp4767-4779, 2000

[4] AG Mignani, R Falciai, L Ciaccheri, "Evanescent Wave Absorption Spectroscopy by Means of Bi-tapered Multimode Optical Fibers", Applied Spectroscopy vol.52, No.4, pp546–551, 1998

[5] AW Snyder, JD Love, "Optical Waveguide Theory", Chapman & Hall, London, 1983

[6] J Rayss, G Sudolski, "Signal of the Evanescent Wave Sensor as a Function of its Length and the Refractive Index of the Surrounding Medium", Proceedings of SPIE vol.4239, pp118–126, 2000

[7] A Banerjee, S Mukherjee, RK Verma, B Jana, TK Khand, M Chakroborty, R Dasd, S Biswas, A Saxena, V Singh, RM Hallen, RS Rajput, P Tewari, S Kumar, V Saxena, A K Ghosha,, J John, P Gupta-Bhaya, "Fiber optic sensing of liquid refractive index", Sensors and Actuators B, vol.123, pp594–605, 2007

[8] C Wochnowski, Y Hanada, Y Cheng, S Metev, F Vollertsen, K Sugioka, K Midorikawa, "Femtosecond-Laser-Assisted Wet Chemical Etching of Polymer Materials", Journal of Applied Polymer Science, vol.100, pp1229–1238, 2006

[9] P Gupta-Bhaya, AK Ghosh, V Saxena, J John, "Design and calibration of low-cost fiber optic sensors for refractive index measurement of turbid liquids", Proc. of SPIE vol.6378, 2006

[10] GF Fernando, B Degamber, "Process monitoring of fibre reinforced composites using optical fibre sensors", International Materials Reviews vol.51, No.2, pp65-106, 2006

CHAPTER SEVEN

Conclusions and Opportunities for Future Work

7.1 Conclusions

The aim of the work described in this thesis was to optimise an early warning system for the initial onset of biofilm growth[1,2,3] for applications including monitoring the formation and subsequent build-up of biofilm, levels of flocculation and scaling in aqueous environments. The research projects encompassed European Commission Research Programmes CLOOPT (FP4) and AQUASTEW (FP5) which are described in more detail in chapter five and appendices four and five. The sensor developed by this project is an intrinsic intensity modulated plastic optical fibre evanescent field biofilm sensor. The sensor operation has been confirmed in-situ by this project.[4] Sensors were demonstrated in harsh and demanding industrial water process systems including heat exchanger cooling systems in Belgium and a paper mill in France, and could sense the very early formation of biofilm, and biofouling removal and control by biocides.[5]

Components of Evanescent Field Sensor – Chapter Three

Commercially available components have been sourced and selected to optimise the sensor to deliver maximum stability, accuracy, reliability and low cost. Several components were custom designed for this project and have stabilised and ruggedised the set-up including:

- an x-y positioner to ensure that the maximum available light is coupled from a laser diode into the POF and secures both in the desired orientation
- a Y-splitter that stabilises the reference signal and optimises the sensing signal by off-axis coupling, ensuring that the high order modes utilised have the largest population due to the Y-splitter, and not removed by mode stripping
- POF to photodiode coupler to ensure that the relative positions of the POF and photodiode and excludes all extraneous light
- a self contained powermeter made from commercially available components in a transimpedence amplifier that rivalled commercially available powermeter. The author of this thesis has refined it to eliminate as much noise as possible by reducing pick-up by components by use of a PCB and housing the circuitry in an isolating solid aluminium case. The resulting module is a much smaller and rugged package that will enable miniaturisation and self-containment at reduce costs

The original experimental setup operated under pressurised conditions which did not reflect the conditions of final usage and the sensing fibre was clamped in position, stripping out the very modes that interacted with the biofilm. The author of this thesis has redesigned and refined the experimental set-up to address these problems.

The growth and removal of biofilms from the sensor with the use of contact lens protein removal systems has been verified with the POF evanescent field sensor developed by this project through intensity monitoring and by imaging using an electron

microscope[6]. This has opened up a new application for the protein removal systems previously used solely for the maintenance of hard contact lenses which are made from PMMA. The biofilm grown by this project has been imaged using an electron microscope and spectrally analysed. Two characteristic peaks were revealed at 486nm and 656nm.

Preparing POF for Sensing - Chapter Four

Termination of POF

A detailed step-by-step description of the procedures involved in terminating fibre ends has been set out in chapter four which refines and establishes good working practice which consistently optimises the ratio of available light coupled into fibre, making the sensor much more sensitive and effective. Improvements in polishing the fibre surface and in procedures in handling the fibres resulted in ten times the power of light previously available to the experiment.

Decladding POF

A simple method of removing the cladding of POF cleanly, efficiently and with consistent reproducible results has been developed which improved, by a factor of 10, the light intensity coupled into the fibre compared to previously. Electron microscope images showed the declad region with a keyed surface of pits and grooves that assists biofilm attachment and any coatings that may be applied since the work contained in this thesis was completed. Fibre core without cladding is now available on special order from Luceat.[7]

Tapering POF

Smaller diameter fibres have a larger proportion of propagating light in the evanescent field, and so tapered fibres were investigated as a way to improve sensitivity. The principle of tapering POF has already been verified by previous researchers working on this project; end tapers are readily produced but the method did not translate to producing mid-length tapers of sufficient quality for sensor purposes. The author of this thesis has automated the process and refined the etching solution to produce mid-length tapers in POF that are optically clear and robust with smooth profiles. The light attenuation during the process was monitored and modelled. The detected light intensity decreased steadily, reflecting the smooth profile of the taper.

Optically clear tapering was achieved by KSC Kuang via heat drawing. The heating and pulling method of producing mid-length tapers readily produced consistent tapers of a few millimetres in length with the cladding still intact and has been proven in use as a strain sensor. The process could be further improved with automated mechanical manipulation and a controlled targeted heat source.

Chemical tapering produces an extended region of tapered and declad fibre that is ideally suited to the biofilm sensor operations. Heat drawing produces very short mid-length tapers with their cladding still intact which are not suited for use in the biofilm sensor as the sensing region is so limited and the cladding would not allow the biofilm to interact with the core.

The work completed in chapter four has informed other research groups who have produced papers,[8,9,10,11,12] citing papers written by the author of this thesis. The groups are carrying out research in etching POF, mPOF and the modelling of the process and in the development of strain sensors.

Plastic Optical Fibre Evanescent Field Biofilm Sensor – Chapter Five

Large diameter step index POF were chosen for the intrinsic evanescent biofilm sensor because it has a large acceptance angle, hence a large NA, therefore supporting a greater population of modes propagating in the fibre core, including fundamental and, more significantly, leaky modes which give rise to the evanescent field and tunnelling rays, the modification of which forms the sensor operation mechanism. By taking tunnelling rays into account, Mignani et al[13] found that the fraction of light power propagating in the medium surrounding the same fibre core had a value within the range of $6x10^{-3}$ to $8x10^{-3}$, an order or magnitude higher than previously evaluated by the same group, which supports the operation of the biofilm sensor developed. The POF develops a positive charge in water,[14] which attracts the negatively charged biofilm,[15] the large diameter also gives more area with a larger radius of curvature onto which the biofilm is able to attach.

Characterisaton of Sensor - Chapter Six

Both declad and mid-length chemically tapered sensors were characterised for their response to refractive index changes. At the time of this research there was no other work published on intensity attenuation due to evanescent field sensing of refractive index changes in POF, we were the only group to characterise POF in this way. Subsequently we have found one other group in Poland, J Rayss and G Sudolski, was doing similar work at the same time as this thesis.[16] Glycerine was used and their various refractive indices were achieved through dilution with water, due to this they did not go beyond a refractive index of 1.410.

Analysis of the percentage of light in the evanescent field due to core diameter has been carried out. More modes are guided in larger diameter fibre core resulting in proportionally less power guided out into the cladding to populate the evanescent field. Decreasing the fibre core diameter results in a higher fraction of power propagating in the modified cladding, the smaller the diameter the fewer modes the supported, the greater the power guided out of the fibre into its cladding as it's diameter decreases. This is the justification for producing a fibre with a region of narrower radius. The larger 1mm POF is easier to use, coupling, terminating etc., tapering a mid length of a fibre would result in effective of coupling together with a greater proportion of light available for evanescent field attenuation. This was in agreement with Mignani et al[13] who also found that reducing the core radius enhanced the fibre absorbance.

Both declad and tapered sensors were characterised for their response to refractive index changes, both illuminated by 660nm wavelength LD. The light intensity detected from the sensor in distilled water at a refractive index of 1.33 was chosen as the reading to normalise about

The normalised output of the declad fibre increased, rising from 1 to 1.0384 when the refractive index. The increased the output of the fibre may be due to the altered scattering and chromatic absorbance properties of the water/sugar solution as increasing amounts of sugar are dissolved. The output of the declad fibre decreased, falling from 1.0384 to 0.0646 when the refractive index increased from 1.40 to 1.46, the oil region of the refractive index medium, a significant change which indicates that this sensor may have sensitive responses in applications connected to oil quality monitoring. The declad sensor was characterised with accuracy of ±0.007 refractive index units (to 2 standard deviations) or 0.5% below n=1.4 and ±0.002 refractive index units (2 standard

deviations) or 0.15% above n=1.4. From 95% confidence limits, the accuracy of the POF was ±0.006 refractive index units (to 2 standard deviations) or 0.4% above 1.4.

As the refractive index increased from 1.33 to 1.36 the normalised output from the tapered fibre stayed unchanged, from 1.38 to 1.45 there was a linear increase of 0.274μW normalised output per 0.01 refractive index change. Beyond 1.45 the tapered fibre was highly sensitive to refractive index change, rising from 1.706μW to 14.11μW. The region between refractive indexes 1.47 to 1.49 showed a linear relationship, the normalised output signal increased 0.5μW for every 0.01 refractive index change. The tapered fibre sensor was characterised with accuracy: ±0.007 (2 st. dev.) or 0.5% below 1.4. ±0.002 (2 st. dev.) or 0.15% above 1.4.

At refractive indices greater than ~1.46, into the oil region, the signal dramatically increased to infinity as the refractive index solution approached that of PMMA. The experimental results matched the theoretical treatment by Mignani et al[13] who discussed the theory of evanescent wave absorption with a view to improving sensitivity by altering the geometry of the fibre core.

The work completed in chapter four has informed other papers[17,18] in developing fibre optic liquid refractive index sensors and process monitoring the curing of epoxies[19].

The work contained in this thesis has been presented and promoted at various conferences around the U.K.

Author Publications

Peer Assessed	**Authors**	**Published in**	**Date Pub.**	**Append**
Automation and dynamic characterization of light intensity with applications to tapered plastic optical fibre	YM Wong PJ Scully HJ Kadim V Alexiou RJ Bartlett	Journal of Optics A: Pure and Applied Optics. Volume 5 pages 51–58	2003	1
Plastic optical fibre sensors for environmental monitoring: Biofouling and strain applications	YM Wong PJ Scully RJ Bartlett, KSC Kuang WJ Cantwell	Blackwell Publishing Ltd Strain Volume 39, pages 151-119	2003	2
Conference Presentations	**Authors**	**Presented at**	**Date Pres.**	**Append**
Chemical Tapering of Plastic Optical Fibres for Devices and Sensors	YM Wong PJ Scully R Bartlett V Alexiou P Eldridge E Sheikh-Bahoum	Poster at EPSRC conference Prep2001	2001	6
Automation and Characterisation of Chemical Tapering of Plastic Optical Fibres	YMWong P JScully HJ Kadim V Alexiou RJ Bartlett	IOP conference Sensors and their Applications XI	2001	7
On-line Measurement of Biofouling at Water Interfaces using Plastic Optical Fibre	PJ Scully RP Chandy YM Wong R Bartlett G Grapin G Jonca G D'Ambrosio FColin N McMillan M O'Neill P Rouxhet	IOP conference Sensors and their Applications IX	2001	8
Tapered Plastic Optical Fibre Evanescent Field Sensors and Applications	YM Wong PJ Scully R Bartlett K Kuang WJ Cantwell	Rank Prize Fund Mini Symposium on Optical Metrology Techniques for Industrial Applications	2002	9
Applications of Plastic Optical Fibre Evanescent Field Sensors	YM Wong PJ Scully R Bartlett	Sensors Paper at Photon02 at Cardiff International Arena	2002	10

The work completed in this has informed projects at various institutions around the world:

- Liverpool John Moores University[11,12] in the modelling of the tapering process
- The University of Manchester[20,21,22] in the design of a POF photon counting OTDR and a perspiration sensor
- The University of Birmingham and Cranfield University[19] to develop sensors for process monitoring of reinforced composites
- National University of Singapore[23,24] informed the design of strain sensor for structural health monitoring
- University of Sydney[9,10] in the chemical tapering of POF and mPOF
- The Indian Institute of Technology Kanpur[17,18] in developing liquid refractive index sensors
- Bremer Institut für Angewandte Strahltechnik Bremen, Germany and The Institute of Physical and Chemical Research, Wako, Japan[8] in chemically etching polymer materials

all of whom have all cited papers written by the author or this thesis as a result of the work contained within this thesis.

7.2 Future Work

The declad process results in a surface with micrometer diameter pits and grooves which may well assist in the adhesion of optically sensitive coatings containing reactants which serve to further optimise POF sensors. Tapered fibres are inherently more sensitive as the tapered region supports fewer modes of light, coating the surface of both the declad and tapered fibres, would further sensitise them. They can be coated with various dopants and dyes that only react with specific chemicals, changing analytes at the core/cladding interface that attenuates the signal to alter the sensors response to chemical or biological measurand. Cladding technology is making advances, most recent and exciting are the advances made in nano-structures.[25]

The declad fibre showed highest sensitivity to refractive indices above 1.40, indicating an alcohol/oil refractometer, the tapered fibre showed even higher sensitivity to refractive indices above 1.47, indicating a great potential as an oil refractometer for use in the food or petrochemical industries for quality control and counterfeit detection to protect company reputation.

Components are constantly being optimised, miniaturised and are becoming cheaper as the demand for smaller, integrated high performance increases. Including these as they become affordable would further improve the sensor range, speed, sensitivity and miniaturisation.

Moore's Law[26] stated that transistor counts had doubled every year; hence the faster and bigger capacities of computers now readily available mean that sensor measurements can include greater detail with increased sampling rates and for longer periods before downloading.

Improvements in mobile telephony, wireless networks make the possibility of remote wireless sensing possible.

The transimpedence amplifier circuit can be refined with the design of a circuit board to further minimise noise, and to be truly self contained, rugged, remote sensing unit combining:

- the launching of light signal
- the sensitive optical fibre
- the detection of the attenuated signal

New structures of optical fibres are constantly being introduced with new sensing opportunities presenting themselves. Single mode FBG consists of short segments of optical fibre that have grating written[27] into them which reflect only particular wavelengths of light and transmits all others. LPFG[28] does not produce reflected light and serves as a spectrally selective absorber. Microstructured POF (mPOF)[29,30] aka 'holey fibres' are the most recent and exciting innovation in optical fibres and bring a myriad of sensing possibilities with them.

Light sources have made great advances since the time of this project. In the early 2000s ultrabright light emitting diodes, LEDs were just emerging and new wavelengths were being introduced. Suitable light sources operated in the infra red and red regions of the spectrum, and in green and blue. Now all colours are available with light power of 200mW+.[31] The possibility of matching interrogating light wavelength to a target measurand absorption spectrum is now reality. The much lower costs now enable the development of throwaway devices. Coupling the available light power from LEDs is the main obstacle at present.

References

[1] PJ Scully, R Philip-Chandy, YM Wong, R Bartlett, G Grapin, G Jonca, G D'Ambrosio, F Colin, N McMillan, P Rouxhet, " Online Measurement of Biofouling at Water Interfaces using Plastic Optical Fibres", Sensors and Their Applications XI/ISMCR, 2001

[2] R Philip-Chandy, PJ Scully, "Plastic Optical Fibre Biofilm Sensor", CLOOPT Progress report, 1 July. Contract: N ENV4-CT97-0634 On-line Measurement for Preventing Fouling When Closing Industrial Process Water Circuit, 1998

[3] R Philip-Chandy, PJ Scully, P Eldridge, HJ Kadim, G Grapin, G Jonca, G D'Ambrosio, F Colin, "An Optical Fibre Sensor for Biofilm Measurement using Intensity Modulation and Image Analysis", IEEE Journal, Selected Topics in Quantum Electronics, JSTQE Optical Sensors Special Issue. vol. 6, 5, pp. 764-772, 2000

[4] R Philip-Chandy, PJ Scully, D Thomas, "A Novel Technique for On-line Measurement of Scale using a Multimode Optical Fibre Sensor for Industrial Applications", Sensors & Actuators B, vol.71, pp19-23, 2000

[5] YM Wong, PJ Scully, RJ Bartlett, KSC Kuang, WJ Cantwell, "Plastic Optical Fibre Sensors for Environmental Monitoring: Biofouling and Strain Applications", Strain, vol.39, No.3, pp115-119, 2003

[6] M O'Neill, ND McMillan, G Dunne, CI Mitchell, B O'Rourke, D Morrin, F Brennan, RMiller, L McDonnell, PJ Scully, "New tensiographic studies on protein cleaning of polymer surfaces". Colloids and Surfaces A., submitted June 2007

[7] Luceat S.p.A Viale F. Marconi 31, Dello (BS), Italy

[8] C Wochnowski, Y Hanada, Y Cheng, S Metev, F Vollertsen, K Sugioka, K Midorikawa, "Femtosecond-Laser-Assisted Wet Chemical Etching of Polymer Materials", Journal of Applied Polymer Science, vol.100, pp1229–1238, 2006

[9] P Hambley, J Canning , G Henry, "Comparison of Tapers in Solid and Microstructured Polymer Optical Fibres", COIN - ACOFT pp24 - 27, 2007

[10] P Hambley, J Canning, "Ultra-fast Tapering of Polymer Fibres for Sensing Applications", Proceedings POF2007, pp15-16, 2007

[11] H J Kadim, "State-Space based Analytical Modelling for Real-Time Fault Recovery and Self-Repair with Applications to Biosensors", IEEE Proceedings of the First NASA/ESA Conference on Adaptive Hardware and Systems, 2006

[12] H J Kadim, " Predictive Analysis for Robust Operation with Applications to Autonomous Biosensors", Second NASA/ESA Conference on Adaptive Hardware and Systems, 2007

[13] AG Mignani, R Falciai, L Ciaccheri, "Evanescent Wave Absorption Spectroscopy by Means of Bi-tapered Multimode Optical Fibers", Applied Spectroscopy vol. 52, No.4, pp546–551, 1998

[14] CLOOPT report August 2000 - internal report

[15] F Gotz, T Bannerman K Schleifer, "The Genera Staphylococcus and Macrococcus", editors: M Dworkin, S Falkow, E Rosenberg, K Schleifer, E Stackebrandt, "The Prokaryotes", chapter 1.2.1, p44, Springer, 2006

[16] J Rayss, G Sudolski, "Signal of the Evanescent Wave Sensor as a Function of its Length and the Refractive Index of the Surrounding Medium", Proceedings of SPIE vol.4239, pp118–126, 2000

[17] A Banerjee, S Mukherjee, RK Verma, B Jana, TK Khand, M Chakroborty, R Dasd, S Biswas, A Saxena, V Singh, RM Hallen, RS Rajput, P Tewari, S Kumar, V Saxena, AK Ghosha,, J John, P Gupta-Bhaya, "Fiber optic sensing of liquid refractive index", Sensors and Actuators B vol.123, pp594–605, 2007

[18] P Gupta-Bhaya, AK Ghosh, V Saxena, J John, "Design and calibration of low-cost fiber optic sensors for refractive index measurement of turbid liquids", Proc. of SPIE vol.6378, 2006

[19] GF Fernando, B Degamber, "Process monitoring of fibre reinforced composites using optical fibre sensors", International Materials Reviews vol.51, No. 2, pp65-106, 2006

[20] C Saunders and P J Scully, "Sensing applications for POF and hybrid fibres using a photon counting OTDR" Meas. Sci. Technol. vol.18, pp615–622, 2007

[21] C Saunders and P J Scully, "Distributed plastic optical fibre measurement of pH using a photon counting OTDR", Journal of Physics: Conference Series vol.15 pp61–66, 2005

[22] J Vaughan, F Gildert, PJ Scully, "Wearable Sweat Sensor using Polymer Optical Fibre", Photon06 conference proceedings, 2006

[23] KSC Kuang, ST Quek, M Maalej, "Assessment of an extrinsic polymer-based optical fibre sensor for structural health monitoring", Meas. Sci. Technol. vol.15, pp2133–2141, 2004

[24] KSC Kuang, M Maalej, ST Quek, "Hybrid optical fiber sensor system based on fiber Bragg gratings and plastic optical fibers for health monitoring of engineering structures", Proc. of SPIE vol. 6174, 2006

[25] SW James, RP Tatum, "Fibre Optic Sensor with Nano-structured Coatings", Journal of Optics A: Pure and Applied, vol.8, pp430-444, 2006

[26] GE Moore, "Cramming more components onto integrated circuits", Electronics Magazine, 1965

[27] KO Hill, Y Fujii, DC Johnson, BS Kawasaki, "Photosensitivity in Optical Fiber Waveguides: Application to Reflection Fiber Fabrication", Appl. Phys. Lett. Vol 32, p647, 1978

[28] AM Vengsarkar, PJ Lemaire, JB Judkins, V Bhatia, JE Sipe, T Erdogan, "Long Period Fiber Gratings as Band-rejection Filters", OFC'95, PD4-2, 1995

[29] MCJ Large, MA van Eijkelenborg, A Argyros, J Zagaril, S Manos, NA Issal, I Bassett, S Fleming, RC McPhedran, CM de Sterke, NAP Nicorovicil, "Microstructured Polymer Optical Fibres: Progress and Promise", SPIE vol.4616, pp105-116, 2002

[30] A Argyros, MA van Eijkelenborg, MCJ Large, I Bassett, "Hollow-core Microstructured Polymer Optical Fiber", Optics Letters vol.31, No.2, pp172-174, 2006

[31] http://www.philipslumileds.com/pdfs/DS23.pdf accessed 3rd April 2009